PB82-166190

REPORT NO.
UCB/EERC-81/12
OCTOBER 1981

STUDIES ON EFFECTS OF INFILLS IN SEISMIC RESISTANT R/C CONSTRUCTION

by

S. T. BROKKEN
V. V. BERTERO

Report to National Science Foundation

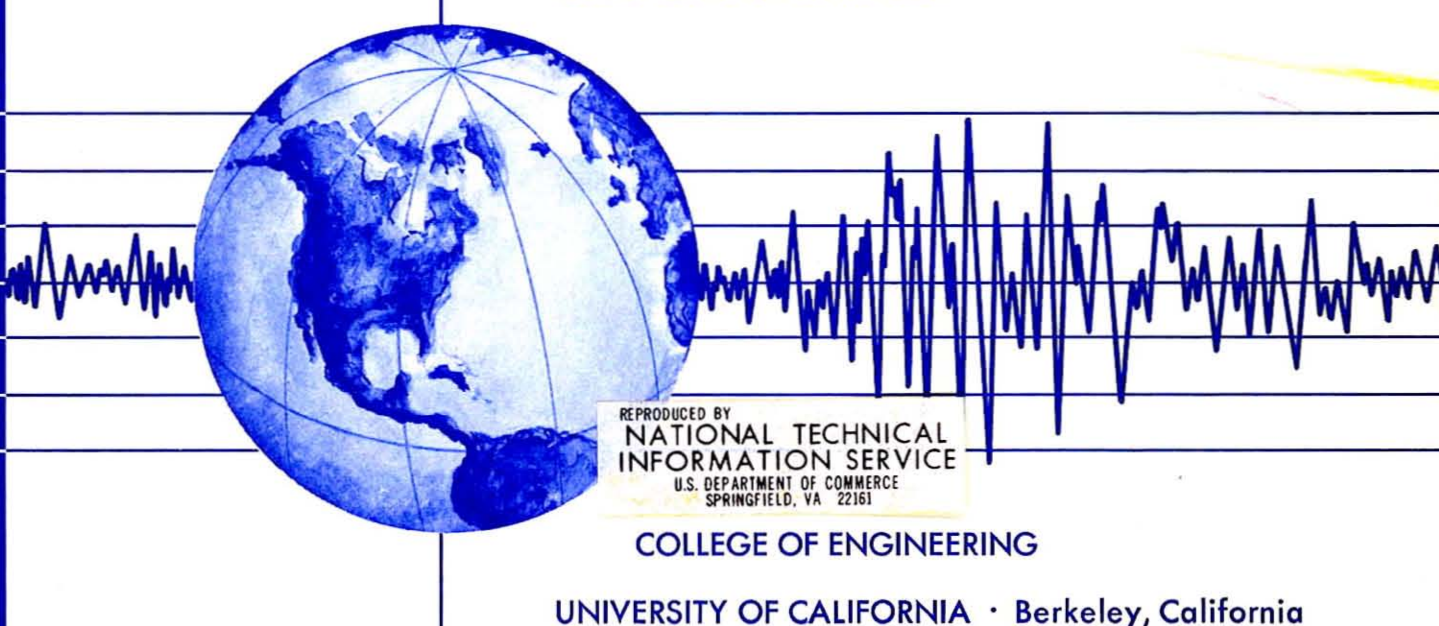

COLLEGE OF ENGINEERING

UNIVERSITY OF CALIFORNIA · Berkeley, California

For sale by the National Technical Information Service, U.S. Department of Commerce, Springfield, Virginia 22161.

See back of report for up to date listing of EERC reports.

50272-101

REPORT DOCUMENTATION PAGE	1. REPORT NO. NSF/CEE-81046	2.	3. Recipient's Accession No. PB82 166190

4. Title and Subtitle	5. Report Date
Studies On Effects Of Infills In Seismic Resistant R/C Construction	October 1981
	6. 053021
7. Author(s) S. T. Brokken and V. V. Bertero	8. Performing Organization Rept. No. UCB/EERC-81/12
9. Performing Organization Name and Address Earthquake Engineering Research Center University of California, Berkeley Richmond Field Station 47th Street & Hoffman Blvd. Richmond, Calif. 94804	10. Project/Task/Work Unit No. 0-22002 11. Contract(C) or Grant(G) No. (C) (G) PFR-79-08984
12. Sponsoring Organization Name and Address National Science Foundation 1800 G Street, N.W. Washington, D.C. 20550	13. Type of Report & Period Covered 14.

15. Supplementary Notes

16. Abstract (Limit: 200 words)

This report summarizes experimental and analytical studies of the quantitative effects of infills in the seismic performance of buildings (particularly in buildings whose structural systems are based on the use of moment resisting frames alone); and the implications of these effects regarding the design of new buildings and retrofitting of existing R/C frame structures have been evaluated.

The first part is concerned with the infill problem and the experimental investigation conducted to study the effects of infill panels on seismic response of reinforced concrete frames. This investigation consisted of a series of quasi-static cyclic and monotonic load tests on 1/3-scale models of the lower 3-1/2 stories of an 11 story-three bay reinforced concrete frame infilled in the outer two bays. The reinforced concrete moment frame was designed for high rotational ductility and resistance to degradation under reversed cyclic shear loads. A number of different panel material and reinforcement combinations were tested.

The analytical studies are described in the second portion of this report. Implications of the experimental results are considered as to how the investigated infills affect the dynamic response of R/C moment resisting frame buildings, as well as considering the effect of these implications on the seismic resistant design and retrofitting of buildings.

17. Document Analysis a. Descriptors

b. Identifiers/Open-Ended Terms

c. COSATI Field/Group

18. Availability Statement:	19. Security Class (This Report)	21. No. of Pages
Release Unlimited		191
	20. Security Class (This Page)	22. Price

(See ANSI-Z39.18) See Instructions on Reverse OPTIONAL FORM 272 (4-77) (Formerly NTIS-35) Department of Commerce

STUDIES ON EFFECTS OF INFILLS

IN SEISMIC RESISTANT R/C CONSTRUCTION

by

S. T. Brokken
Senior Engineer
URS/John A. Blume & Associates, Engineers
Formerly Graduate Student
University of California, Berkeley

V. V. Bertero
Professor of Civil Engineering
University of California, Berkeley

Report to Sponsor:
National Science Foundation

Report No. UCB/EERC-81/12
Earthquake Engineering Research Center
College of Engineering
University of California
Berkeley, California

October 1981

ABSTRACT

Although it is widely recognized that infills play an important role in the seismic performance of buildings, particularly in buildings whose structural systems are based on the use of moment resisting frames alone, little reliable information is available regarding the quantitative effects of infills. This report summarizes studies conducted at Berkeley in which these effects have been studied experimentally and analytically, and the implications of these effects regarding the design of new buildings and retrofitting of existing R/C frame structures have been evaluated. The report, therefore, has been divided into two main parts.

The first, which covers the first five chapters, is concerned with the infill problem and the experimental investigation conducted to study the effects of infill panels on seismic response of reinforced concrete frames. This investigation consisted of a series of quasi-static cyclic and monotonic load tests on 1/3-scale models of the lower 3-1/2 stories of an 11 story-three bay reinforced concrete frame infilled in the outer two bays. The reinforced concrete moment frame was designed for high rotational ductility and resistance to degradation under reversed cyclic shear loads. A number of different panel material and reinforcement combinations were tested. For reasons of economy, ease of construction, favorable mechanical properties, and efficiency of different types of masonry infill, it was concluded that the most promising panel configuration consisted of solid brick laid in mortar reinforced with two mats of welded wire fabric, one bonded to each side of the wall in a layer of cement stucco (mortar).

The results of analytical studies are described in the second portion of this report (Chapter Six). The implications of these experimentally obtained results are considered as to how the investigated infills affect the dynamic response of R/C moment resisting frame buildings, as well as considering the effect of these implications on the seismic resistant design and retrofitting of buildings.

ACKNOWLEDGEMENTS

The research reported herein was sponsored by the National Science Foundation under Grant No. PFR 79-08984, "Seismic Behavior of Structural Components." Subproject No. 0-22002 is focussed on studies of R/C wall-frame structural systems. Any opinions, discussions, findings, conclusions, and recommendations are those of the authors and do not necessarily reflect the views of the National Science Foundation.

All testing was conducted in the Structural Engineering Laboratory of the Department of Civil Engineering, University of California, Berkeley.

The authors would like to acknowledge particularly the contributions of Development Engineers Barry Lotz and Don Clyde to the construction and testing involved in this investigation. The authors would also like to express their appreciation to Wes Neighbor, who assisted with the testing phase of specimens, and to Jose Sandoval, graduate student, who also assisted in the fabrication and testing of some of the specimens. Additional acknowledgement is due to M. C. Randall and S. Gardner for editing this report, and D. Ullman and R. Steele for preparing the illustrations.

TABLE OF CONTENTS

LIST OF TABLES

LIST OF FIGURES

I. INTRODUCTION

1.1 Statement of Problem

While in the process of structural design it is necessary for the designer to utilize a mathematical model of the structural system, in practice the actual structure may be quite different from the designer's idealization. Numerous parameters may influence this occurrence, one of the most striking being a tendency to neglect "nonstructural" components which are not envisioned by the designer as necessary contributors to the response of the structure. An example is the presence of infill elements which consist simply of a panel, frequently masonry, placed in the plane of a structure frame, partially or completely filling either the height or width. It is of paramount importance to realize that the effect of such "nonstructural" components may be quite objectionable and may have a significant impact upon the seismic resistance of the structure. Hence there exists a real need for a rational design-oriented approach which takes into consideration the effects of such elements.

Furthermore, the proper use of these infill elements can be of great value in strengthened and stiffened existing frame structures. For this reason, and due to the lack of reliable data concerning the effects of such elements on structural response, it was decided to conduct the studies reported herein. This investigation is a continuation of the research reported in Ref. 1.

1.2 Objectives and Scope

The ultimate objective of this research is to improve the behavior and, therefore, the seismic-resistance of buildings whose structural systems consist of reinforced concrete frames infilled with panels, i.e., infilled frames. To achieve this objective a series of experimental and analytical work has been performed.

Although the studies reported herein are concerned particularly with experimental work, analytical predictions based on the results obtained in the experiments are also reported.

Experimental work was conducted on a 3 1/2-story x 1 1/2-bay subassemblage selected for study from the end frame of the prototype structure. This subassemblage was built to 1/3 scale, infilled with panels and instrumented as required, and then tested. A total of 18 tests were conducted to investigate the relative performance of various types of infilling materials and construction techniques. Specific details concerning techniques and materials as well as results are presented in the body of this report.

The effects of infills on the seismic resistant R/C construction are studied analytically, after evaluation of the obtained experimental results. Finally, recommendations for the design of seismic-resistant infilled frame structural systems, as well as for retrofitting of R/C moment resisting frames, are formulated.

II. SELECTION OF BUILDING TO BE STUDIED

2.1 General Remarks

To facilitate these studies it was decided to select a reasonably simple prototype building. The prototype building was the same as that described in Ref. 1. Biggs and Grace [2] had a series of five hypothetical buildings designed by a practicing structural engineering firm using conventional design procedures. The buildings were apartment house-type construction with intentionally simple and symmetrical architecture and structure. Because many typical infilled frame-type structures are in the 10- to 15-story range in height, it was decided to use the 11-story reinforced concrete frame from this series of hypothetical buildings.

2.2 General Description of Prototype Building

The prototype building selected consists of an 11-story reinforced concrete space frame, 60 x 200 ft (18.3 m x 61 m) in plan, with uniform 9 ft (2.75 m) story heights and a one-way slab floor system. Typical plan and end frame elevation views are shown in Figs. 1 and 2. Some modifications have been made to the design by Biggs and Grace [2], and will be discussed in subsequent sections.

2.3 Design and Analysis

In order to check the service condition design by Biggs and Grace [2] to identify any possible modifications to the prototype, a preliminary bare frame design was first carried out. Dead loads were computed based on the data given in Ref. 2, and live loads were taken to be 50 psf (1.04MPa). Design was based on the provisions of the 1970 UBC [3]. Using Sections 2615 and 2630 of the UBC, critical design load combinations were given by:

$$1.5\ D + 1.8\ L$$

$$1.40\ (D + L \pm E)$$

$$0.9\ D \pm 1.25\ E$$

Equivalent static lateral loads representing the effects of seismically induced inertial forces were computed according to two procedures:

(1) The building was modeled using TABS, a computer program specifically developed for static and dynamic structural analysis [4]. The model used the original member sizes, and considered the effects of finite column widths and beam depths. Young's modulus for concrete was calculated in accordance with Section 8.3.1 of the 1971 ACI Code [5] using f'_c equal to 4000 psi (27.58 MPa). The contribution of the floor slabs to beam stiffness was included in accordance with Section 8.7.2 of the 1971 ACI Code. Reduction in beam flexural stiffness due to cracking was considered by using an effective moment of inertia equal to 40 percent of that of the uncracked section. This ratio was subsequently checked and found to be valid for the final beam designs. The fundamental period of vibration of the 11-story frame structure was calculated to be 1.30 secs. Based on this value, equivalent static lateral forces were calculated by Section 2314 of the 1970 UBC, using a value of Z equal to 1.0 (Zone III), and a value of K equal to 0.67, corresponding to a ductile moment-resisting frame. This nomenclature is defined in Ref. 3.

(2) Although Section 2314 of the 1970 UBC does not explicitly specify a design response spectrum for calculating equivalent lateral forces, its base shear calculation formula implies the spectrum shown in Fig. 3. In accordance with Section 2630(a) of the 1970 UBC, this equivalent spectrum was scaled up by a factor of 1.40, resulting in peak spectral response accelerations of 0.093 g, as shown in this same Fig. 3. Newmark's maximum spectral values for a standard basis earthquake were scaled to produce the equivalent Zone 3 ground spectrum which, when modified in accordance with Ref. 6, would also produce maximum spectral response accelerations of 0.093 g in buildings with 3 percent critical damping, founded on firm soil. This amount of damping was used because it is a realistic value for a clean, reinforced concrete frame responding in the elastic range. Assuming 3

percent damping in all modes, the root-mean-square (RMS) combination of the first five modes, as computed by TABS [4], was used to calculate an envelope of equivalent story shears. The base shear obtained by this second method was within a few percent of the UBC base shear. In the upper floors, however, the second method gave story shears which were larger and considered more realistic. Therefore, these were used in combination with gravity loads to compute the forces required for member design. For consistency, the story shears computed by the second method were factored to give a base shear equal to that of the UBC method. Load combinations were computed using the TABS program. The members were designed to meet the 1971 ACI Code and its Appendix A ("Special Provisions for Seismic Design"), using Grade 60 steel and f'_c equal to 4000 psi (27.58 MPa).

2.4 Revised Design

The original columns of Ref. 2 measured 12 in. x 30 in. (305 mm x 762 mm). The results of the preliminary design indicated that, owing to their low shear-span ratio, such columns might have low resistance to cyclic shear reversals. Therefore, the preliminary design was revised for columns measuring 18 in. (457 mm) square. This revised service load design was carried out by the 1971 ACI Code and its Appendix A, with the following exceptions:

(1) Beams were designed for the shear consistent with the development of their maximum moments (ϕ = 1.0) at sections located at a distance of two-thirds the clear span apart. Such a hinge placement could be developed under combined lateral and gravity loads. The total shear was assumed to be carried by the transverse steel alone.

(2) Columns were designed for the shears consistent with the development of maximum balance point moments (ϕ = 1.0) acting in opposite senses at a distance d/2 from adjacent beam faces (double curvature, with the inflection point at column mid-height). Again, shear was assumed to be carried by steel only. This is a very con-

servative assumption for columns, where the axial force is assumed to be the compressive force corresponding to the balance point of the moment-axial force interaction diagram.

(3) Beam-column connections (joints) were designed with transverse reinforcing sufficient to resist the shear produced by the development of maximum moments (acting in the same sense) in the framing beams at the column faces.

The final service condition design was similar to that of Ref. 2.

2.5 Design Modifications for Strong Ground Motions

Because the revised bare frame design indicated that the selected prototype was basically satisfactory, it was decided to continue with this prototype. The previous design was now modified to resist strong earthquake ground motions.

Lateral forces were calculated using the ground spectrum suggested by Newmark: $u_{g\ max} = 0.50$ g, $u_{g\ max} = 24$ in./sec. (610 mm/sec.), and $u_{g\ max} = 18$ in. (457 mm). The building was assumed to be founded on rock or firm soil, with 5 percent critical damping in all modes, and an available displacement ductility of 5.0. Then current procedures [7] were used to compute the reduced elasto-plastic design response spectra (Fig. 4), which were much more severe than the service condition spectra of Fig. 3. The critical load combination was taken as the sum of:

(1) Story shears from the RMS combination of the first five modal responses to the reduced elasto-plastic design response spectra shown in Fig. 4; plus

(2) Factored gravity loads (1.5 D + 1.8 L), with the live load reduced for tributary area by Section 2306 of the 1970 UBC. These factors were used instead of (0.9 D + 1.2 E) because the latter are less critical for columns, such as those used here, whose moment

resistance does not decrease significantly for axial loads less than the balance point axial load. It is recognized that the maximum gravity loads calculated using (1.5 D + 1.8 L) are conservative. The factors were used to account in an approximate manner for the potential effects of concurrent vertical accelerations.

This load combination and the building geometry were used as input to BADAS-2, an elasto-plastic design program [8]. This program found the required member resistance by storywise optimization. The necessary beam and column resistances at each floor level were very close to those obtained by hand calculation using a sidesway collapse mechanism consisting of a one-story subassemblage. Member design was carried out using realistic material properties. Park and Kent's stress-strain curves for confined concrete [9] were used with f'_c = 4000 psi (27.58 MPa). Spalling was assumed to take place at a concrete strain of 0.0035. Because the actual average yield stress for Grade 60 deformed reinforcing bars is about 68 ksi (469 MPa), that value was used instead of the nominal 60 ksi (414 MPa). Strain hardening was assumed to begin at a steel strain of 0.007 with a strain-hardening modulus of 1500 ksi (10,343 MPa). A maximum (and ultimate) stress of 95 ksi (655 MPa) was assumed to be reached at a steel strain of 0.15.

Beam designs were checked using the computer program RCCOLA [10] which calculated moment-curvature relationships using the section geometry and material properties discussed above. No ϕ factors were used. Sufficient closely-spaced transverse steel was provided for the following purposes:

(1) To resist all the shear consistent with the development of ultimate moments at hinge regions located at a distance of one-half the clear span apart (Fig. 5). It was found that this hinge location pattern might result from extreme combinations of vertical and lateral loads. The hinge separation was reduced from that used in the revised design of Section 2.4 because it was considered desirable to

design more conservatively against loss of ductility due to shear failure produced by cycles of extreme reversal;

(2) To provide the rotational ductility (as calculated by the formulas of Mattock [11] and Corley [12]) consistent with the assumed available overall displacement ductility of 5.0; and,

(3) To reduce the unsupported length of the longitudinal steel so that longitudinal steel buckling would be prevented or delayed even after the onset of strain hardening.

To simplify design detailing and to improve hysteretic behavior under full deformation reversals, the beams were designed with equal top and bottom longitudinal reinforcement. To allow for the formation of hinge regions away from the column faces due to combinations of lateral and vertical loads, all beams were designed with equal reinforcement carried along their entire length.

Using the RCCOLA program [10], moment-axial force interaction curves were calculated for several trial column sections and compared with the critical moment-axial force combinations calculated by the BADAS-2[8] computer program. To obtain increased resistance to cyclic shear reversals, it was decided to use spiral reinforcing instead of the rectangular hoops used in the revised bare frame service load design. Columns at each joint were designed to resist the combined action of 1.2 times the joint forces (moments and shears acting at the interfaces of the beams and the joint) consistent with the development at these interfaces of the ultimate moment capacities of the framing beams, acting in the same sense (Fig. 6). Spiral reinforcement was designed to accomplish the following:

(1) Resist all the shear consistent with the development of maximum column moments in opposite senses at a distance d/2 from the beam faces limiting each clear story height, i.e., column double curvature over a height equal to the clear story height less two lengths of d/2 each, with the inflection point located at the

column midheight (Fig. 7);

(2) Protect the longitudinal steel against buckling, even in the strain-hardening range; and

(3) Provide the necessary confinement as prescribed by A.6 of Appendix A of the 1971 Code.

Figure 8 shows the moment-axial force interaction diagram calculated (using the RCCOLA program) for the final column design. Because of the relatively high percentage of longitudinal steel, the moment capacity is not sensitive to variations in axial force at or below the balance point axial force. This figure also shows two moment-axial force interaction curves which apply when shear capacity controls. The first of these, calculated considering the shear resistance of the concrete only, represents the internal force combinations expected to produce shear cracking under monotonically increasing loads. The second curve, calculated considering the shear resistance of spirals only, represents the flexural capacity (governed by shear) under full cycles of reversed loading.

Because it was anticipated that the model would be constructed to one-third scale, the design of all members was carried out using bar sizes which, when divided by three, would result in available deformed bar sizes. A "strong column-weak girder" design philosophy was used. The columns were assumed to remain elastic except at the base of the building. They were designed for rotational capacities corresponding to story drift indices of at least 0.02, even under maximum factored gravity loads. The critical regions of all members were designed for rotational ductility ratios of at least 5.0, consistent with the assumed available overall displacement ductility ratio of 5.0 used in constructing the reduced elasto-plastic design response spectrum.

2.6 Selection of Basic Structural Subassemblage

If the subassemblage were of a configuration such that it could be isolated from the prototype frame by separation only at sections corresponding to inflection points in the beams and columns, then the problem of reproducing boundary values during testing would be considerably simplified. Inflection points will not necessarily remain in a fixed position, and this movement may introduce some modeling error which must be tolerated. It was decided to use a multi-panel subassemblage providing increased accuracy in the duplication of boundary conditions in panels located away from points of load application.

Maximum force levels in a typical building structure are generally reached at or near the base of the structure due to the predominance of the fundamental mode in the response. Therefore, it was decided to locate the subassemblage in the lower three and one-half stories of the end frame. Elastic symmetry considerations (neglecting geometric stiffness) imply that zero moment and zero vertical displacement imposed at the frame center line satisfy the proper force and displacement boundary conditions at this point for the beams. However, the structure is not completely symmetric in the inelastic range due to different axial load levels in the columns caused by the overturning moment from floors above. These different axial load levels change the plastic hinge moments of the column sections and hence cause a variation from symmetry. Thus, in the inelastic range, constraining ends of the cantilever beams of the model to zero vertical displacement and zero moment does not exactly satisfy the force and displacement boundary conditions. To satisfy these boundary conditions would require modeling both halves of the frame (i.e., all three bays). This was an unacceptable alternative due to limitations of space, time and cost. In addition, the effects introduced by variation from these boundary conditions are believed to be small. Therefore, the prototype subassemblage shown in Fig. 9 (three and one-half stories high by one and one-half bays wide), was selected for the studies described in Ref. 1 and was also finally adopted for the studies reported herein. Design details of frame elements of the subassemblage are shown in Fig. 10.

III. EXPERIMENTAL STUDY

3.1 General Remarks

As discussed in Chapter II, it was decided to test a three and one-half story by one and one-half bay subassemblage from the end frame, as shown in Fig. 9, using to the extent possible a previously developed shear wall testing facility at the structural engineering laboratory where the tests were to be conducted. This placed a series of constraints on the final details regarding the test specimen, the results of which will be discussed subsequently.

3.2 Selection of Test Specimens: Model Scale

Many parameters are greatly influenced by model scale. For example, aggregate interlock plays an important role in the behavior of cracked regions, having a potentially large effect on energy dissipation characteristics. Also, the bond properties of reinforcement vary with the bar size. Furthermore, effects of fabrication errors increase as the scale is decreased. Hence geometric scaling introduces modeling errors, some of which cannot be avoided. Thus the subassemblage should be modeled to the largest scale which can be accommodated, ideally full size. Given the number of stories in the subassemblage and the dimensional and capacity limitations of the testing facility, one-third scale was deemed to be the largest feasible.

3.3 Instrumentation and Data Acquisition System

It is convenient to divide the required data into four primary categories, namely, (1) all actions (loads) applied to the specimen; (2) overall response parameters; (3) contributions of different sources of deformation to overall and local response; and (4) local behavior of critical regions of interest.

Loads were applied using hydraulic jacks and were monitored using calibrated load cells connected in line with the actuator shafts. Passive forces, i.e., forces developed in connecting struts used to maintain correct displacement boundary values which were loaded by being acted upon by the specimen and hence capable of supplying only resisting forces in a passive manner, were monitored using force transducers consisting of four-arm strain gauge bridges.

Overall response parameters were considered to consist of the lateral displacements at the various floor levels and interstory displacements between these floor levels. Lateral displacements were measured using linear potentiometers attached to fixed reference points. Interstory displacements were considered obtainable by subtracting lateral displacements at appropriate floor levels.

The primary contributions to different sources of deformation of concern are shear distortion, flexural distortion, and rigid body motion of the specimen. Shear distortion was measured with the use of two diagonal linear potentiometers between two successive floor levels (Fig. 11). Rigid body motion was measured using three dial gauges placed around the foundation of the specimen. Flexural deformation was obtained by subtracting the shear displacement from the specimen displacement.

The extent of instrumentation varied considerably from test to test for the following reasons: (1) the frames for specimens 1, 2, and 3 were originally constructed and tested by Klingner [1], thus limiting the extent of possible instrumentation on these specimens to that which could be accommodated using existing provisions for instrumentation; (2) weldable microdot gauges in critical regions were frequently unsuitable for use in subsequent tests due to their being subjected to strains well beyond their capacity; and (3) concrete gauges were used only on specimens 4 and 5 to measure the force in the panel diagonal corresponding to the so-called equivalent strut. These gauges provided limited information due to panel cracks passing through the gauge length relatively early in testing. (See Figs. 11 and 12 for details regarding instrument placement.)

Output from all instrumentation was read at discrete intervals using a high-speed data acquisition system with 128 channel capacity. Some channels were also monitored continuously with X-Y-Y' recorders.

3.4 Fabrication of Specimens

Frame Construction. Frame construction details were identical for all specimens with the following two exceptions: (1) details necessary for attaching instruments; and (2) details necessary for infill anchorage to the frame.

Typical frame construction proceeded as follows. The reinforcing bars for frame construction were bent and tied. Threaded pins for attaching instrumentation were silver-soldered to reinforcing steel as required. Weldable strain gauges were spot-welded in their appropriate locations. The entire steel cage was then placed in formwork designed for horizontal casting, which was used because it simplified formwork and specimen construction. Formwork was varied as required according to the different arrangements of steel protruding from the frame into the panel openings for infill anchorage. Specimens were cast in a single pouring operation with concrete batched and mixed at the laboratory. Twelve batches were nominally required per specimen. After seven days the formwork was stripped and specimens were placed in a vertical position for infilling.

For frames infilled with reinforced hollow unit masonry, work proceeded as follows. Blocks were laid in running courses with horizontal courses sawcut as required to permit placement of horizontal steel which was lap spliced to column dowels. The first few courses were generally laid prior to lap splicing vertical steel to dowels projecting from the underside of the beam above. Remaining courses were laid using units which were sawcut to permit being slipped sideways onto the vertical steel. All courses were fully grouted as work proceeded. The gap between the top of the panel and the beam of the floor above was filled with stiff mortar.

Construction of infill panels consisting of solid split bricks with exterior welded wire fabric reinforcement proceeded as follows. Split bricks were laid in mortar infilling the frame opening. Cross ties were left in the mortar bed as a provision for holding the welded wire fabric mat flat for subsequent construction stages. After the panel was allowed to sit undisturbed for at least 24 hours, two mats of welded wire fabric were attached to it, one on each side, with care taken to tie the wire mesh flat against the brick using the cross ties already in position. A bonding agent was then applied to both sides of the panel to assure good bonding between the mortar cover and brick. A mortar cover 5/8 in. thick was applied to each side (face) of the infill panels in two layers. It was difficult to maintain uniform panel thickness using this method, and it is believed that better quality control could be attained easily in the field, especially if pneumatically applied concrete is used.

3.5 Testing Procedure

The loading sequence for each test consisted of the following: (1) The column jacks were connected to the specimen, and column loads were applied to simulate unfactored dead plus live loads. The cantilever beam struts were left free during this step. (2) The cantilever beam struts were connected and tightened only enough to remove any play in the strut pin connections corresponding to the direction in which the specimen was to be loaded. (3) The horizontal jack was connected to the specimen. (4) The desired loading program was then applied. Overturning moment from stories above the subassemblage, as calculated from analysis, was applied automatically using a preset transfer between the horizontal and column jacks through the MTS servocontrol system. (5) Upon completion of the loading program the horizontal jack was removed from the specimen and the cantilever beam struts were disconnected. (6) Axial loads were removed and the column jacks were disconnected from the specimen.

The ratio between the lateral force and corresponding overturning moment was calculated by an elastic analysis of the entire end frame. Analyses were conducted on both the bare frame and the infilled frame. Transfer ratios as applied to these specimens are shown in Figs. 13 and 14 respectively.

During the course of testing, increasing panel degradation resulted in the behavior of the infilled frame tending toward a bare frame type of response, i.e., as the level of panel damage increased, the panel contributed less and less to the lateral strength and stiffness of the frame, and hence behavior at this point was dominated by the frame response. Therefore, during infilled frame tests, the associated overturning moment was modified to that of the bare frame during the loading program at a point dependent upon the extent of the transition toward a bare frame type of response.

3.6 Repair Methods

Typically, after completion of an infilled frame loading program, panel replacement was required at only one level, as severe panel damage was generally confined to one level only. The remainder of the damaged panel was removed, with care taken to retain reinforcing steel (or WWF*) protruding from the frame which was cast in place for panel reinforcement anchorage. Spalled concrete was removed from the columns leaving only sound concrete. In general, the column cores were in good condition and showed no visible signs of distress, a consequence of the excellent confinement provided by the closely-spaced transverse spiral steel. Panel anchorage steel sometimes suffered some damage, and was repaired by chipping concrete away to allow the welding of a new piece of reinforcing steel to the stub (No. 2 bar) or, for tests in which welded wire fabric reinforcement was used, any necessary repair to the anchorage fabric was performed by brazing. The columns were then reformed and the cover was recast in a horizontal position. After the column forms were stripped, the specimen was lifted and placed in a vertical position for infilling. Infilling proceeded using construction methods described previously (Section 3.4) with new panel reinforcement lap spliced as required to the frame anchorage steel.

Strengthening Methods. During tests 7 and 9 the spiral trans-

* WWF, i.e., Welded Wire Fabric.

verse steel was observed to fracture in critical plastic hinge regions of the columns in the first story, thus causing immediate brittle shear failure at that location in the column. This made any type of repair impossible and rendered this story level useless in subsequent testing. Therefore it was decided to strengthen this floor level so panels in other floor levels could be tested.

Strengthening was achieved by placing a rather substantial amount of reinforcing steel in the panel opening and casting this floor level solid (6-inch thick). Vertical steel was concentrated at both sides of the bay, and was anchored at the top by being passed through holes drilled in the second floor beam. Thus the steel formed a continuous U-shape (no splices) with the curved portion of the U passing through the second-floor beam, and both ends of the U terminating at the footing. Anchorage was achieved at the footing by welding the reinforcement to anchorage angles (see Figs. 15 and 16) which were secured under bearing plates used in prestressing the specimen to the reaction blocks.

IV. EXPERIMENTAL RESULTS

4.1 General Remarks Concerning Data Reduction and Data Presentation

A series of 18 tests has been performed on 5 models of the subassemblage chosen for study. Tests were conducted using a variety of panel configurations to provide information regarding different panel materials and reinforcing details. An overview of this testing series may be seen in Table 1; the mechanical characteristics of materials are summarized in Table 2.

Most of the experimental results are presented as load, H, vs. interstory displacement, Δ, hysteresis loops (Fig. 17 to 34). The horizontal force plotted in these hysteresis loops includes corrections for the horizontal components of the force applied by the column jacks, which may be a very significant correction at large values of specimen displacement. For tests in which the panel failure occurred in the first floor, the horizontal force in the hysteresis curves includes a correction which accounts for the horizontal component of force from the first-floor beam strut (BM-1) (See Fig. 10a) which was part of the system used to impose the correct boundary conditions on the subassemblage.

Interstory displacements, corresponding to the stories that failed, were obtained by subtracting readings from respective linear potentiometers measuring lateral displacements of the specimen at appropriate floor levels. Shear displacements were obtained from diagonally placed linear potentiometers in each story level.

4.2 Failure Mode and General Observations Concerning Specimens

4.2.1 Test Specimen No. 1 (Model No. 1 - Fig. 17)

Model No.1 was originally built and tested once by Klingner [1], who obtained a first-story failure leaving the second- and third-story panels intact. The specimen was repaired for use in the present study by recasting column cover as required in the first-story level and re-infilling the same level with an unreinforced fully grouted clay brick panel. Thus the specimen for this test consisted of fully grouted clay brick panels in all three stories, the first-story panel being unreinforced, with the second- and third-floor panels having 0.6 percent steel in both the vertical and horizontal directions. The specimen was subjected to several service load cycles, and then loaded monotonically to failure. The specimen was then given a displacement reversal sufficient to return it to zero displacement upon unloading.

General observations:

(1) The failure mode involved only the first-story panel. After crushing of the panel at midspan of the diagonal compression strut, the frame formed a sidesway mechanism with hinges at the top and bottom of the first story in both columns.

(2) Panel damage in the first story was well distributed considering this panel was unreinforced.

(3) An air mattress supported on shored plywood was used to balance the dead load of the first-story panel. This prevented loose panel material from falling out of the plane of the panel. Some of these pieces were relatively sizable and continued to carry load as the panel continued to crush at increasing values of displacement. Thus the air mattress appeared to have retarded break-up of the panel.

(4) The frame panel interface cracked, but no significant relative lateral displacement was observed between the frame and panel. Large relative lateral displacements were apparent across horizontal cracks within the panel.

(5) Plastic hinges in the columns did not form at their idealized locations for the obtained failure mechanism (top and bottom of columns in first story). Plastic hinges formed into the bay opening, thus decreasing the distance between the hinges. This was caused by panel material stiffening corners of the frame.

For an overview of panel damage, see Figs. 35 and 36.

4.2.2 Test Specimen No. 2 (Model No. 1, Repair 1 (R1) - Fig. 18)

Model 1 was repaired after Test 1 by removing all remaining panel material and all spalled column cover from the first-story level. The column cover was recast and a prefabricated unreinforced clay brick panel was positioned and grouted in place in the first-story level. Panels in the second and third story had sustained only minor damage and required no repair.

The specimen was then loaded cyclically with full load reversals and, after ductility one, with full displacement reversals until the maximum displacement capacity of the horizontal jack was reached in the negative displacement direction. At that point, full displacement reversals were not possible and the specimen was cycled to the maximum displacement that the jack could impose. (Fig. 18)

General observations:

(1) The failure mode involved only the first story, beginning with crushing of the infill and finally with the frame forming a single story sidesway mechanism with hinges at the top and bottom of the first story in both columns.

(2) Interior panel damage was concentrated in very few diagonal cracks. Cracking within the panel was very poorly distributed.

(3) Separation between the bounding frame and the panel occurred very early in the test. Relative slip was observed between the panel and the frame and crushing of panel material occurred along the entire first-story column height on the right side, as well as adjacent to the left column extending up from the base approximately one-third of the first-story column height. Crushing of panel material also occurred along the entire length of the base of the first-floor panel (see Figs. 37 and 38).

(4) Virtually no crushing occurred within the panel, i.e., away from panel boundaries.

4.2.3 Test Specimen No. 3 (Model No. 3 - Fig. 19)

Model No. 3 was originally built and tested once by Klingner [1] who obtained a combined second- and third-story failure leaving the first-story panel intact. The model was repaired for use in this study by removing remnants of the second- and third-story panels and casting a 2-in. thick panel of lightweight concrete (LWC) with a steel percentage = 0.6% in both vertical and horizontal directions in each of these two floor levels. Thus Test Specimen No. 3 had a first-story panel of fully grouted concrete block (ρ = 0.6%) and second- and third-story panels of 2-in. thick LWC (ρ = 0.6%). Specimen 3 was loaded monotonically. (Fig. 19)

General observations:

(1) The failure mode involved only the first story and was triggered by crushing of the infill acting as diagonal compression strut, with the frame finally forming a sidesway mechanism with hinges at the top and bottom of the first story in both columns.

(2) Cracking occurred but no significant relative lateral displacement was observed between the frame panel interface.

(3) First-story panel damage was well distributed with the exception that relatively little cracking was observed in the lower portion of the first-story panel below the point where the lap splice of the vertical steel terminated. This portion of the panel had more effective vertical steel as it consisted of both the dowel and the reinforcement for which the dowel provided anchorage (see Figs. 39 and 40).

4.2.4 Test Specimen No. 4 (Model No. 2 - Fig. 20)

Model No. 2 was originally built and subjected to two tests by Klingner [1]. In the first of these tests, the model was tested as a bare frame subjected to a monotonic loading program. In the second test the same frame was infilled with fully grouted clay brick panels (ρ = 0.6%) in all three floor levels and subjected to a cyclic loading program. In this second test a combined first- and second-story panel failure was observed by Klingner with a sidesway mechanism consisting of plastic hinges at the base of the first story and at the top of the second story in both columns. Three plastic hinges occurred in the first-floor beam, one at each of the three beam-to-face-of-column connections. The repair of Model 2 for use in test No. 4 of the present study consisted of recasting the concrete cover on the columns as required, installing a new clay brick panel (ρ = 0.6%) in the first story, and repairing the second-story panel with grout since it was not sufficiently damaged to warrant panel replacement. The specimen was subjected to cyclic load inducing full displacement reversals (Fig. 20).

General observations:

(1) The failure mode involved only the first story with the frame forming a sidesway mechanism with hinges at the top and bottom in both columns after the failure of the first floor panel.

(2) Horizontal cracks extending completely across the first-floor panel developed early in the test. Locations of every major horizontal crack coincided with a mortar bed containing horizontal steel in the masonry (see Fig. 41).

(3) Cracking occurred but no significant relative displacement was observed at the frame panel interface.

(4) First signs of panel crushing were observed at the right hand side of the panel, see Fig. 42. This crushed zone spread completely across the panel and proceeded to enlarge somewhat (see Figs. 43 and 44).

(5) A considerable amount of debris was produced by spalling panel material.

4.2.5 Test Specimen No. 5 (Model No. 1, R2 - Fig. 21)

Model No. 1 was now repaired by removing the remaining first-story panel (from Test 2) and strengthening this first-story level by placement of special reinforcement and casting this level solid with 6 in. of concrete as previously discussed in Section 3.6. This strengthening was necessitated by the permanent residual deformation remaining in the right column along with evidence of some core damage. The resulting specimen for Test No. 5 was a 6-in. thick reinforced concrete strengthened first story, and clay brick panels ($\rho = 0.6\%$) in the second- and third-floor levels.

The specimen was loaded monotonically with one full displacement reversal. (Fig. 21)

General observations:

(1) The failure mode involved only the third story, the frame forming a single-story sidesway mechanism with hinges at the top and bottom of the third story in both columns, after failure of the infill.

(2) A horizontal crack was observed to extend completely across the third-floor panel approximately 2 in. from the top of the panel. This crack was very significant as it evidenced poor shear transfer across this crack leading to locally concentrated forces imposed by the columns transmitting shear to each side of the panel adjacent to this crack. (Fig. 45)

(3) Crushing was observed at the top right corner of the third-floor panel. (Figs. 45-47) Nearly vertical cracking was observed in the same panel adjacent to the left column. Relative lateral displacement was observed across the horizontal crack previously mentioned.

(4) Crushing was observed at the top of the panel across the horizontal crack previously observed in this region. This was accompanied by further crushing and increasing crack widths on the south and north sides of the column, respectively (Figs. 46 and 47).

4.2.6 Test Specimen No. 6 (Model No. 1, R3 - Fig. 22)

After the failure of the third-story panel in Test 5, the remaining panel material was removed, the column cover recast, and the third floor infilled with a 2-in. thick cast in place reinforced concrete (R/C) panel ($\rho = 0.6\%$). Thus, for Test 6 the subassemblage had a 6-in. R/C solid first story, clay brick ($\rho = 0.6\%$) in the second story and 2-in. R/C ($\rho = 0.6\%$) in the third story. The specimen was subjected to a cyclic loading program. (Fig. 22)

General Observations:

(1) The failure mode was a single-story mechanism involving only the second story. This mechanism was triggered by sliding shear of the infill followed by its crushing.

(2) Cracking was uniformly distributed throughout the second-story panel.

(3) Failure was initiated by crushing at the bottom of the second-story panel at the beam panel interface. Panel material began to spall along this interface accompanied by some crushing of panel material in the lower corners of the panel.

(4) On continued displacement reversals panel material continued to be spalled by interaction with the columns, the effect of which is shown in Fig. 48.

(5) The effective reinforcement percentage in this panel was greater than 0.6%, as dowels extended up from below approximately 12 in. and down from above approximately 12 in., leaving a 4-in. strip in the midpanel region when the vertical steel percentage was actually the design value.

4.2.7 Test Specimen No. 7 (Model No. 2, R1 - Fig. 23)

The previously failed first-story panel from Test 4 was removed, and the column cover was recast in this first-story region. This bay opening was now infilled with a fully grouted clay brick panel (ρ = 0.15%). Thus, for this test the infill panels in the subassemblage consisted of three clay brick panels, first story ρ = 0.15%, second- and third-stories ρ = 0.6%. The specimen was subjected to a cyclic loading program. (Fig. 23)

General observations;

(1) Failure occurred involving only the first story, the frame forming a sidesway mechanism with hinges at the top and bottom of the first story in both columns.

(2) Very early in testing, a horizontal crack was observed to

extend almost completely across the first-story panel. This crack coincided with the location of the cut-off point of dowels splicing vertical panel steel. Significant relative lateral displacements and subsequent crushing was observed across this crack (see Figs. 49 and 50).

(3) A spiral steel fracture occurred on the left column, the occurrence of which was aggravated by the previously mentioned horizontal crack meeting this column, which introduced a significant shear force concentration at this point (see Figs. 51 and 52).

(4) As loading of the specimen was continued, shear deformation in the left column concentrated in the spiral fracture area imposing very large displacements across the zone of now essentially unconfined concrete, causing the column core in this region to degrade quickly. The core of this column in the spiral fracture region was observed to have crushed, with the longitudinal steel having buckled. At this point, the plywood diaphragm, which was shored in position with 2 by 4 in. (50.8 mm x 101.6 mm) wood studs under the first-floor panel to support the air mattress used to balance the dead load of the panel, was interacting with frame due to the unexpected extreme vertical displacements encountered. An unknown but significant portion of the axial load of the left column was now carried by this plywood 2 by 4 in. stud system.

4.2.8 <u>Test Specimen No. 8</u> (Model No. 3, R1 - Fig. 24)

For use in Test No. 8, the failed concrete block first-story panel from Test 3 was removed, and the cover on the first-story columns was recast. The first story was then infilled with a new concrete block panel (ρ = 0.6%). No repair was necessary to the second- and third-story panels.

Thus the specimen for Test 8 had a virgin concrete block panel (ρ = 0.6%) in the first story, and lightweight concrete panels (ρ = 0.6%) in the second and third floors.

The specimen was loaded with a cyclic loading program. (Fig. 24)

General observations:

(1) Failure occurred involving only the first-story panel; this was triggered by sliding shear and then crushing of the infill. Finally the frame formed a sidesway mechanism with hinges at the top and bottom of the first story in both columns.

(2) A horizontal crack consisting of different segments in the same horizontal mortar bed and ultimately becoming a continuous horizontal crack approximately 10 in. below the first-floor beam began to form and subsequently propagated completely across the first-story panel. The location of this crack coincided with a mortar bed containing horizontal steel. Significant relative lateral displacement was observed across this crack in addition to spalling of material along the crack. Figures 53, 54 and 55 show this crack in initial, intermediate and advanced stages.

Spalling of masonry continued along this horizontal crack, the damage aggravated by displacement reversals. Spalled masonry began to fall free from the panel producing a very large horizontal gap completely across the panel, as well as a very large amount of debris (see Figs. 56, 57 and 58).

(3) The spiral steel on the left column fractured in the first story, concentrating shear deformation in this region of the column (see Fig. 59). The specimen was then returned to a zero displacement position and unloaded.

4.2.9 Test Specimen No. 9 (Model No. 3, R2 - Fig. 25)

After the first-story panel failure and the first-story spiral steel fracture which occurred on the left column during Test 8, the subassemblage was repaired as follows. Spalled cover along with the core in the region of the spiral fracture of the left column was removed. Care was taken to straighten the longitudinal steel. New spiral steel was lap spliced to the spiral in the region of the spiral fracture. The column was then formed, and this section of the core along with the column cover was recast. The cover was also recast on the right column.

Thus the specimen for Test 9 consisted of lightweight concrete panels ($\rho = 0.6\%$) in the second and third stories. There was no infill panel in the first-story level. The specimen was subjected to cyclic loading with full displacement reversals (Fig. 25).

General observations:

(1) The first story was a soft story and most of the deformation was concentrated at this level, even in the initial elastic cycles.

(2) The sidesway mechanism observed was a single-story mechanism with plastic hinges at the top and bottom of the first story in both columns.

(3) A spiral steel fracture occurred in the mid-portion of the right column, followed by a spiral steel fracture on the left column, (see Fig. 25).

4.2.10 Test Specimen No. 10 (Model No. 3, R3 - Fig. 26)

After spiral steel fractures in both first-story columns of Model No. 3, R2, repair of this model was accomplished by strengthening the first-floor level, casting it as a solid 6-in. thick panel with additional reinforcement (see Section 3.6).

Thus the subassemblage for this test consisted of a 6-in. reinforced concrete first floor, and lightweight concrete panels ($\rho = 0.6\%$) in the second- and third-floor levels.

The specimen was subjected to a cyclic loading program. (Fig. 26)

General observations:

(1) Failure occurred in the second-story panel forming a sidesway mechanism consisting of plastic hinges in the second-story columns only. This mechanism was triggered by crushing of the infill.

(2) Failure was initiated by crushing at the bottom left corner of the second-story panel. From this initial area, crushing propagated along the lower beam panel interface and then up into the mid-panel region and horizontally across to the right column (see

Fig. 60).

(3) The top column hinge in both columns was formed at some distance from the bottom level of beam. This was caused by interaction of columns with still intact sections of the upper part of the panel, thus decreasing the distance between column hinges and increasing the shear force transferred through the columns.

(4) On continued deformation reversals, crushing continued in the panel and a zone developed across the panel in which no panel material remained (see Fig. 61).

4.2.11 Test Specimen No. 11 (Model No. 3, R4 - Fig. 27)

After Test 10, a new lightweight concrete panel (ρ = 0.6%) was installed in the second-floor level of Model 3. Thus the subassemblage had lightweight concrete panels (ρ = 0.6%) in the second- and third-floor levels, and a strengthened 6-in. thick first story. The specimen was subjected to a monotonic loading program. (Fig. 27)

General observations:

(1) After initial crushing of the infill at the second story, the failure occurred in the second-story forming a side-sway mechanism consisting of plastic hinges in the second-story columns only.

(2) The failure sequence was very similar to Test 10 with crushing beginning in the lower left corner of the second-story panel, propagating up into the panel and horizontally across to the right column (see Figs. 62, 63 and 64).

(3) The position of plastic hinges in the column was significantly affected by panel presence, the hinge locations being almost identical to the positions observed in Test 10.

4.5.12 Test Specimen No. 12 (Model No. 1, R4 - Fig. 28)

After Test 6, the cover of the second-floor columns was recast, and this story level was then infilled with a clay brick panel, (ρ = 0.15%). Thus the subassemblage for this test had a 6-in. thick reinforced concrete first story, a fully grouted clay brick (ρ = 0.15%) panel in the second story, and a 2-in. thick reinforced concrete panel (ρ = 0.6%) in the third-story level. The specimen was subjected to a monotonic loading program. (Fig. 28)

General observations:

(1) Failure occurred involving only the second story, the frame forming a single-story sidesway mechanism with hinges in the second-story columns.

(2) Crushing of the second-story panel began in the lower left corner adjacent to the first-floor beam. This crushing continued, reducing the shear transferred from the second-story panel into the first-floor beam. Therefore the left column was subjected to severe shear and distortion due to the relative displacement between the beam and panel occuring after the onset of crushing. This is evidenced by the shear crack which subsequently developed at the base of the second-story column. (See Figs. 65 and 66, note particularly the relative displacement of the vertical lines drawn on the panel in the last photograph.)

(3) The column spiral at the base of the left second-story column fractured, causing an immediate decrease in lateral load capacity of approximately 11.2 kips. (Fig. 28)

4.2.13 <u>Test Specimen No. 13</u> (Model No. 2, R2 - Fig. 29)

After the severe first-story column damage inflicted on this specimen during Test 7, it was necessary to strengthen the first-story level as discussed in Section 3.6 to make the model suitable for use in this test. Thus, for Test 13 the specimen had a 6-in. thick reinforced concrete first story and clay brick panels (ρ = 0.6%) in the second- and third-story levels. The specimen was subjected to a cyclic loading program. (Fig. 29)

General observations:

(1) Failure occurred in the third story. It was triggered by shear sliding failure of the panel. This lead to the frame forming a single-story sidesway mechanism consisting of hinges at the top and

bottom of the third-story columns.

(2) Panel cracking was very well distributed in the second- and third-story levels. Cracking at the frame-panel interface along both panel sides and the panel bottom was observed in the third-story level early in testing.

(3) Failure was initiated by sliding at the bottom of the third-story panel at the beam panel interface. Crushing of both lower corners of the panel subsequently occurred along with spalling along the beam panel interface and up both sides of the panel adjacent to the columns. (See Figs. 67, 68 and 69.)

4.2.14 Test Specimen No. 14 (Model 2, R3 - Fig. 30)

Following the third-story failure of the panel in Test 13, Model 2 was repaired by recasting the cover on the third-story columns and then casting a 2-in. reinforced concrete panel (ρ = 0.6%) in the third-story level. Thus the subassemblage for this test had a 6-in. thick reinforced concrete first story, a 2-in. thick reinforced concrete (ρ = 0.6%) third story, and clay brick panel (ρ = 0.6%), the lower boundary of which was repaired with grout following the combined first- and second-story failure obtained by Klingner in testing this model with all virgin clay brick panels. The specimen was subjected to a monotonic loading program. (Fig. 30)

General observations:

(1) After an initial sliding shear failure of the infill and its crushing, the final failure occurred in the second story, forming a side-sway mechanism consisting of plastic hinges in the second-story columns only.

(2) Shear crushing occurred at the top left corner of the second-story panel forming a zone 2 in. (5 cm) below the second-floor beam which propagated across the panel and was met by a horizontal crack forming in the same mortar bed, having originated at the other side of the panel. This horizontal crushed zone subsequently extended completely across the panel, and crushing occurred at the right side of

the panel caused by the concentration of shear force at this location due to the poor transfer of shear across the horizontal crack. (Figs. 70-71)

(3) The positions of plastic hinges in both columns were affected as these positions were constrained by the ability of the frame to crush or pull away from the panel, the former being governed by the compressive strength of the panel and the latter by the panel reinforcement, an effect of the frame-panel anchorage.

4.2.15 Test Specimen No. 15 (Model No. 4, Virgin - Fig. 31)

This frame specimen was constructed as a bare frame with no steel projecting into the bay openings. Thus the specimen for this test is a completely bare frame with no infill panels at any floor level. The specimen was loaded with a cyclic loading program. (Fig. 31)

General observations:

(1) The observed failure mechanism was, as expected and according to the design philosophy, strong column-weak girder. Plastic hinges occurred in the columns only at the base and in the beams at every beam-face-of-column connection, a total of 11 locations. The resulting sidesway mechanism involved all three floor levels.

4.2.16 Test Specimen No. 16 (Model No. 5, Virgin - Fig. 32)

This frame specimen incorporated two layers of welded wire fabric (identical to that used in the panel as reinforcement) cast in place with the frame to anchor the panel steel. The frame was infilled with three panels consisting of split brick with a welded wire fabric mat covered with a cement mortar (stucco) on each side of the panel (ρ = 0.4%). Mesh orientation was 90° for both the panel mesh and the anchorage mesh. (See Section 3.4 for fabrication details.) The final panel thickness was 2-1/2 inches. The specimen was loaded with a cyclic loading program. (Fig. 32)

General observations:

(1) The failure mechanism was a single-story mechanism with

plastic hinges at the top and bottom of the first-story columns. The failure was initiated by shear cracking of the infill followed by shear crushing of this infill.

(2) Interconnecting shear cracks in two directions began to form a shear crushing type failure resulting in a horizontal failure surface approximately 12 in. below the first-story beam in the mid-panel region. Significant relative displacements were observed across this zone and, with increasingly large displacements, the welded wire fabric began to have individual wires breaking in tension (see Figs. 72 and 73).

(3) A horizontal crack began to develop in the second-story panel but, as damage worsened in the first-story panel, the strength and stiffness of the subassemblage was reduced sufficiently in the first story level so that damage did not worsen in the second floor beyond the development of this initial failure plane.

(4) The anchorage of the panel to the frame was excellent due to the very well distributed steel placement. However, upon panel removal after this test, some of the mesh cast into the frame was observed to have been sheared off by relative displacement (sliding) between the frame and panel. In addition, along the height of the columns some of the anchorage steel failed in tension.

(5) A relatively small amount of debris was produced during this test.

4.2.17 Test Specimen No. 17 (Model No. 5, R1 - Fig. 33)

The first-story level, the panel of which was heavily damaged from Test 16, was removed. The columns were recast as necessary and anchorage wire fabric was mended as required by brazing. The first story was then infilled with a panel consisting of split brick with welded wire fabric reinforcement using the same construction details and methods as were used for infilling the virgin frame in Test 16. The horizontal crack which developed through the whole infill cross-section in the second-floor panel from Test 16 was repaired by removing loose material at the panel surface and applying a layer of cement mortar over the now exposed wire fabric. The specimen was subjected to a monotonic loading program. (Fig. 33)

General observations:

(1) The horizontal crack in the second-story panel, which occurred in Test 16 and was repaired for the present test, occurred again at the same location, apparently due to inadequate repair of this second-story panel following Test 16. This horizontal crack should have been repaired by chipping away the damaged material completely through the cracked region and replacing this material with cement mortar, rather than by removing damaged material only at the surface and applying a new cement mortar cover. This ultimately proved to be of no major consequence as the second-story panel, even in this semi-damaged condition, was capable of sustaining sufficient lateral resistance to fail the first-story panel. Thus, the sidesway mechanism attained was a single-story mechanism with plastic hinges in the top and bottom of both first-story columns.

(2) Failure of the first-story panel was initiated by crushing along a horizontal band approximately 8 inches below the first-floor beam. Crushing along this horizontal band continued as the lateral displacement was increased (see Figs. 74-75, note the damage in the second-story panel).

(3) Relative slip between the frame and boundary was observed, particularly at the bottom of the second-story panel and at the top of the first-story panel, indicating a failure of good shear transfer at these locations.

(4) A relatively small amount of debris was produced during this test.

4.2.18 Test Specimen No. 18 (Model No. 4, R1 - Fig. 34)

The bare frame from Test 15 was repaired by epoxy injection at all damaged sections, i.e., at beam-face of column connections (nine locations) and the base of both columns. The members of the frame were then drilled to attach an anchorage system for the panel reinforcement. This anchorage system consisted of steel plates attached to the beams with anchor bolts at 8 in. O.C. and to the columns with bolts at 4 in. O.C. Wedge anchors were used in the column and the third-story beam. The first- and second-story beams were drilled completely through, and nuts were secured to plates on both sides of the beam to secure anchorage plates for welded wire fabric (WWF) reinforcement anchorage (see Figs. 77-81). The WWF was placed with the reinforcement oriented at 45°. The specimen was loaded with a cyclic loading program. (Fig. 34)

General observations:

(1) The mode of failure was combined first-, second- and third-story panel failure with plastic hinges forming in the first-, second- and third floor beams at the beam-face of the column connections and at the base of both columns.

(2) Separation between the panel and bounding frame occurred very early in the test, initially in the first-story panel and then in the second-story panel and finally in the third-story panel. Very large relative lateral displacements were observed at the frame-panel interfaces, particularly in the first and second stories (see Fig. 76).

(3) Failure was controlled by the integrity of the frame-panel anchorage system. The welded wire fabric draped around the anchorage plate fractured at numerous locations where the fold occurred.

V. EVALUATION OF RESULTS

5.1 Introductory Remarks

The effect of the loading program, the type of infill material, and the type and arrangement of panel steel and anchorage system, will be evaluated in this section. The evaluation of these parameters is necessary in order to provide an adequate basis on which to make design recommendations. The significance of these parameters should become clear with the evaluation performed in the various portions of this chapter.

5.2 Effect of Loading Program, Monotonic vs. Cyclic

In order to obtain a good understanding of the effect the loading program plays in the response of the test specimens, it is necessary to compare tests in which this is the only parameter varied. The following pairs of test specimens appear suitable for comparison: 1 and 2, 3 and 8, 16 and 17, 6 and 14, 10 and 11, and finally, 5 and 13. The first three of these pairs failed by a first-story-failure mechanism, the next two pairs in a second-story mechanism, and the last pair in a third-story mechanism.

5.2.1 Test Specimens Nos. 1 and 2 (Fig. 17 and 18)

The first-story panels tested for both Specimens 1 and 2 were *unreinforced* but fully grouted, clay brick. These first story panels were virgin panels at the time of testing. The only parameter intentionally varied in these two tests was the loading program, Specimen 1 being loaded monotonically and Specimen 2 cyclically.

Specimen 1 failed by crushing of the first story panel at about midspan of the diagonal corresponding to the compression strut. No significant relative displacements (sliding) were observed between the panel and bounding elements of the frame (see Fig. 35).

Specimen 1 attained a peak load of 55.2 kips (245.5KN), an interstory yield displacement of .15 in. (3.8mm), and an interstory first-story displacement ductility of 19.5 with a strength reduction at the displacement corresponding to this ductility of 30 percent. (Fig. 17)

The first story panel of Specimen 2 (cyclic) separated from the bounding elements of the frame very early in the test and the subsequent failure was controlled by sliding and crushing of the panel perimeter to accommodate the frame displacement around the panel. This early panel separation was certainly aggravated by the cyclic loading program, but also by the presence of low strength boundary grout (below desired strength) anchoring the panel of Test 2 in the bay opening. However, given the relative ease with which panels in subsequent tests were observed to separate from the bounding elements of the frame when subjected to cyclic loading programs, it is likely that the presence of this low strength grout did not alter the behavior exhibited by this panel. This is because when separation of the panel occurs in a case such as this, where the panel is unreinforced and hence no dowel action is available, the only mechanisms for transmitting lateral forces through the panel are friction and aggregate interlock acting between the panel and frame, and by strut action of the panel acting in compression through opposite corners. The frictional and aggregate interlock mechanisms degrade quickly with the cyclic loading program, and in this test when the strut mechanism began to develop, crushing occurred alternately in the lower corners, with damage propagating forming a crushed zone along the entire panel bottom. The right side of the panel was also crushed as the panel proceeded to slide along the frame boundaries (see Figs. 37 and 38). As the displacements through which the frame was cycled were increased, crushing in these two zones propagated.

Specimen 2 attained a peak load of 35.3 kips (157. KN), an interstory yield displacement of .10 in.(2.54mm) and an interstory first-story displacement ductility of 39.0 with a strength reduction at this ductility of 10.0 percent. The reader is referred to Fig. 18 where it is observed that the panel suffered a rather significant strength loss initially, as the first cycle following the yield cycles exhibits a strength reduction of 35.0 percent. The strength subsequently increases at successive displacement peaks. Inspection of Fig. 82 and comparing curves No. 2 (this specimen), and No. 9 (soft-first-story frame mechanism), shows that the resistance being obtained for this specimen is a few percent greater than that of the first-story frame mechanism. This slightly greater strength is provided by the panel compression strut which picks up some load as the shear distortion in the first-story level reaches a sufficiently large value. The increase in strength is limited as panel material continues to crush while the compression strut is loaded. Thus the ductility values can be misleading if not correctly interpreted, as a small yield displacement at low strength is attributable to the poor behavior of this panel under cyclic loading, and the consequent strength and deformation capacity are provided by the frame alone.

Comparison of Specimen 2 with the complete bare frame (Specimen 15) response envelope (Fig. 82) shows that Specimen 2 was afforded a substantial increase in lateral load capacity on account of forcing a soft-story mechanism to occur (similar to Specimen 9). Note, however, that the displacement plotted for Specimen 15 is the tip displacement at the top of the specimen (not the first-floor interstory displacement). Since Specimens 2, 9, and 15 were cycled to approximately the same tip specimen displacements, it is evident that most of the deformation is concentrated in the first-story level of Specimens 2 and 9, thus requiring much larger inelastic rotations in local regions to sustain comparable tip specimen displacements relative to Specimen 15. The increase in strength provided by forming a soft-story frame sidesway mechanism is not necessarily beneficial, as brittle failure of frame elements due to shear failure may occur (particularly in the columns) if the frame elements are not adequately designed and constructed for sufficient shear and inelastic rotation capacity.

Concluding remarks:

For Specimens 1 and 2 it is seen that the difference in the loading program alters the basic mechanism by which the panel fails. It is also important to note that an air mattress supported by a shored plywood diaphragm was used under the first-story panels in both tests to balance the panel dead load. The presence of this out-of-plane support system is believed to have retarded significantly the degradation of both panels and hence the maximum computed ductilities for each of the two tests are misleadingly high. Without this support system it is believed that both first-story panels, or significant portions thereof, would have fallen out-of-plane almost immediately after yield of the specimens, the result being immediate conversion to a soft-first-floor bare frame mechanism.

It is realized that testing of the subassemblage horizontally does subject the panel to having to support its own dead load out-of-plane if an air mattress system is not used. However, it is believed that in the actual prototype structure, no significant increase would be achieved in out-of-plane stability (due to the panel being vertical) on account of concurrent out-of-plane accelerations the panel would be subjected to, in the case of actual earthquake ground motions.

The main point, therefore, is the change in type of mechanism from a complete bare frame mechanism to a soft-first-story mechanism. Note that when the infill is not reinforced and not anchored to the building frame, the cyclic loading program has a very great effect in reducing the peak strength from 55.2 kips to 35.2 kips, a reduction of 36 percent. Consequently, tests of unreinforced masonry infills under monotonically increasing load and/or deformation may provide misleading results regarding its behavior under a more generalized type of loading.

5.2.2 Test Specimens Nos. 3 and 8 (Figs. 19 and 24)

The first story panels tested for both Specimens 3 and 8 were fully grouted concrete block with 0.6% reinforcement. The first-story panel of Specimen 3 was part of the original Klingner [1] test series and was subjected to one previous cyclic loading program having a peak load of approximately 60 kips, the resulting failure mechanism involving the second- and third-floor levels. The first-floor panel of Specimen 8 was a virgin panel at the time of testing. Specimen 3 was loaded monotonically and Specimen 8 cyclically.

Specimen 3 (monotonic) failed by crushing of the first-story panel acting as a diagonal compression strut, horizontal cracking occurred in several of the panel mortar bed joints, but none of these cracks extended more than half the distance across the panel and hence did not form a single weak section. Thus performance of Specimen 3 was governed principally by the crushing resistance of the first-floor panel along its diagonal.

Specimen 3 attained a peak load of 67.9 kips (302. KN), an interstory yield displacement of 0.28 in. (7.1mm), and interstory first-story displacement ductility values of 6.7 with a strength reduction of 30% and 8.1 with a reduction of 35%.

In Specimen 8 (cyclic) a horizontal crack began to form segmentally in different portions of the same mortar bed in the first-floor wall panel. These different segments connected forming a continuous horizontal crack which extended completely across the first-story panel approximately 10 in. below the first-floor beam. This is significant as shear across this section had to be carried by the boundary elements (columns) and in the panel region by aggregate interlock, friction and dowel action. After several cycles it was evident that shear transfer across this horizontal crack was poor, as large relative displacements (sliding) were observed across this crack. This caused a shear concentration in the boundary columns at both sides of the panel where they met this crack. Panel material began to spall along the entire length of the crack and crushing of panel material began to occur adjacent to both columns. A spiral steel fracture occurred on the left column in line with the horizontal orientation of the crack, thus, failure of Specimen 8 was governed by the shear capacity of the first-floor panel across the weak section where this horizontal crack formed, and the cyclic shear capacity of the columns.

Specimen 8 attained a peak load of 46.7 kips (207.7KN), an interstory yield displacement of 0.14 in.(3.6mm), and interstory first-story displacement ductility values of; 12.4 with a 19% strength reduction, 16.9 with a 21.5% reduction, 19.9 with a 39.9% reduction, and 24.3 with a 50% reduction.

Concluding remarks:

The first-story panel of Specimen 8 failed prematurely due to development of a horizontal crack which was incapable of transmitting sufficient shear force to fully develop the compressive capacity of the panel along its diagonal strut. The sliding shear failure of this surface was certainly aggravated by the cyclic loading program, as displacement reversals across this cracked region had a tendency to quickly degrade the mechanisms carring shear across this crack, namely; friction, dowel action, and aggregate interlock.

The higher ductility values observed in Specimen 8 and lower reductions in peak strength are easily explained by noting that the premature failure of the first-story panel of Specimen 8 (relative to Specimen 3) resulted in a lower yield displacement value at a lower yield force than would be attained otherwise. The lower yield force results in the subassemblage having a smaller percent strength reduction necessary to attain the bare frame mechanism lateral capacity, and the low yield displacement results in higher ductility values at given values of lateral displacement. See Fig. 83 for the response envelopes of Specimen 3 and 8.

5.2.3 Test Specimens Nos. 16 and 17 (Figs. 32 and 33)

Panels tested for Specimens 16 and 17 consisted of solid split brick, both sides reinforced with welded wire fabric (WWF) in a layer of cement stucco. Anchorage for the panel reinforcement for both tests was provided by WWF cast in place in the beams and columns as required. Test 16 was loaded cyclically and Test 17 monotonically.

In Specimen 16 failure was initiated by interconnecting shear cracks in two directions forming a shear crushing type failure resulting in a horizontal failure surface approximately 12 in. below the first story beam in the mid panel zone. (See Fig. 72 and 73.) This region then propagated completely across the panel and formed a continuous horizontal failure surface across which large displacements were observed. Crushing of panel material occurred at both sides of the panel adjacent to where this crack met the columns. Thus failure of Specimen 16 was governed by the cyclic shear capacity of the first-floor panel.

During test of Specimen 16, some horizontal cracking occurred in the second-story level, but did not propagate and never actually initiated failure of this floor level. The second-story panel was only repaired, but not replaced, following the test of Specimen 16. This is important to note as the same model was used in Specimen 17 with this repaired second-story panel being a component of the structural subassemblage. The significance of this will be discussed below with the consideration of Specimen 17.

Specimen 16 attained a peak load of 71.0 kips (316. KN), an interstory yield displacement of 0.30 in. (7.6mm), and interstory first-story displacement ductility values of: 4.2 with a 14% strength reduction, and 7.3 with a 32% reduction.

In the test of Specimen 17, the repaired second-floor panel of the subassemblage quickly recracked and showed visible distress early in the test, evidencing inadequate repair of this second-story panel following test of Specimen 16. However, sufficient shear was capable of being transmitted across this zone in the second-floor level to fail the first-story panel. The ability of the second-floor panel to supply adequate resistance in its damaged condition is partially explainable by the lower stucco strength present in the first-floor panel (3.26 ksi, 22.5MPa) relative to that in the second-floor panel (5.29 ksi, 36.5 MPa), and also explainable by the higher moment/shear ratio in the first-floor panel due to its lower position in the subassemblage. In addition, the monotonic loading program did not tend to degrade the shear transfer mechanisms operating across the damaged portion of the second-floor panel (friction, aggregate interlock and dowel action). A cyclic loading program with its resulting deformation reversals would have degraded these mechanisms considerably. Thus, since the second-story panel did maintain sufficient strength under monotonic loading to fail the first-floor level, no substantive difference would be expected from the first-story panel response of this test if a less damaged second-story panel had been present in the subassemblage.

Failure of the first-story panel of this test was initiated by shear crushing along a horizontal band approximately 8 inches below the first-floor beam. This location coincided with the end of the welded wire fabric (WWF) splice anchoring the WWF of the panel to the WWF cast in place in the frame. Crushing continued along this zone and then down at approximately 45° angle to the base of the left column as the lateral displacement increased (see Figs. 74 and 75).

Specimen 17 attained a peak lateral load of 61.3 kips (272.7 KN), an interstory yield displacement of 0.36 in. (9.1mm), and an interstory first-story displacement ductility value of 3.1 with a 6% strength reduction and a ductility of 6.3 with a 12.4% strength reduction.

Concluding remarks:

The failure of both Specimens 16 and 17 was controlled by a shear crushing mechanism operating through approximately the same zone in the first-story panel of both specimens. Thus the different loading programs did not alter the basic mechanism of panel failure.

Specimen 17 (monotonic) did have significantly less peak lateral resistance than Specimen 16. This is an unexpected result when the failure of both specimens is controlled by the same mechanism. This result is explainable by noting that the cement stucco cover of the first-story panel of Specimen 16 had a compressive strength of 5.39 ksi (37.2MPa) and that of Specimen 17, 3.26ksi (22.5MPa). Although this variation in material properties caused Specimen 17 to attain a lower peak lateral resistance than would otherwise be expected, it did have a beneficial effect on the specimen's post yielding response. That is, Specimen 17, after reaching its maximum resistance, exhibited a much smaller strength reduction in lateral load capacity relative to Specimen 16 corresponding to interstory displacements at comparable ductilities. This is accountable to both: (1) The usually smaller strength reduction associated with lower strength materials; and (2) the effect of loading history (less degradation occurs under monotonic loading program). (See Fig. 86.)

The important point is that even with the low strength first-floor stucco, the infill provided an increase in initial stiffness of 169% and an increase in strength of 155%. Furthermore, even under a cyclic loading program, the specimen offers considerable dissipation of energy and excellent containment of debris (debris is contained primarily within the panel so as not to cause a hazard by falling debris or blockage of passageways required for emergency exit) as was observed up to an interstory displacement of 2.4 in. (interstory drift = .067).

5.2.4 Test Specimens Nos. 6 and 14 (Figs. 22 and 30)

The second-floor panels tested in Specimens 6 and 14 were fully grouted clay brick panels with 0.6% reinforcement in each direction. Both panels were part of the original Klingner test series [1], and both panels were subjected to several loading programs each during the current investigation as a component of the structural subassemblage. Thus neither is truly representative of a virgin specimen. Specimen 6 was loaded cyclically and Specimen 14 monotonically.

Test 6 failed by sliding shear occurring at the bottom of the second-floor panel. As displacements increased, spalling at the beam panel interface occurred and both sides of the panel began to crush starting in the lower corners and working up the sides of the columns alternately as the loading direction varied cyclically forming a second-story mechanism (see Fig. 48).

Specimen 6 attained a peak load of 80.0 kips (356.KN), an interstory yield displacement of 0.27 in. (6.9mm) and interstory second-story displacement ductiliy values of; 2.79 with a 3.26% strength reduction, 3.9 with a 19.8% reduction, and 16.4 with a 56.2% reduction.

The failure of Specimen 14 was initiated by a sliding shear failure occurring at the top left panel corner (see Fig. 70). This was followed by horizontal cracking forming a continuous zone approximately 2 inches below the top of the second-story panel across which crushing and horizontal displacement was observed. Panel crushing also occurred adjacent to the right column from midheight of the second-story panel upward, caused by sidesway of the second-story column moving into the panel (see Fig. 71).

Specimen 14 attained a peak load of 83 kips (369.KN), an interstory yield displacement of 0.36 in. (9.1 mm), and interstory second-story displacement ductility values of 2.2 with a 1.4% strength reduction, 2.9 with a 28.9% reduction, 5.1 with a 40% reduction, and 8.4 with a 45.1% reduction.

Concluding remarks:

Specimens 6 and 14 failed by very similar mechanisms, each developing a critical section along a beam framing the panel, in one case at the top of the panel and in the other case at the bottom. Failure of both specimens was controlled by the shear capacity of the panel, the location of the failure surface being influenced by local imperfections present in the panels as well as by the high stresses produced at the boundary elements. The different loading programs in these two tests did not produce a significant difference in the failure of these specimens. Significantly more degradation is evident in the cyclically loaded specimen at large displacements (see Fig. 84).

The important point is the considerable increase in strength and initial stiffness offered over that of the bare-frame specimens, representing a 540% increase in interstory stiffness over the completely bare frame and an increase in peak strength of approximately 195%. The response of Specimens 6 and 14 were not significantly affected by the different loading programs up to an interstory displacement of 1.8 inches (45.7 mm).

5.2.5 Test Specimens Nos. 10 and 11 (Figs. 26 and 27)

The second-floor panels in both Specimens 10 and 11 were lightweight concrete with 0.6% reinforcement in both vertical and horizontal directions. The second-floor panel of Specimen 10 had been previously subjected to two cyclic and one monotonic loading programs as part of the structural subassemblage of Specimens 8, 9 and 3, respectively. The loads to which this panel were subjected in the previous tests were significantly below the second-floor panel's capacity and are not believed to have had a significant effect on the results of Specimen 10. The second-story panel of Specimen 11 was a virgin panel. Specimen 10 was loaded cyclically and Specimen 11 monotonically.

Specimens 10 and 11 were observed to fail in a very similar manner. (See Figs. 60, 61, 62, 63, and 64.) In both specimens failure was initiated by crushing of the infill which occurred in the bottom left corner of the second-story panel, followed by propagation of this crushing along the lower beam panel interface to approximately the center line of the bay. This zone then propagated up into the panel and then horizontally across the mid-panel region to the right column.

Specimen 10 (cyclic program) had a peak load of 93 kips (414. KN), an interstory second-floor yield displacement of 0.20 in. (5.1mm), and interstory second-floor displacement ductilities of 3.1 with a 13.7% strength reduction, 4.3 with a 24.5% reduction, 5.6 with a 54.4% reduction, and 6.6 with a 54.8% reduction.

Specimen 11 (monotonic program) has a peak load of 100.0 kips,(445. KN), an interstory second-floor yield displacement of 0.20 in. (5.1mm), (i.e., practically the same stiffness as Specimen 10), and interstory second-floor displacement ductility values of 3.1 with a 20% strength reduction, 3.7 with a 26.3% reduction, 6.0 with a 40% reduction, and 7.95 with a 50% reduction.

Concluding remarks:

The cyclic loading program is seen not to affect very much the failure mechanism observed under monotonic loading. Specimen 11 under a monotonic program of loading is seen to possess slightly larger ductility values with less strength reduction, which is as expected. (See Fig. 85.) In this case, the lateral load - interstory displacement curve of the critical story obtained under monotonic loading, can be considered as a good envelope of the hysteretic behavior under cyclic loading.

5.2.6 Test Specimens Nos. 5 and 13 (Figs. 21 and 29)

The third-story panels for both Specimens 5 and 13 were fully grouted clay brick with 0.6% reinforcement in each direction. Both panels were part of the original Klingner test series [1], and hence neither specimen was representative of a virgin specimen. Specimen 5 was loaded monotonically and Specimen 13 cyclically.

In Specimen 5 the third-story panel failed prematurely developing a continuous horizontal crack in a mortar bed approximately 2 in. below the top of the panel. Large relative displacements occurred across this crack evidencing poor shear transfer. Crushing occurred at the top right corner of the panel due to the concentration of shear at this location accountable to this crack. (See Figs. 45, 46 and 47.)

Specimen 5 had a peak load of 68.6 kips (305. KN), an interstory third-floor yield displacement of 0.38 in. (9.7mm), and interstory third-floor displacement ductility values of 2.0 with a 6.2% reduction, 2.6 with a 19.9% reduction, 5.3 with a 31.0% reduction, 6.6 with a 31.8% reduction, and 8.0 with a 38.3% reduction.

In Specimen 13 failure of the third-story panel was initiated by sliding occurring at the lower beam panel interface. This sliding caused the panel initially to be crushed beginning at the lower left corner. The lower corners of the panel then proceeded to be crushed alternately (depending upon the loading direction) and propagated upwards along the columns as the cyclic loading program continued. Crushing also propagated along the entire lower beam panel interface, and the panel began to crack and break up propagating from this lower beam panel interface moving upward into the panel due to interaction with the steel dowels (No. 2 bars) originally cast in place in the beams. (See Figs. 67, 68, and 69.)

Specimen 13 had a peak load of 76 kips (338. KN), an interstory third-floor yield displacement of 0.44 in. (11.2mm), and interstory third-floor yield displacement ductility values of 1.75 with a 19.3% strength reduction, 2.26 with a 48% reduction, 4.5 with a 49.5% reduction, 6.8 with a 56.6% reduction, and 9.0 with a 58.9% reduction.

It is interesting to note that the shear strength of these two specimens was somewhat smaller than those obtained in Specimens 6 and 14, which were of the same construction. The differences in overall behavior were not very large.

Concluding remarks:

The lower peak lateral resistance attained for Specimen 5 (versus Specimen 13) is other than would generally be expected. That is, with all other factors being equal, a monotonic loading program will generally result in higher peak lateral specimen resistance than cyclic loading programs. The deviation from this normally expected result may be explained as being due to the presence of a weak mortar joint at the top of the third-floor panel in Specimen 5. This weak section caused Specimen 5 to fail prematurely by a mechanism not controlled by the compressive capacity of the panel along its compression diagonal. Specimen 13 also failed by a mechanism not controlled by the diagonal compression strut, but by sliding occurring between beam and panel at the panel bottom. Thus the two failures are seen to be very similar, both being controlled by a weak horizontal surface, in the case of Specimen 5, a weak mortar bed between horizontal masonry courses at the panel top, and in Test 13, between the beam below and the first course of block in the third-floor panel. Even with the premature failure of Specimen 5, it is seen to have better post-yielding behavior than Specimen 13 (due to the greater degradation occurring under cyclic loading). See Fig. 88.

5.2.7 Conclusions Regarding Effect of Loading Program

It has been seen that of the six pairs of specimens considered, in four of these pairs, 6 and 14, 10 and 11, 16 and 17, 5 and 13), the failure observed was controlled by the same basic mechanism, irrespective of the difference in load program. In the remaining two pairs (1 and 2, 3 and 8) the specimen loaded cyclically failed prematurely, relative to the mechanism observed under monotonic load program. The observation that in four of the six pairs of specimens considered here failure was controlled by the same basic mechanism, does not imply that the effect of the cyclic vs. monotonic load program is negligible. The cyclic load program is seen to aggravate any potentially critical region which may be present in the panel due to imperfections or stress concentrations from various sources. Possible sources include local variations in material properties (such as a mortar joint), high stresses encountered due to lap splicing of steel reinforcement, stress concentrations at panel-boundary interfaces, and construction flaws such as poorly made construction joints between successive horizontal courses of masonry, as may be required due to a work stoppage. Additionally, the cyclic program has a greater tendency to follow preferred cracking orientations, particularly in horizontal mortar courses, a single joint of which was frequently observed to be cracked continuously across a panel from column to column, which rarely occurred under monotonic load program. Interconnecting shear cracking from the cyclic load program was more severe than unidirectional cracking experienced under monotonic load program, as the cyclically loaded panels tended to break up faster and the subsequent behavior was very dependent upon the ability of the panel steel to hold pieces of the panel together. The specimens loaded cyclically generally tended to yield at lower lateral force levels and at smaller yield displacement values than their monotonically loaded counterparts. Note that the reason for the variation of the two specimen pairs for which this generalization is not correct is easily explainable.

In Specimen pair 5 and 13 this is explainable by the weak horizontal mortar bed in Specimen 5, causing this specimen to yield at a lower lateral displacement and lateral force than Specimen 13. Note that the tangent stiffness of these two specimens is comparable. (Stiffness values given for all specimens are tangent stiffnesses computed at the positive 30 to 40 kip lateral force range, and for Specimen 5, it is before full development of this horizontal crack.) In Specimen pair 16 and 17, the mortar cover on the first-floor infill panel of Specimen 17 had a too low compressive strength and thus a detrimental impact upon the stiffness and strength (61.3k vs. 70.7k), (22.7 KN vs. 314.5 KN) of Specimen 17 relative to Specimen 16.

After a certain amount of interstory displacement, the lateral resistance of the specimens, particularly those subjected to a cyclic load program, tends toward the resistance of the soft-story-frame mechanism corresponding to the story in which panel failure has been observed. The lateral resistance usually remains somewhat higher than the corresponding soft-story-frame mechanism (unless severe column degradation occurs) due to the reduction in distance between plastic hinges occurring in the columns and the consequent increase in shear force transmitted through these elements.

5.3 Effects of Type of Infill

5.3.1 Clay Brick Infills (First Story Failure)

First the response of clay brick specimens failing by a first story mechanism will be considered. Figure 82 compares the response envelopes of the appropriate clay brick specimens. The response envelopes of Specimen 9 (in which only the second- and third-floor levels were infilled, producing a soft-first-story frame mechanism) and of the complete bare frame specimen are also included in this figure for comparison. It should be noted that the curves shown in Fig. 82 represent the interstory displacement, and not the total displacement at the top of the specimen, with the exception of Specimen 15, as shown in the figure.

Initially it would appear that there is significant scatter in the results obtained from these specimens. This is not the case when the results are examined in detail. First compare Specimens 1 and 4 in Fig. 82, not only are the initial stiffnesses* [187 k/in. (32.7 KN/mm) and 206 k/in. (36.1 KN/mm) for Specimens 1 and 4 respectively] and maximum strength [55.2 vs. 54.5 kips (245.4 vs. 242.4 KN)] of these two specimens very similar, but also the response envelopes up to approximately 1 in. (25.4 mm) lateral interstory first-floor displacement, are also very similar. The response of these two specimens, however, diverges considerably at displacements larger than 1 inch. This closely matched initial response and consequent divergence is explainable as follows: Specimen 1, in which the bricks were unreinforced, was loaded monotonically and hence did not experience the fast-panel deterioration associated with a cyclic load program acting on an unreinforced panel; the effect of the cyclic load program, as occurred in the case of Specimen 2 was previously discussed in Section 5.2.1. Specimen 4, where the infill panel is broken up as a consequence of the cyclic load program, had sufficient panel reinforcement (ρ = 0.6% for both vertical and horizontal panel steel) to hold the various fragments together. This resulted in very good response of the specimen under cyclic loading until gross panel deterioration from the cyclic displacement reversals spalled a continuous band of masonry horizontally

---

* The values of initial stiffness given herein were obtained by post frame-panel bond separation as explained in miscellaneous stiffness evaluation comments following Section 5.3.5.

across the entire panel, thus causing divergence from the response envelope of Specimen 1. That is, as this horizontal spalled zone developed across the panel (Fig. 43), there was no longer panel material available continuously along the compression diagonal, making mobilization of strut resistance impossible at attainable values of shear distortion. However, there was still a significant contribution being afforded by the panel to the lateral resistance of the frame, even with the panel in this severely damaged condition. This contribution was from the still intact portions of the panel occupying the corner regions of the frame. This material (anchored to the frame by the reinforcing steel acting as dowels) stiffened the corners of this first-floor bay opening and resulted in shortening the effective, or unsupported, length of the columns working in flexure. This behavior resulted in a decrease of the distance between plastic hinges in each of the columns and, therefore, an increase of the shear force transmitted by the columns, and thereby an increase in the lateral resistance of the first-story collapse mechanism. See Fig. 44 for a photograph of the column of Specimen 4, evidencing this stiffening type of behavior from interaction with the panel material in the frame corners. The subsequent drop in strength of Specimen 4 to below the envelope of the first-floor soft-story mechanism (Specimen 9), which occurred at a displacement of about 2 in. (50.8mm) is due to degradation in shear resistance of the columns, particularly the left column, due to the shorter distance between plastic hinges and the resulting greater curvature in that column. Note that the final load cycle in the test of Specimen 4 (Fig. 20) imposed an interstory first-floor displacement of $\pm$ 2.87 in. (72.9mm), which corresponds to an interstory drift of 0.080 for the 36 in. (914mm) story height of the model. This is a very large interstory drift, demanding an even larger plastic hinge rotation in the concrete columns, due to the shorter distance between plastic hinges.

The response envelope of Specimen 2, when compared to that of Specimen 4, shows the significant function that panel reinforcement and frame panel anchorage play in the specimen's response. Specimen

2 had a stiffness of 236 k/in.(41.3KN/mm), as compared to Specimen 1 [206 k/in. (36.1KN/mm)], Specimen 4 [187 k/in. (32.7KN/mm)], and Specimen 7[124k/in.(21.7 $\frac{KN}{mm}$)]. Thus the initial contribution of the unreinforced first-story panel of Specimen 2 (cyclically loaded) is even somewhat larger than that of a heavily reinforced panel such as Specimen 4. However, the maximum strength was considerably lower [35.3 vs. 54.5 kips (157. vs. 242.2 KN)] and the post-yield behavior is completely different. This is as expected, as without adequate panel reinforcement, when the specimen is subjected to a cyclic load input, the stiffness and strength degrade very quickly, and in this case approximates very closely the bare-frame response envelope at an interstory drift of about 1 in. (25.4mm). However, Specimen 2 exhibits slightly more strength than the bare frame envelope; this is due to that part of the panel remaining which requires additional force to crush it.

The response envelope of Specimen 7 is between the response of Specimen 2 and Specimens 1 and 4. (See Fig. 82.) Specimen 7 failed by a completely different mechanism than Specimen 2 (see Figs. 37, 38, 49, 50, 51, 52), evidencing that the light reinforcing used in Specimen 7, ρ = .15% corresponding to 12 in. (305mm) spacing to steel bars each way in the panel, provided sufficient dowel action to maintain adequate continuity between the bounding frame and the panel, but failed to provide sufficient continuity to significantly retard breakup of the panel. Note that Specimen 7 consisted of the repaired subassemblage from Specimen 4, the left column of which was previously observed to experience severe degradation, causing the lateral resistance of Specimen 4 to drop below that of the soft-story frame mechanism. In Specimen 7 when this same column was subjected to an interstory drift of about 1.3 in. (33.0 mm), its spiral reinforcing steel fractured; leading to a drop in its shear capacity (See Figs. 44 and 52) to below that of the soft-story frame mechanism at the first-floor interstory drift index of 0.036.

Concluding remarks:

The addition of an infill of clay bricks to a bare-moment-resisting frame with very ductile and specially shear reinforced members produced the following main effects:

(1) The reinforced infill increases significantly the initial stiffness of the complete bare frame from 35 k/in.(6.1KN/mm) to 206 k/in. (36.1KN/mm), which represents an increase of 488%. This increase is reduced when the bare frame first-floor interstory stiffness (without an infill panel) is taken as a basis of comparison (Specimen 9). In this case the increase in initial stiffness is 240%.

(2) The use of reinforcement in the infill did not contribute to a significant increase in the initial stiffness.

(3) The use of clay brick infill increased the maximum lateral resistance in cases of monotonically increasing load from 12.5 k (55.6KN) to 55.2 k (245.5KN) (342%) with respect to the complete bare frame and from 27.4 k (121.9KN) to 55.2 kips (245.5KN) (101%) when compared with the first-story bare frame.

(4) Due to the effect of cyclic loading in the case of an unreinforced infill, the strength increase was only from 12.5 to 35.3 kips (55.6 to 157.0KN) (182%) with respect to the complete bare frame and 27.4 to 35.3 kips (121.9 to 157.0KN) (28%) with respect to the first-floor soft-story frame (Specimen 9).

(5) Even in the case of cyclic loading with full reversal, the properly reinforced infill (Specimen 4) gives an increase of 209% in initial stiffness and a 101% increase in peak lateral resistance when compared to a frame with just a first-floor soft story. The increase is of 434% in initial stiffness and 336% in peak lateral resistance when compared with that of a complete bare frame.

(6) The average panel nominal unit shear stress was estimated to be 368 psi (2.54 MPa) in Specimen 4.

5.3.2 Clay Brick Infills (Second- and Third-Story Failures)

Figure 84 compares the response envelopes of clay brick specimens which failed in a second-story sidesway mechanism. Specimens

6 and 14 are observed to have very little difference in their overall behavior as shown by their response envelopes up to an interstory displacement of 1.5 in. (38.1mm) (interstory drift index = 0.042), as was previously concluded with the effect of the load program. Specimen 12 had significantly less peak lateral resistance and stiffnes [63.2k, 167 k/in. (281KN, 29 $\frac{KN}{mm}$)] than either Specimen 6 [80. k, 238 k/in. (355.8 KN, 41.7 $\frac{KN}{mm}$)] or Specimen 14 [83. k, 210 k/in. (369 KN, 37 $\frac{KN}{mm}$)]. This low strength and stiffness of Specimen 12 is most likely attributable to a variation in material properties, as the second-story panels of Specimens 6 and 14 were from the original Klingner test series and were approximately three-years-old at the time of testing, having had a long period of time to cure relative to the second-story panel of Specimen 12, which was newly constructed. No information regarding mechanical characteristics of materials was available for Specimen 12, and data available for Specimens 6 and 14 were from the original Klingner test series [1]. In spite of the smaller contribution of the infill in Specimen 12 to the lateral strength and stiffness relative to Specimens 6 and 14, it is still seen that this type of infill offers a substantial increase to the strength [63.2 k vs. 12.5 k (281.1KN, 55.6KN)], initial stiffness [167k/in. vs. 35 k/in. (29.2, 6.1 $\frac{KN}{mm}$)] and energy absorption and dissipation capacities of the complete bare frame structural subassemblage. While Specimens 6 and 14 had an average unit nominal shear stress in the panel at peak lateral resistance of 541 psi (3.73 MPa) and 561 psi (3.86 MPa) respectively, this average shear stress in Specimen 12 was 427 psi (2.94 MPa). Considering that the f'_m found by Klingner for the infill was 3500 psi (24.1 MPa) the observed average shear stress represents a strength of 7.2 $\sqrt{f'_m}$ (psi) (.597 $\sqrt{f'_m(\text{MPa})}$)

Figure 88 compares the response envelopes of the two clay brick specimens (5 and 13) which failed in a third-story sidesway mechanism. The response of these two specimens has been discussed previously with the consideration of effect of load program. It will only be pointed out here that the initial stiffness and strength of these two specimens compare favorably, having a maximum variation of 10 percent to an interstory displacement of 1.25 in. (31.7 mm) (interstory drift index = 0.035).

Specimens 5 and 13 had an average panel unit nominal shear stress at the peak lateral resistance of 463 psi (3.19 MPa) and 514 psi (3.54 MPa). Although these values are somewhat smaller than those obtained where failure occurs in the second story, they are very close. This indicates that the main parameter in the failure of the infill panel is the shear stress, and that the effect of bending stress is small in the second- and third-story.

Concluding remarks:

(1) The interstory stiffness of the frames infilled with clay brick panels failing in the second story, having an average of 205 k/in. (35.9KN/mm), and that of the specimens failing in the third story, having an average of 186 k/in. (32.6KN/mm), compare favorably with the initial stiffnesses observed with similar infilled frames failing in the first story, which had an average of 206 k/in. (36.1KN/mm). Thus the larger M/V ratio occurring at successively lower levels in the subassemblage does not significantly alter the initial interstory stiffness, or in other words, this stiffness is controlled by the shear deformation rather than flexure.

(2) Higher peak lateral resistances were observed in the second- and third-floor levels relative to the first. Of the specimens failing in a second-story panel sidesway mechanism, Specimens 6 and 14 had an average increase in peak lateral resistance of 48%, and Specimen 12 an increase of 15% relative to the first-floor panel failure (Specimen 4). The average increase obtained in peak lateral resistance of the specimens failing in a third-story panel sidesway mechanism was 31.5% relative to the first-floor panel failure (Specimen 4). Therefore, it appears that for the specimen failing in the second- and third-story, the moment did not affect the failure, while in the case of those specimens failing in the first story, the bending moment was high enough to affect the lateral resistance of this first story.

5.3.3 Concrete Block Infills

Figure 83 illustrates the response envelopes of the only two concrete-block specimens tested, both failing in a first-story panel mechanism. These two specimens have been compared previously under consideration of the effect of the load program, and the divergence of the response envelopes was explained as being due to the development of a horizontal crack in Specimen 8 precipitating failure of this specimen by a different panel mechanism than Specimen 3, i.e., a sliding shear failure vs. crushing of the diagonal compression strut. Specimen 3 developed a maximum average panel unit nominal shear stress of ν_u = 459 psi (3.16 MPa), and Specimen 8 a ν_u = 316 psi (2.18 MPa). The strength of Specimen 8 dropped to below the first floor bare frame (soft story) envelope due to a spiral steel fracture on the left column in the first-story level. This fracture occurred at an interstory drift index of 0.089 which can be considered as sufficiently high for infilled frame buildings of up to 11 stories.

The results obtained from Specimen 8 are very significant because they emphasize the following points:

(1) The critical importance of workmanship with regard to the peak lateral strength of the specimen, particularly when the specimen is subjected to cyclic load, including deformation reversals. The initial stiffness is not affected greatly by workmanship.

(2) In spite of the considerable reduction in strength observed in Specimen 8, the peak lateral resistance was still 70 percent higher than that offered by the bare frame soft first-story specimen.

(3) The importance of very ductile frame elements (beams and particularly columns). Brittle column behavior can lead to very sudden and catastrophic collapse, once panel failure has been initiated. In Specimen 8 column failure was observed (as a

result of severe loading from first-story collapse mechanisms sustained in this subassemblage during the test of Specimen 8, and in the previous tests as part of Specimen 3), resulting in a sudden drop of strength.

Concluding remarks:

Addition of an infill of concrete block produced the following main effects:

(1) The initial stiffness increased from 35 k/in. (6.1 KN/mm) for the complete bare frame to 212 k/in. (37.1 KN/mm) in the case of Specimen 3, or to 250 k/in. (43.8 KN/mm) in the case of Specimen 8. This represents an increase in stiffness of 506% to 614% for Specimens 3 and 8 respectively, relative to the completely bare frame.

This increase is smaller when compared to the first-floor soft story frame which had an initial stiffness of 60.5 k/in. and represents an increase of 250% to 313% for Specimens 3 and 8 respectively.

(2) The maximum lateral resistance increased from 12.5 kips (55.6 KN) for the complete bare frame to 67.9 kips (302. KN) for Specimen 3 and 46.7 kips (208. KN) for Specimen 8. This represents an increase in lateral load capacity of 443% for Specimen 3 and 273% for Specimen 8. With respect to the strength of the first soft story bare frame whose peak strength was 27.4 k (122. KN), this represents an increase of 148% and 70% respectively.

(3) Specimen 8 was observed to develop an interstory drift index of .089 before dropping below the capacity of the soft story frame mechanism (Specimen 9).

Specimen 3 was observed to develop an interstory drift index of .056, although it could have been loaded to a larger deformation, while maintaining a 78% increase in strength over the response of the soft first story frame envelope. At this interstory drift there was no evidence of severe damage to the frame elements, which means that the specimen could have sustained considerably more displacement without dropping below the Specimen 9 strength or load-interstory displacement curve.

5.3.4 Lightweight Concrete Infills (Second-Story Failures)

Figure 85 compares the response envelopes of the only two lightweight concrete specimens tested, Specimens 10 and 11. Both of these specimens were observed to fail in a second-story mechanism. Specimens 9 and 15 are also included in Fig. 85 for comparison. The overall behavior of the two specimens compares very favorably, with Specimen 11 (monotonic) having slightly higher peak strength and stiffness [100 k, 409 k/in. (445. KN, 72. KN/mm)]than Specimen 10 [92.7 k, 358 k/in. (412. KN, 63. KN/mm)]. This represents a 14% difference in initial stiffness and an 8% difference in peak lateral resistance. Specimens 10 and 11 developed an estimated maximum average panel unit nominal shear stress of ν_u = 626 psi (4.32 MPa), and ν_u = 676 psi (4.66 MPa), respectively. The response envelopes begin to diverge at an interstory displacement of approximately .9 in. (22.9mm) due to the faster degradation occurring under cyclic loading. This corressponds to an interstory drift index of .025.

Concluding remarks:

(1) The initial stiffness increased from 35 k/in. (6.1 KN/mm) for the complete bare frame to 358 k/in. (62.7 KN/mm) in the case of Specimen 10 and to 409 k/in. (71.6 KN/mm) for Specimen 11. This is an increase of 922% and 1068% for Specimens 10 and 11 respectively. When compared to the first-floor soft story frame (k = 60.5 k/in., 10.6 KN/mm), the respective increases in initial stoffnesses are 492% and 576% respectively.

(2) The maximum lateral resistance increased from 12.5 k (55.6 KN) for the complete bare frame to 92.7 k (417. KN) and 100 k (445. KN) for Specimens 10 and 11 respectively. This represents respective increases of 642% and 700%. When compared to the first-floor soft story frame, this represents increases of 238% and 264%, respectively.

(3) When the horizontal force-lateral displacement graphs (Figs. 26 and 27) are examined, it is observed that the response is almost perfectly elastic followed by a very rapid loss in

lateral load capacity. The available ductility of these specimens is suspect at large values of lateral displacement. However, the strength increase afforded to the subassemblage is so great that in practice it may be possible to place such infills in buildings so that earthquake ground motion is resisted elastically. It should be noted that the use of lightweight concrete infill panels will have significant cost disadvantages in practice if they are cast in place, and it would be preferable to use an actual shear wall type of construction. If the lightweight concrete panels are precast, the cost savings would be significant, but probably outweighed by the difficulty of obtaining good anchorage of the precast unit to the bounding frame.

5.3.5 Welded Wire Fabric Reinforced Infills

The welded wire fabric panels tested in Specimens 16, 17, and 18 were 2.5 in. (63.5mm) thick while panels tested in all other specimens had a 2.0 in. (50.8 mm) thickness. This makes direct comparison of the response envelopes of Specimens 16, 17, and 18 with those of other panel specimens misleading, because for a given value of lateral force there is a lower level of average panel shear. For this reason, two sets of response envelopes are given for Specimens 16, 17, and 18; one set defined by the lateral force-displacement relation (exacly as done for all other specimens), and the other is the first set of envelopes with the ordinate (horizontal force) multiplied by 2.0/2.5 to account for the difference in average panel shear in Specimens 16, 17, and 18. These two sets of response envelopes are referred to as unfactored and factored, respectively.

Figure 86 compares the unfactored response envelopes of welded wire fabric specimens. Specimens 16 and 17 were compared previously with the evaluation of the load program. The response envelope of Specimen 18 is seen to correspond very closely to those of Specimens 16 and 17, with some divergence occurring after a first-floor interstory displacement of 2 in. (50.8 mm) corresponding to a interstory drift index = 0.056. This divergence is not a surprising result, as in both Specimens 16 and 17 failure was initiated by shear crushing in the first-story panel, whereas in the case of Specimen 18, failure was controlled by the deterioration of the frame panel anchorage system. The close agreement of the response envelope of Specimen 18 to that of Specimens 16 and 17 is thus not an expected result, but demonstrates that similar increases in strength and deformation capacities are attainable with very different types of panel behavior.

Specimen 16 had an initial stiffness of 292 k/in. (51.1 KN/mm), Specimen 17, 118 k/in. (20.7 KN/mm) and Specimen 18, 203 k/in. (35.6 KN/mm). The difference in the initial stiffnesses of Specimens 16 and 17 (which had the same two mat WWF cast in place anchorage system) is accountable to the lower strength stucco on the first panel of Specimen 17 (3.26 ksi) (22.5 MPa) relative to Specimen 16 (5.29ksi) (36.5 MPa). This variation in material properties affected greatly the elastic in-plane stiffness of the panel, and hence the subassemblage.

Figure 87 consists of the factored response envelopes of Specimens 16, 17, and 18. These curves should be used for comparison with response envelopes of other panel tests.

Factored stiffness values (by 2.0/2.5) should also be used for comparison to other tests. These stiffnesses are 234 k/in. (41.0 KN/mm), 94 k/in. (16.5 KN/mm), and 162 k/in. (28.4 KN/mm) respectively for Specimens 16, 17, and 18.

Specimen 16 attained an average panel shear ν_u = 382 psi (2.63 MPa), Specimen 17 ν_u = 331 psi (2.28 MPa), and Specimen 18 ν_u = 310 psi (2.14 MPa) at peak lateral resistance.

Concluding remarks:

(1) In spite of the low stiffness and strength of the split brick used in these infills, the initial stiffness of the infilled frames was very similar to those obtained with clay bricks, even if the factored values are used.

(2) The unfactored peak strengths were in all cases higher than those obtained using clay bricks. The factored peak strengths were practically the same as that obtained with the clay bricks in which a higher percentage of panel reinforcement was used ($\rho = 0.6\%$ vs. $\rho = 0.4\%$). This is also confirmed by comparing the values of the average panel unit nominal shear stress [341 vs. 370 psi (2.35 vs. 2.55 MPa)].

(3) Analysis of the hysteretic behavior of Specimens 16 and 18 (Figs. 32 and 34) and comparison of such behavior with similar behavior obtained from Specimens 2, 4 and 7 (Figs. 18, 20, and 23), clearly shows that the energy absorption and energy dissipation capacity of the WWF infilled frames were as good or better than those obtained from reinforced clay brick infills.

(4) Considering the above observed mechanical behavior and the easier, quicker and more economical construction potential of the WWF infills when compared with all other types of infills used in this investigation, it is concluded that WWF infills similar to those used in this investigation offers great potential for seismic-resistant construction. This great potential is not only for the cases of design and construction of new buildings, but perhaps even more important, for cases of retrofitting existing buildings where bolted anchorage of the WWF seems to be an ideal solution.

5.4 Effect of Infills on the Building Dynamic Characteristics

The use of infills that interact with the building frame decreases its fundamental period T_1 computed neglecting the contribution of such infills. The problem is to determine the proper stiffness that should be used. This depends on the problem at hand. If the problem is to estimate the initial stiffness of the whole building when it will be subjected to just service excitations, the results show that the stiffness values given in this report are somewhat lower than the real initial tangent stiffness. If the building had been subjected already to moderate lateral excitations then the contribution of the infilled frame system to the natural period calculations should be based on the structural stiffness of the subassemblage after bond separation between the panel and frame occurs. This is because in the event of significant earthquake ground motion where the structural response of the infilled frame system may enter the post yield region of the response envelope, the structural period will have been modified by the occurrence of this separation, and hence the use of this bond separated stiffness in the calculation of the structures period should result in a more accurate estimation of the actual dynamic characteristics of the structure under a critical excitation.

It should be noted that most stiffness values presented in the text of this report for infilled frame specimens have been estimated as a secant stiffnesses from a 30 to 40 kip range (133.4 to 177.9 KN). The stiffnesses of some specimens have been calculated in the 20 to 30 kip range (89.0 to 133.4 KN) when excessive panel degradation had already occurred in the 30 to 40 kip range (133.4 to 177.9 KN), for example, Specimen 2. The values of the measured initial tangent stiffness and of the estimated effective stiffness are given in Table 3. The interstory stiffness of the 1/3-scale model of the prototype is actually twice that measured in the test of the corresponding specimen.

5.5 Conclusions from Experimental Studies

In summarizing the concluding remarks made in the evaluation of each of the main parameters considered in this chapter, as well as analyzing results obtained in Reference 1, it can be concluded that:

(1) The interstory lateral stiffness of bare moment resisting R/C frames is significantly increased by the addition of infills. The initial tangential interstory lateral stiffness of virgin infilled specimens was more than 10 times the similar stiffness of the bare moment resisting frame. Since this stiffness deteriorates very quickly at service lateral load, an effective interstory stiffness at service load level has been introduced. This effective interstory lateral stiffness of virgin infilled frames was 5.3 to 11.7 times the lateral stiffness of the bare frame, depending on the type of infill, the smallest being for clay brick infill and the largest for lightweight concrete infill.

This lateral stiffness does not seem to depend upon how the panel is reinforced, i.e., it is practically the same for unreinforced and reinforced infills. It appears, however, to be sensitive to how well the infill is made, particularly to the workmanship along the interfaces of the infills and the boundary frame elements. The minimum observed service lateral stiffness was that of Specimen No. 17, which consisted of a repaired specimen. For this case the service lateral stiffness was 3.4 times that of the bare frame. The lateral stiffness deteriorates with cyclic loading, particularly if it includes deformation reversals. The degree of deterioration depends upon the type of reinforcement of the panel, and particularly in the way that the infill is attached to the frame.

(2) The maximum lateral strength of the bare moment resisting R/C frame is significantly increased by the addition of infill. In case of virgin infilled specimens, the peak lateral strength was 4.8 to 5.8 times that obtained for the bare frame. For cases of repaired and/or retrofitted specimens, the peak strength was 2.8 to 8.0 times that of the bare frame, depending on the type of infill, the way that infill is attached to the frame, and the loading program to which it was subjected. The maximum lateral resistance has been obtained with lightweight concrete infills, and the minimum with clay brick. For cases of monotonically increasing lateral load, the peak strength does not seem to be affected very much by the amount of reinforcement used in the infill.

(3) Hysteretic behavior under cyclic loading depends upon the type of infill, the amount and arrangement of reinforcement and the way that the panel is attached (anchored) to the frame. The cyclic loading of unreinforced infills leads to considerable deterioration in stiffness and strength when compared with the values observed in monotonic loading.

The peak strength under cyclic loading is in general somewhat smaller than that obtained under monotonic loading, and deteriorates as the severity of deformation and number of cycles increases, but remains somewhat larger than the strength of a frame with a soft story corresponding to the story in which damage of the infill concentrates. Excellent hysteretic behavior has been obtained with the use of solid brick infills reinforced with welded wire fabric.

(4) While the maximum lateral strength in cyclically loaded and/or deformed specimens depends on several parameters (see Conclusions 2 and 3), the final mechanism of failure is what can be defined as a somewhat strengthened soft story frame. Thus the energy dissipated by an infilled R/C frame would always be considerably larger than a bare soft story frame, provided that the columns of the infilled frame have been properly designed against the story shear corresponding to the infilled frame and for the required or desired deformation capacity of the frame.

(5) The hysteretic behavior of welded wire fabric reinforced infills not only has been excellent but also has resulted in significantly less production of debris. The debris produced was effectively contained within the panel. This was not the case with unreinforced infills in which considerable debris was produced, and since in these unreinforced infills there is nothing to protect against this debris falling, it constitutes a hazard.

(6) The addition of infills to a moment reducing frame introduces significant changes in the dynamic characteristics of the frame and, therefore, of the building. In the linear elastic range the periods and mode of vibrations are significantly affected by the infills. In the inelastic range the dissipation of energy takes place through mechanisms completely different from that in which a ductile moment resisting frame dissipates energy. In the infilled specimens the large inelastic deformations were concentrated in one story.

VI. EFFECTS OF INFILLS IN DESIGN AND RETROFITTING OF SEISMIC RESISTANT BUILDINGS

6.1 Introductory Remarks

The results presented herein, as well as those obtained in the previous investigation by Klingner and Bertero [1] and by other researchers, have shown clearly that the infill affects significantly the stiffness, strength, and deformation capacity (i.e., ductility, and energy absorption and dissipation capacities) of the bare frame. All these effects result in changes in the dynamic characteristic of the building in which the infill is used. From the practical viewpoint of seismic resistant design of new buildings, as well as of proper retrofitting of existing buildings, the question that should be answered is how the infill will affect the seismic response of the buildings and how these effects should be considered in the design and retrofitting procedures of these buildings.

This is not an easy question to answer because, as will be discussed herein, the degree in which the infill affects the above mechanical characteristics of the structure depends on how the infill is constructed and particularly how it is integrated (anchored or connected) to the bare structure of the building. The infills not only modify the available (supplied) strength, stiffness, damping, hysteretic behavior and deformation capacity of the building structure, but these changes also introduce modifications in the demands of these same response parameters to any given earthquake ground motion. The addition of infills brings an increase in the building mass. This increase in mass has two main effects: (1) the reactive mass is increased; and (2) the period, T, of the structure is increased. While the increase in reactive mass brings a direct increase in the inertia forces that will be developed for any given acceleration to which this mass will be subjected, the effect of a relative increase in the period T on the response of the structure depends on the interacting final dynamic characteristics of the building and ground motions. Furthermore, while the addition of the infills by virtue of its mass increases the period T, it also introduces an increase in stiffness which decreases the T. These opposite interacting effects as well as the change in the effective viscous damping and changes in the mechanisms of dissipation of energy by inelastic deformation, make it difficult to arrive at definite conclusions regarding the final effects of the infill. An evaluation of the effects of infills on most of the above parameters is presented first. This is done considering the two sides of the design equation, i.e., considering the effects on the demand as well as on the supplies. From this evaluation some final observations are made regarding the probable effects of infills on the overall dynamic response and, consequently, on the seismic resistant design and retrofitting of buildings.

6.2 Effects of Infill on the Lateral Stiffness, K, Supplied to the Structure

The evaluation is first based on the results obtained in the models that have been tested. Then they are extrapolated to the prototype by just considering the scale effects, i.e., the stiffness in the prototype, K^p, is equal to the stiffness in the model, K^m, multiplied by the length scale L_s, i.e.,

$$K^p = K^m \times L_s \tag{1}$$

Furthermore, the lateral stiffness that will be evaluated and compared is the one based on the effective interstory lateral stiffness at service load level rather than on the initial tangent lateral stiffness and/or that based on total displacement of the specimen tested.

6.2.1 Results on Models

(1) Bare Frame. The lateral stiffness of the subassemblage tested based on the interstory drift, K^s_{bf} was evaluated at 35 k/in. (see Table 3). This value is shown in Fig. 90 where it is compared with the values obtained for some of the infilled frame subassemblages tested. As discussed in Sec. 5.4, the lateral stiffness of the model

frames are twice those of the subassemblages tested.

(2) Infilled Frames. The values of K_I^S obtained for the specimens tested varied from 118 k/in. to 409 k/in. (20.7 to 71.7KN/mm) with an average of 221 k/in. (38.7KN/mm). When the values obtained for the same type of infills are averaged, the K_I^S varied between 163 to 383 k/in. (28.6 to 67.1KN/mm). For clay brick the K_I^S was very consistent and averaged a value close to 200 k/in. (35.0KN/mm). For the concrete block the K_I^S averaged 231 k/in. (40.470KN/mm). When the infill was made of lightweight concrete cast in place, the K_I^S averaged 383 k/in. (67.1KN/mm). The smallest K_I^S was obtained with the solid brick panels reinforced with wire fabric: K_I^S averaged 163 k/in. (28.6KN/mm).

(3) Infilled vs. Bare Structure. Considering averages of the values obtained for the same type of infills, the following main relative increases in K_I^S are obtained: minimum increase is $\frac{163}{35} = 4.66$ and the largest $\frac{383}{35} = 10.94$ being the average about $\frac{221}{35} = 6.31$.

(4) Effect of K_I^S on Period, T, of Building. This effect depends upon the interrelated effect induced by the associated mass and stiffness of the infills, i.e., how the total mass of the building, M, changes relative to the stiffness with the addition of infill. Different results can be obtained depending on the assumption of how M changes; see Table 4.

(a) Same M, i.e., it is assumed that the same infills also exist in cases where the structure is considered as a bare frame, i.e., the infills are structurally isolated or, in the cases where they are not structurally isolated they are not considered to act structurally. In this case comparing the period of just one infilled frame, T_{if}, with that corresponding to one bare frame, T_{bf}, we will have that on the average

$$T_{if}^{+} = \frac{1}{\sqrt{6.31}} T_{bf} = 0.40\ T_{bf}.$$

The smallest decrease is for the use of exterior welded wire fabric. In this case

$$T_{if}^{+} = \frac{1}{\sqrt{4.66}} T_{bf} = 0.46\ T_{bf}$$

The largest decrease is in the use of lightweight concrete panels cast in place

$$T_{if}^{+} = \frac{1}{\sqrt{10.94}} T_{bf} = 0.30\ T_{bf}\ .$$

Regarding how these values would affect the period of the whole building, it will depend on how many of the total number of frames in one direction are infilled. If it is assumed that all the frames are infilled, then the above periods also represent the change in period of the buildings. Therefore, any of the infill, even the most flexible one, will produce a significant change in the period of the building.

Since the above case can be considered as an upper bound in the change of T, a lower bound can be obtained considering the case that only 4 (which is the smallest of shear walls recommended by ATC recommendations [13]) of the 11 frames are infilled.

Average change $$T_{if}^{-} = \sqrt{\frac{(11x1)}{(7x1) + (4x6.31)}}\ T_{bf} = 0.58\ T_{bf}$$

Lowest change $$T_{if}^{-} = \sqrt{\frac{(11x1)}{(7x1) + (4x4.66)}}\ T_{bf} = 0.65\ T_{bf}$$

Highest change $$T_{if}^{-} = \sqrt{\frac{11x1}{(7x1) + (4x10.94)}}\ T_{bf} = 0.47\ T_{bf}$$

As can be seen, for even this lower bound case, there is a significant change in T, if the M does not change.

(b) M Increases with Addition of Infills. As an extreme case it can be considered that no infill at all (i.e., no partitions) are used in case of the bare frame structure. Then the changes in mass for each infilled frame of the model will be approximately 7.90 k. (35.1KN). The total mass of the building model is 23144 k/27g = 857 k/g $(3814\frac{KN}{g})$.

Case that 11 Frames Are Infilled. The increase in reactive mass amounts $\frac{11 \times 7.90}{857} = 0.10$, i.e., 10%. The changes in the T_{if} are as follows:

Average change
$$T^{+}_{if} = \sqrt{\frac{[857 + (11x7.90)] \times 1}{857 \quad x \quad 6.31}}\ T_{bf} = 0.42\ T_{bf}$$

Lowest change
$$T^{+}_{if} = \sqrt{\frac{[857 + (11x7.90)] \times 1}{857 \quad x \quad 4.66}}\ T_{bf} = 0.49\ T_{bf}$$

Highest change
$$T^{+}_{if} = \sqrt{\frac{[857 + (11x7.90)] \times \quad 1}{857 \quad x \quad 10.94}}\ T_{bf} = 0.32 T_{bf}$$

As can be seen, the effect of change in mass on the T for this particular building is very small (smaller than 7 percent).

Case that Four Frames Are Infilled. Increase in reactive mass amounts $\frac{4 \times 7.90}{857} = 0.04$, i.e., 4%. The changes in T_{if} are as follows:

Average change
$$T^{-}_{if} = \sqrt{\frac{[857 + (4x7.90)]}{857}} \times 0.58\ T_{bf} = 0.59\ T_{bf}$$

Lowest change
$$T^{-}_{if} = 1.0183 \times 0.65\ T_{bf} = 0.66\ T_{bf}$$

Highest change $\quad T_{if}^{-} = 1.0183 \times 0.47\, T_{bf} = 0.48\, T_{bf}$

6.2.2 Interpretation of Model Results Regarding Behavior of Prototype Building

All the above results which were obtained considering a model of the building in the length scale $L_s = 3$, can be translated to the prototype by proper consideration of the effects of this scale. Accordingly the periods of the prototype, T^p, would be given by the period computed for the corresponding model, T^m, multiplied by the length scale. The period of the prototype bare frame building, therefore, would be

$$T_{bf}^{p} = 3 \times T_{bf}^{m}$$

Considering that the effective interstory stiffness for the model of the bare frame based on the measured stiffness of the tested specimen is equal to 35 k/in. x 2 = 70 k/in. and considering that there are 11 frames in the building of Fig. 1 and its total mass is 857 k/g, the T_{bf}^{m} results to be

$$T_{bf}^{m} = 2\pi \sqrt{\frac{857\ \mathrm{K}}{(70\mathrm{x}11)\ \frac{\mathrm{K}}{\mathrm{in}} \times 386\ \frac{\mathrm{in}}{\mathrm{sec}^2}}} = 0.338\ \mathrm{sec.}$$

and consequently

$$T_{bf}^{p} = 3 \times 0.338\ \mathrm{sec.} = 1.01\ \mathrm{sec.}$$

It is of interest to compare this value estimated from experimental results, with the one estimated analytically in the design of the prototype bare frame which was 1.30 sec.

In conclusion, all the results obtained above for the periods of the model infilled frame can be translated directly to the periods of the corresponding prototype infilled frame by just multiplying them by the length scale factor 3. The period values in seconds for the proto type infilled building are given in Table 4.

6.3 Effects of Infill on the Supplied Strength to the Building

These effects are again evaluated on the basis of the results obtained in the tests of the specimens (model subassemblages) making different assumptions regarding the number of frames that are infilled in the real building. The evaluation of the strength is based on the estimation of the base shear strength V_n that the model of the building could have resisted. This estimation in turn will be based on the measured lateral resistance of the specimen tested, $(V_n)^s$ which is equal to the maximum lateral force H plotted in the diagrams of Figs. 17 through 34 and summarized in Table 1.

6.3.1 Base Shear Strength of Bare Frame

As shown in Fig. 31, the bare frame specimen in Test 15 was capable of resisting a maximum lateral force of $H = (V_n)^s = 12.5$ kips (55.6KN). This means that a 1/3-scale model of the complete frame would have been capable of resisting a total base shear, $(V_n)^m_{bf}$, of 25K (111.3KN). Therefore, the total lateral resistance of the model of the complete building, if the only resisting structural element were the 11 bare frames, would amount to 11 x 25 k = 275 kips (1224 KN).

6.3.2 Base Shear Strength of Infilled Frames

This varied considerably depending on the type of infills, as well as on the loading program, that was used. As shown and discussed in Chapter V and summarized in Table 1, the measured lateral resistance of the specimens tested varied from a minimum of 35.3 kips (157.KN) to a maximum of 100 kips (445.KN), which means a variation on the total $(V_n)^m_{bf}$ from 70.6 kips (314.KN) to 200 kips (890KN). As discussed below, this variation was due to the different types of infill.

In evaluating the supplied strength to the prototype building or its model from the results obtained in the test of the model subassemblages, it is necessary to distinguish the two bounds considered previously, i.e., an upper bound based on the assumption that all 11 frames are infilled, and a lower bound assuming that only

4 of the 11 frames are infilled. The final results obtained from this evaluation are summarized in Table 5. In the case that 11 frames are infilled, the supplied or available lateral strength of the building V_n will be directly obtained from the results of the specimens tested $(V_n)^s$, since

$$V_n = (V_n)^m \times L_s^2 = [(V_n)^s \times 2]\, L_s^2.$$

When only 4 of the 11 frames are infilled, the determination of V_n requires analysis of the load-deformation relationship of the infilled frames, and that of the bare frame (Figs. 17-34), and an assumption regarding the in plane flexibility of the floor system (diaphragm). To simplify the discussion, it will be assumed that the diaphragm is rigid and that no torsion is developed.

As illustrated in Fig. 91, the infilled frame reaches its peak "elastic" strength at a displacement (interstory drift) somewhat smaller than the one at which the bare frame reaches its maximum lateral strength. Thus it is clear that to obtain the elastic strength of the building we cannot add the peak strength of the bare frame to that of the infilled frame. For each different type of infill it would be necessary to analyze the load-deformation of the infilled frame together with that of the bare frame. From inspection of the results obtained it has been concluded that a lower bound of the strength can be obtained by considering that when the infilled frame reached its peak "elastic" strength the bare frame has developed a resistance equal to half of its maximum strength, i.e., that the

$$[(V_n)_{bf}^m]\ (\delta_{if})_{max} = 2\times[1/2\ (V_n)_{bf}^s] = 2 \times 6.25 \text{ kip} = 12.5 \text{ kips } (55.6\text{KN}).$$

(1) $(V_n)_{uif}^m$ <u>for Unreinforced Infill</u>. This type of infill resulted in the lowest lateral resistance. According to the result obtained for Test Specimen 2 (Fig. 18), $(V_n)_{uif}^m$ becomes $35.3 \times 2 = 70.6$ kips (314.KN). In spite of this low value, it still

represents an increase of 182% with respect to the resistance of the bare frame, i.e., $(V_n)^m_{uif} = 2.82\ (V_n)^m_{bf}$.

Then for the case of all 11 frames being infilled

$$(V_n)^+_{uif} = 2.82\ (V_n)_{bf}$$

In case that only 4 frames are infilled

$$(V_n)^-_{uif} = \frac{7\ (0.5) + 4\ (2.82)}{11}\ (V_n)_{bf} = 1.34\ (V_n)_{bf}.$$

(2) $(V_n)^m_{rif}$ <u>for Reinforced Hollow Masonry Infill</u>. The smallest lateral resistance measured during the experiments for this type of infill was 39.2 kips (174.4KN) (Specimen 7, Fig. 23) which has only 0.15% of reinforcement. This means a $(V_n)^m_{rif} = 39.2 \times 2 = 78.4$ kips (348.8KN) which represents an increase 214% with respect to the similar strength of the bare frame. In the case of infills reinforced with 0.6% of vertical and horizontal reinforcement the smallest resistance measured was 46.7 kips (207.8KN) (Specimen 8, reinforced concrete blocks, Fig. 24), which means a $(V_n)^m_{rif}$ of $46.7 \times 2 = 93.4$ kips (415.6KN). This in turn represents an increase in base shear strength of 274% with respect to the similar strength of bare frame. As summarized in Table 5 the observed increase for this type of infill, reinforced with $\rho = 0.6\%$ were

Smallest $(V_n)^m_{rif} = 3.74\ (V_n)^m_{bf}$

Average $(V_n)^m_{rif} = 5.20\ (V_n)^m_{bf}$

Largest $(V_n)^m_{rif} = 6.64\ (V_n)^m_{bf}$

Then for the case that all the 11 frames of the building are infilled

$\rho = 0.15\%$ {Smallest $(V_n)^+_{rif} = 3.14\ (V_n)_{bf}$

$$\rho = 0.60\% \quad \left| \begin{array}{ll} \text{Smallest} & (V_n)^{+}_{rif} = 3.74\ (V_n)_{bf} \\ \text{Average} & (V_n)^{+}_{rif} = 5.20\ (V_n)_{bf} \\ \text{Highest} & (V_n)^{+}_{rif} = 6.64\ (V_n)_{bf} \end{array} \right.$$

In case where only 4 of the 11 frames are infilled

$$\rho = 0.15\% \quad \{\text{Smallest} \quad (V_n)^{-}_{rif} = \frac{7(0.5) + 4(3.14)}{11} = 1.46\ (V_n)_{bf}$$

$$\rho = 0.60\% \quad \left| \begin{array}{ll} \text{Smallest} & (V_n)^{-}_{rif} = \dfrac{7(0.5) + 4(3.74)}{11} = 1.68\ (V_n)_{bf} \\ \text{Average} & (V_n)^{-}_{rif} = \dfrac{7(0.5) + 4(5.20)}{11} = 2.21\ (V_n)_{bf} \\ \text{Highest} & (V_n)^{-}_{rif} = \dfrac{7(0.5) + 4(6.64)}{11} = 2.73\ (V_n)_{bf} \end{array} \right.$$

(3) $(V_n)^{m}_{rif}$ <u>for Solid Split Brick Reinforced with Welded Wire Fabric</u>. The three specimens tested (16, 17, and 18, Figs. 32, 33, and 34) resisted maximum lateral forces of 70.7, 57.3, and 61.3 kips (314.6, 255., 272.8KN) respectively. This means an average $(V_n)^{m}_{rif}$ of 126.2 kips (561.6KN), which in turn means a 405% increase in strength with respect to the bare frame.

For the case that all the 11 frames are infilled

$$\text{Smallest} \quad (V_n)^{+}_{rif} = 4.58\ (V_n)_{bf}$$

$$\text{Average} \quad (V_n)^{+}_{rif} = 5.05\ (V_n)_{bf}$$

$$\text{Highest} \quad (V_n)^{+}_{rif} = 5.65\ (V_n)_{bf}$$

In case that only 4 of the 11 frames are infilled

$$\text{Smallest} \quad (V_n)^{-}_{rif} = \frac{7(0.5) + 4(4.58)}{11} = 1.98(V_n)_{bf}$$

$$\text{Average} \quad (V_n)^{-}_{rif} = \frac{7(0.5) + 4(5.05)}{11} = 2.15(V_n)_{bf}$$

$$\text{Highest} \quad (V_n)^{-}_{rif} = \frac{7(0.5) + 4(5.65)}{11} = 2.37(V_n)_{bf}$$

Considering that this is the simplest way of infilling frames (either new or for retrofitting of already constructed moment resisting frames) with reinforced masonry, and also more attractive from an economical point of view, the increase in strength is very significant, being on the average practically the same as that obtained when using reinforced hollow masonry with a larger amount of reinforcement (0.6% vs 0.4%). Even in the case where the measured strength is reduced to consider that the models of the subassemblages for this type of infill had a thickness of 2.5 in. (63.5mm) rather than the 2.0 in. (50.8mm) of the other infills, the increase in strength is still very significant, as shown by the following values.

In case all the 11 frames are infilled

Smallest $(V_n)^{+}_{rif(2")} = 3.66\ (V_n)_{bf}$

Average $(V_n)^{+}_{rif(2")} = 4.04\ (V_n)_{bf}$

Highest $(V_n)^{+}_{rif(2")} = 4.52\ (V_n)_{bf}$

In case where only 4 of the 11 frames are infilled

Smallest $(V_n)^{-}_{rif(2")} = 1.65\ (V_n)_{bf}$

Average $(V_n)^{-}_{rif(2")} = 1.79\ (V_n)_{bf}$

Highest $(V_n)^{-}_{rif(2")} = 1.96\ (V_n)_{bf}$

(4) $(V_n)^{m}_{rif}$ <u>for Reinforced Lightweight Concrete Infill.</u> The two specimens tested (10 and 11, Figs. 26 and 27), resisted maximum lateral forces of 93 and 100 kips (413.8 and 445.KN). Therefore, on the average these results represent an increase in V_n of 672% with respect to bare frame, or $(V_n)^{m}_{rif} = 7.72\ (V_n)^{m}_{bf}$.

If all the 11 frames of the building are infilled

$$\text{Average } (V_n)^+_{rif} = 7.72\ (V_n)_{bf} \begin{cases} \text{Minimum } 7.42\ (V_n)_{bf} \\ \text{Maximum } 8.00\ (V_n)_{bf} \end{cases}$$

In case that only 4 of the frames are infilled

$$\text{Average } (V_n)^-_{rif} = \frac{7x(0.5) + 4(7.72)}{11} = 3.12\ (V_n)_{bf} \begin{cases} \text{Minimum } 3.02\ (V_n)_{bf} \\ \text{Maximum } 3.23\ (V_n)_{bf} \end{cases}$$

6.4 Effects of Change in Period, T, on the Estimation of the Demands

The dynamic response depends, of course, not only on the dynamic characteristics of the building (T, ξ, V_n, and μ) but also on the dynamic characteristics of the ground motions. Thus to draw definite conclusions regarding the effects of infills on the dynamic response, one needs to be able to predict the type of ground motions that could be expected at the building site, and then find the critical ground motions for the problem at hand. Due to lack of information regarding future earthquake ground motions, one way of getting an idea of possible effects is to study the effects of a possible suite of earthquake ground motions. The easy way to obtain a clear idea of what can be the effects of the changes in T over the response is to analyze the response spectra of ground motions. In doing so we have to distinguish the following two cases: linear elastic and inelastic response.

Before discussing these two cases, it is necessary to define the mass of the building, the period of the building with bare frame, and to adopt an effective viscous damping ration ξ.

6.4.1 Mass M of the Building

Because the numerical estimations conducted in section 6.2.1(4) have shown that the two main effects of the change in mass are small for this particular building, for the sake of simplicity it will be assumed that the mass is the same, whether the structure of the building is considered as bare frame, or infilled frame. Thus the lateral mass of the prototype building is assumed to be $2314\frac{k}{g}$ $(102990\frac{KN}{g})$.

6.4.2 Period of the Bare Frame Building

To illustrate how the initial stiffness of the bare frame can affect the influence of infills, the two following periods of the bare frame will be considered: the T_{bf}^{p} estimated from test results equals 1.01 secs. and the one obtained analytically, i.e., 1.30 secs.

6.4.3 Damping Ratio of the Bare Frame Building

It has been assumed that for the service earthquake ground motion, $\xi = 3\%$ and for the extreme earthquake ground motion, $\xi = 5\%$. Although the addition of infills may introduce considerable change in ξ, usually increasing it for large deformations (because of the friction along the cracking that develops in the infills and between the boundaries of the infill and the frame, values of $\xi = 12\%$ have been measured), for simplicity's sake, the ξ for the infilled frame building is assumed to be the same as for the bare frame building under strong ground motions, i.e., $\xi = 5\%$.

6.4.4 Linear Elastic Response

Assuming a linear elastic response spectra as suggested by Newmark and Hall [6] for a maximum effective peak acceleration of 0.5g (Fig. 92), it is clear that because of variation in T, there will be significant changes if force, as well as displacement demands, when the infills are considered.

6.4.5 Effect of Changes in T on Seismic Force Demands, V_{if}^{D}

As a consequence of the decrease in T induced by the effect of the infills (from 1.30 sec to 0.52 sec on the average, ranging from 0.60 sec in the lowest decrease, to 0.39 sec in the case of the largest decrease) in the case that all the frames are infilled the demands in design seismic forces increases about 141%, 141%, and 141% for the average, lowest and largest decrease in T (see Table 6). Figure 92 illustrates the increase in force demand for the case of T changing from 1.30 secs to 0.39 secs. It should be noted that for the sake of simplicity it is assumed that the total seismic force demand is directly given by the first mode response, i.e., the response of the structure is considered as that of a single degree of freedom having the total mass M of the building and the periods computed in Table 5. In the case that $T_{bf}^{p} = 1.01$ sec, the addition of infills changes this value to 0.40 sec, 0.46 and 0.30 secs for the average, lowest and highest decreases. This change causes the following corresponding approximate increases in seismic force demands: 86%, 86% and 86%.

Table 6 shows also the estimated increases for the case that only 4 of the 11 frames are infilled. The minimum increase is 56%. Increases in seismic forces of the order of 56% and, of course, 141%, are very significant and cannot be neglected. It is clear that for the type of ground motions represented in the selected elastic response spectra, the more flexible the bare frame the larger the increase in the seismic forces attracted by the addition of the infill.

6.4.6 Effect of Changes in T on Deformation Demands

As is shown in Table 7, as a consequence of the increase in stiffness (decrease in T), when all the frames are infilled, the deformation response decreases 66%, 56%, and 82% for the cases of the average, lowest and largest decrease in T_{if} considering $T_{bf}^{p} = 1.30$ secs. Figure 92 illustrates the estimations of the maximum displacements for the case of $T_{bf}^{p} = 1.30$ secs and $T_{if} = 0.39$ secs., considering the structures as single degree of freedom systems. For the case of $T_{bf}^{p} = 1.01$ secs, the decreases are 76%, 66%, and 85% respectively. For the case where only 4 of the 11 frames are infilled, the decreases are also shown in Table 7 and vary from 33% to 60%. These decreases in deformation are very significant and have beneficial effects. The smaller the deformation the smaller the damage, either of the structural or nonstructural components, and the smaller the P-Δ effects, which are two of the main drawbacks in the use of just a bare moment resisting frame. Even in the case of the more flexible infill (the one based on use of wire fabric), and when only 4 frames are infilled, the reduction is very significant, 33%. There is no doubt that this reduction in elastic deformation demand is a significant advantage in the use of infills.

6.5 Overall Effect of Infills on Strength Demand and Strength Supply

In light of the results presented and discussed above in Sections 6.3 and 6.4, it is now possible to reach some observations regarding the overall effects of infills on seismic behavior of infilled reinforced concrete frames when compared with behavior of bare moment resisting frames as far as lateral strength is concerned.

6.5.1 Supplied Strength vs. Strength Demand Based on Linear Response

In Section 6.4 it has been seen that due to the increased stiffness (decrease in T), there can be an increase in seismic force demands that in the case of linear elastic response, and for the case of T_{bf}^{p} = 1.30 secs, and assuming that all the frames of the building are infilled amounts to 141% when compared with that corresponding to the demands for a building with just bare frames. In case of T_{bf}^{p} = 1.01 secs, the increase in seismic force demands is about 86%. It has been shown in Sec. 6.3 and summarized in Table 5 that the addition of infills to all the bare frames of the building results in an increase of the supplied (available) base shear strength of 182% as a minimum and 700% as a maximum. It can be concluded that in case that all the frames are infilled the increase in supplied strength exceeds considerably the increase in strength demand and, therefore, it would appear advantageous to infill all frames, in all cases, even with unreinforced masonry. However, this will be only correct if it is possible to assume that the building will be able to supply the elastic strength that is demanded. In the case that only 4 of the 11 frames are infilled, similar comparison shows that the increase in demand for the case of $T_{bf}^{p} = 1.30$ secs varies from 56 to 141% and when $T_{bf}^{p} = 1.01$ sec it varies from 57 to 86%. On the other hand the increase in the supplied strength varies from 34%, which is the minimum for unreinforced masonry, to a maximum value of the lower bound of 223%. Comparison of the values obtained for the supplied and demanded strength for similar specimens shows that except for the unreinforced masonry and the reinforced masonry with $\rho = 0.15\%$, all other infills result in a supplied strength larger than the demanded strength. Thus from the point of view of "elastic" strength it appears that the use of all types of infills considered in this investigation, when properly reinforced with $\rho \geq 0.4\%$ are advantageous. Therefore, it remains to find out what intensity of ground motion the supplied "elastic" strength will be capable of resisting. This is evaluated below, considering that in the design of the building, the total weight was estimated in 23144 kips (102991.KN), i.e., W = M.g = 23144 kips (102991.KN).

Estimation of Lateral Resistance and Intensity of Ground Motion

These estimations are summarized in Table 8.

(1) The 11 Frames are Infilled. Then the lateral strength of the 11 prototype infilled frames, $(V_n)_{if}$, will be $(V_n)_{if}^{m} \times 11 \times L_s^{2}$. Because the L_s of the models is 3, then the strength scale factor is $(3)^2 = 9$.

(a) Unreinforced Infills. Considering the lower value obtained for this type of infill $(V_n)_{uif} = (70.6k \times 11) \times (9) = 6989$ kips (31103KN). This shear represents an overall lateral seismic resistant coefficient, C, of

$$C = \frac{6989}{23144} = 0.30$$

Because this infilled frame building has a T = 0.52 secs (see Table 8), it could resist "elastically" ground motions with an effective peak acceleration of about 0.12g if this ground motion has the dynamic characteristics of the earthquake ground motions considered by Newmark and Hall [6] in their smoothed elastic design response spectra and a $\xi = 5\%$ is assumed (Fig. 92).

(b) Reinforced Hollow Masonry Infill. Considering an average strength $(V_n)^m_{rif}$ = 130k (578.5KN), $(V_n)_{rif}$ = 130k x 11 x 9 = 12870 kips (57272KN) which results in a

$$C = \frac{12870}{23144} = 0.56$$

Having T = 0.52 sec, this type of infilled frame could resist "elastically" earthquake ground motions with effective peak acceleration up to approximately 0.22g if the motions have dynamic characteristics similar to that considered by Newmark and Hall [6] and a $\xi = 5\%$ is assumed (Fig. 92).

(c) Solid Split Bricks Reinforced with Welded Wire Fabric. Considering the average strength obtained for this type of infill

$$(V_n)_{rif} = 126.2 \times 11 \times 9 = 12494 \text{ kips } (55597\text{KN}).$$

This results in a

$$C = \frac{12494}{23144} = 0.54$$

Having T = 0.60 sec, this type of infilled frame building could resist "elastically" the effects of earthquake ground motions having an effective peak acceleration of about 0.21g if these motions have elastic response spectra as that shown in Fig. 92.

(d) Reinforced Lightweight Concrete Infill. As shown in Section 6.3.2 (4), the averaged strength available for this type of infill

$$(V_n)_{rif} = 193^k \times 11 \times 9 = 19107 \text{ kips } (85026\text{KN}).$$

This yields a

$$C = \frac{19107}{23144} = 0.83$$

Having T = 0.39 sec, this type of infilled frame could resist "elastically" the effects of ground motions having an effective peak acceleration of about 0.21g if the response spectra of these motions are like the ones illustrated in Fig. 92.

(2) Only 4 of the 11 Frames Are Infilled. For this case, the total base shear strength supplied to the building that can be expected, according to the results obtained in the tests of the models and assuming a lower bound for the combined resistance of the seven bare frames and the four infilled (See Sec. 6.3.2), and the intensity of the ground motions, a_{ep}, that the building can resist "elastically"

if these motions have elastic response spectra like that illustrated in Fig. 92 are as follows:

(a) Unreinforced Infills.

$$(V_n)_{uif} = (7 \times 12.5^k + 4 \times 70.6^k)\ 9 = 3329 \text{ kips } (14814.KN).$$

As shown in Table 5 this represents an increase of 34% over the similar strength of the bare frame building.

The overall lateral seismic resistant coefficient C corresponding to this $(V_n)_{uif}$ is estimated as

$$C = \frac{3329}{23144} = 0.14$$

Since considering a $T_{bf} = 1.30$ sec the $T_{if} = 0.75$ secs this structure can resist a ground motion having an $a_{ep} = 0.07g$. Note that for the bare frame building the $C = \frac{2475}{23144} = 0.11$, and considering a $T_{bf} = 1.30$ secs the corresponding max $a_{ep} = 0.10g$

(b) Reinforced Hollow Masonry Infill.

$$(V_n)_{rif} = (7 \times 12.5 + 4 \times 130) \times 9 = 5468 \text{ Kips } (24333.KN)$$
$$= 2.21\ (V_n)_{bf}$$

$$C = \frac{5468}{23144} = 0.24$$

considering $T_{if} = 0.75$ secs: $a_{ep} = 0.13g$

(c) Solid Split Brick Reinforced with Welded Wire Fabric.

$$(V_n)_{rif} = (7 \times 12.5^k = 4 \times 126.2^k) \times 9 = 5330 \text{ kips } (23705KN)$$
$$= 2.15\ (V_n)_{bf}$$

$$C = \frac{5330}{23144} = 0.23$$

considering $T_{if} = 0.84$ secs: $a_{ep} = 0.14g$

(d) Reinforced Lightweight Concrete Infill

$$(V_n)_{rif} = (7 \times 12.5^k + 4 \times 193^k) \times 9$$

$$= 7735 \text{ kips } (34421.\text{KN}) = 3.13\ (V_n)_{bf}$$

$$C = \frac{7735}{23144} = 0.33$$

considering $T_{if} = 0.61$ secs: $a_{ep} = 0.17g$

As can be seen from analysis of the above results, even when only four frames are infilled, the use of infill considerably increases the supplied lateral shear strength to the building when compared with the bare frame. The increase varies from 34% to 234% depending on the type of infill. However, only for infills reinforced with $\rho \geq 0.4\%$ can the infilled frame building resist a higher intensity ground motion than the bare frame building.

6.5.2 Comparison of Supplied Strength vs. Strength Demands Based on Linear Elastic Response of Whole Buildings

Before comparing these two strengths, it should be noted that the lateral force demands, as well as the maximum effective peak acceleration a_{ep}, have been estimated according to the response spectra illustrated in Fig. 92. Keeping this in mind in the comparison, the following observations may be made:

(1) Case Where All Frames Are Infilled. Unreinforced masonry infills could be used advantageously (i.e., elastic strength supplied larger than elastic strength demands) in seismic regions in which the peak effective acceleration, a_{ep} is $\leq 0.12g$, which, according to the ATC recommendations [13], is for most of the U.S. In the case of reinforced lightweight concrete infills, these infills could be used without the danger of any significant damage in seismic regions in which $a_{ep} \leq 0.32g$, which means they could be used in regions of very severe earthquake ground motions. The maximum value specified by ATC [13] for a_{ep} is 0.40g. Similarly, the solid split

bricks reinforced with wire fabric could be used in seismic regions where $a_{ep} \leq 0.21g.$, i.e., areas 1, 2, 3, 4, and 5 of ATC map area classification.

(2) <u>Case Where Only 4 of the 11 Frames Are Infilled.</u> Unreinforced masonry could be used in seismic regions where the $a_{ep} \leq 0.07g$, i.e., in regions located in the U.S. area classified as 1 and 2 in the map area classification recommended by ATC [13]. The solid split bricks reinforced with welded wire fabric could be used advantageously with respect to bare frame in regions where $a_{ep} \leq 0.14g$ (i.e., for all 1, 2, and 3 areas according to ATC map area classification), without danger of suffering serious damage. Similarly, reinforced lightweight concrete infill could be used in areas where $a_{ep} \leq 0.17g$, i.e., ATC areas 1 through 4.

It can be concluded that infilling moment resisting frames with properly reinforced panels offers advantages when designed so that the frames would remain in the elastic range during the most severe earthquake ground motion that can occur in the region. The question that remains is, what would happen if these infills were subjected to deformations larger than those corresponding to its maximum "elastic" strength? Can the infilled frame survive such deformations without severe damage? In attempting to answer it is necessary to analyze the inelastic behavior of infills in the infilled frames, and how this behavior affects the performance of the frames. In this analyses it is convenient to distinguish the following cases.

(1) Case of unreinforced masonry infill and properly designed ductile moment resistant frame.

(2) Case of unreinforced masonry infill and moment-resisting frame when details do not satisfy the requirement of ductile moment resisting frame.

(3) Reinforced infill and properly designed ductile moment resistant frame.

(4) Reinforced infilled and non-ductile moment resistant frame.

6.6 Effect of Infill on the Inelastic Response of the Building

6.6.1 Ductile Moment Resisting Frame Infilled with Unreinforced Masonry

According to results obtained in experiments conducted on Specimens 1 and 2, (Figs. 17 and 18) and observations made during the tests (Figs. 35 through 38), it becomes clear that under cyclic loading (Fig. 18) as soon as the panel reaches its maximum strength, which occurs with very small amounts of inelastic deformations (approximately 1.5 times that which will correspond to linear elastic behavior, i.e., given a displacement ductility ratio of about 2.5), after this there is a reduction in strength to a value that is close but somewhat higher (10%) than that which was observed in the experiments conducted with a first soft story frame (Specimen 9) about 23 kips (102KN), $(V_n)^m$ = 46 kips (204KN), and then an increase up to a value of about 30 kips $(V_n)^m$ = 60 kips (267KN) up to a displacement ductility, μ_δ of about 39. (See Section 5.2.1). It should be noted that after a μ_δ of 2.5, some portions of the unreinforced infill started to spall out.

The above observations indicates that if initial stiffness, strength, and energy dissipation (ductility) were the only considerations in selecting a building structural system, the use of properly designed unreinforced masonry to infill properly designed ductile moment resisting frame would be highly beneficial compared to bare ductile moment resisting frame. Unreinforced masonry would be appropriate for regions in which the seismic risk level of the site is such that the amount of inelastic behavior required to dissipate energy imposed a displacement ductility demand, μ_δ, not larger than 2.5. This is so if the ground motions of the building site have such dynamic characteristics that they result in elastic and inelastic response spectra similar to that shown in Figs. 92 and 93.

As shown in previous sections, while the addition of the unreinforced infill to the bare frame with a T_{bf} = 1.30 secs resulted in an increase in strength demand of about 141% in the elastic range, the increase in supplied strength was about 182%. Now if an analysis using an inelastic response spectra similar to those shown in Fig. 93, but for $\mu_\delta = 2.5$ is conducted, the increase in strength demand due to the decrease in T from 1.30 secs to 0.52 secs is found to be 138%, while the increase in the supplied strength is 182% for μ_δ up to 2.5. Therefore, it appears that as far as strength is concerned, ductile moment resistant frame with unreinforced infills, can be used advantageously in regions where a_{ep} is ≤ 0.26 g if all the 11 frames are infilled, or $a_{ep} \leq 0.22$ g if only 4 of the 11 frames are infilled. However, the real problem with this kind of infill is not the initial stiffness or the strength, but the fact that as soon as maximum strength is reached, the masonry units can shatter and large portions of the infill spall out. In the case of earthquake response this is like an explosive failure with a large portion of unreinforced masonry scattering about. This type of explosive failure of unreinforced masonry infills has been typically observed after moderate to severe earthquake ground motion. In general it is inadvisable to use unreinforced masonry infills except in cases where the response demands will not exceed the elastic range and where out-of-plane failure of the infills can be restrained.

6.6.2 Nonductile Moment Resisting Frame Infilled with Unreinforced Masonry

Except for cases where the building can resist elastically the effect of the most severe earthquake ground motion, this type of structural system should not be used. Its use should be limited to regions of very low seismic risk level, i.e., regions where $a_{ep} \leq 0.12$ g if all the frames are infilled or $a_{ep} \leq 0.07$ g if only 4 of the 11 frames are infilled. The reasons are: First, as soon as the maximum strength is reached a large part of the infill fails and flies out. As soon as the infill fails there can be a failure (collapse) of the nonductile frame. This is because the explosive type of failure of the infill leads the infilled frame to behave like one soft story frame with very large demands in shear and plastic rotations in the columns and/or the beams or beam-column joints adjacent to the failed infilled panel. As these elements have not been designed to resist such demands, the explosive failure of the unreinforced masonry usually will lead to the collapse of the frame.

6.6.3 Properly Designed Ductile Moment Resistant Frame Infilled with Reinforced Masonry or Concrete Panels

(1) Reinforced Masonry Infills. As noted in Section 6.5.1, frames infilled with reinforced masonry can resist elastically the effects of ground motions with an $a_{ep} \leq 0.22$ g if all the frames are infilled or an $a_{ep} \leq 0.13$ g if only 4 of the 11 frames are infilled, while the bare frame system can resist elastically $a_{ep} \leq 0.10$ g. Furthermore, the infilled frames offer the advantage that the resulting lateral deformations are considerably smaller than those that occur if bare frames are used. Analysis of the inelastic behavior obtained in the experiments conducted on these types of infills show that the maximum strength is reached at a deformation of 0.28 in. which can be considered as two times the deformation which would result if a linear elastic behavior with the initial tangential stiffness occurs.

At the average peak strength of the reinforced masonry infill $(V_n)^m_{rif}$ = 130kips (578 KN) = 5.2 $(V_n)^m_{bf}$ considering that it can develop at $\mu_\delta = 2$ without any loss of strength means that the reinforced masonry infilled frame building on the average can resist seismic ground motions (of the types given a design response spectra as that of Figs. 92 and 93) having the following effective peak accelerations.

Case Where All 11 Frames Are Infilled

For T = 0.52 secs: a_{ep} = 0.40 g
T = 0.40 secs: a_{ep} = 0.38 g

Case Where 4 of the 11 Frames Are Infilled

For T = 0.75 secs: a_{ep} = 0.26 g
T = 0.54 secs: a_{ep} = 0.18 g

In the case that the infill consisted of solid split bricks reinforced with two layers of WWF since the infilled frame can develop a $\mu_\delta = 4.2$ with a reduction of only 14% in strength, it becomes evident that this type of structural system can resist earthquake ground motions having the following a_{ep} if the elastic and inelastic design response spectra of these ground motions are like those shown in Figs. 92 and 93.

Case Where All 11 Frames Are Infilled

For $T = 0.60$ secs: $a_{ep} = 0.77$ g

$T = 0.46$ secs: $a_{ep} = 0.59$ g

Case Where 4 of the 11 Frames Are Infilled

For $T = 0.84$ sec: $a_{ep} = 0.55$ g

$T = 0.66$ sec: $a_{ep} = 0.44$ g

In the case of a building with bare ductile frame--for a $T_{bf} = 1.30$ secs it would require to develop a $\mu_\delta \geq 6.1$ to be able to resist a ground motion with an $a_{ep} = 0.55$ g, and in case $T_{bf} =$ 1.01 secs it would require a $\mu_\delta \geq 5.6$ to resist a ground motion with 0.44 g. Since the experiment has shown that the bare frame structure can develop a $\mu_\delta = 6.1$ without any significant loss in strength, it would appear that there is no advantage in using infills except when the majority of the frames are infilled. However it should be recognized that for a bare frame structure to develop a $\mu_\delta = 6.1$, it would have to undergo lateral displacements considerably larger than that needed for an infilled frame building to develop $\mu_\delta = 4.2$. Furthermore, in case of the infilled frame, most of the damage will be developed in just one or two stories where the inelastic deformations concentrated.

Thus it appears that from strength and damage viewpoints, this type of infilled frame can be used advantageously for buildings located in the most severe seismic region of the U.S. Some cautions should be considered before applying this observation in a general sense. It can be applied only to cases similar to those assumed in this study, such as:

(a) Buildings up to 11 stories when the frames are designed with the same design criterion as the one used in the specimens tested.

(b) Ground motions have dynamic characteristics similar to those for which the smoothed linear elastic design response spectra shown in Fig. 92 has been derived.

(c) Ground motions and inelastic behavior of structures that permit the use of Newmark-Hall [6] rules for deriving the inelastic design response spectra firectly from the elastic one, through the use of displacement ductility ratio.

Regarding assumption (a), this is necessary because the inelastic deformation in this type of structure is usually concentrated in one or two stories; the larger the number of stories of a building, the larger will be the demand in the story in which the inelastic deformation is concentrated. Furthermore, the frame has to have very ductile members because the inelastic demands at the story in which the inelastic deformations concentrate, would be very large. This problem has been discussed by Park and Paulay [14], who show that the required column curvature ductility factor, ϕ_{uci}/ϕ_{yci}, can be typically expressed as $\phi_{uci}/\phi_{yci} = 12.54\ r - 3.2$ where r is the number of the story to the top of which the deflections are to be measured.

In the case of solid split bricks reinforced with WWF, the specimens were deflected, producing an interstory drift of 2.4 in. at the story where inelastic deformation was concentrated. (See Figs. 32 and 33.) This drift, which means an interstory drift ratio of 0.07, was achieved without any serious (significant) spalling of debris. This interstory drift, when translated in ductility displacement means μ_δ = 2.4 in./0.17 in. = 14 (see Fig. 91), which was attained with a reduction of strength of 32%. Therefore, this specimen could resist the following effective peak accelerations, a_{ep}, without danger of failure (collapse).

Case Where 11 Frames Are Infilled

For $T = 0.60$ secs: $a_{ep} = 2.05$ g

$T = 0.46$ secs: $a_{ep} = 1.54$ g

Case Where 4 Frames Are Infilled

For $T = 0.84$ sec: $a_{ep} = 1.62$ g

$T = 0.66$ sec: $a_{ep} = 1.31$ g

The interstory drift ratio of 0.07 is very large, demanding large rotations in the columns. The columns of the specimen were capable of developing these rotations because of their special design and detailing. The columns were capable of inducing an interstory drift index of 4 in./32 in. = 0.12 without losing flexural strength. (See Figs. 18 and 22.) Nonductile R/C columns cannot develop the plastic rotations required to obtain such an interstory drift ratio. Note that if an 11 story frame develops a complete collapse mechanism through plastic hinges at the beams, the interstory drift required to achieve the same displacement as the one with a soft story requiring an interstory drift index of 0.07 would be approximately 0.07/11 = 0.006.

Limitation (b), that the ground motion should have dynamic characteristics resulting in an elastic response spectra as that illustrated in Fig. 92. This is necessary because it may well be that a ground motion can occur having the highest frequency content agreeing with the fundamental period of the infilled building and inducing a response larger than the one considered in the response spectra adopted.

Limitation (c) is necessary in view of the possible occurrence of ground motions with long severe acceleration pulses [15].

In conclusion it can be stated that the use of specially designed ductile moment resistant frame infilled with reinforced masonry, particularly solid split bricks with W.W.F., can be used advantageously for even the most severe seismic regions of the U.S., provided the number of stories is limited, say to 11.

A designer could be tempted to design as ductile only the members of the bottom story of the infilled frame. In the case of infilled frames, once inelastic deformations start to occur they concentrate in a very few stories, usually the bottom ones, while all the others remain in the elastic range of behavior. Although to design in this manner appears logical and can lead to considerable economy, the designer must be aware that the results obtained in these investigations, as well as in others, clearly show that for such a design to work it must be assured that the inelastic deformation will actually concentrate in the weakest spot, i.e., the story that is designed as ductile. This is not an easy task. The uncertainties involved in predicting the critical seismic response of buildings are so large that conservative precautions should always be taken. Furthermore, the strength, stiffness and deformation capacity of masonry infills are very sensitive to quality control of the materials and workmanship. To believe that it is possible to control "exactly" where inelastic deformations can occur in a real building is too optimistic.

(2) Reinforced Lightweight Concrete Infills. An analysis of the results obtained with the reinforced lightweight concrete infills (Figs. 26 and 27) clearly shows that it is possible to resist elastically seismic ground motion up to $a_{ep} = 0.32$ g. Furthermore, from the results obtained it is also clear that the specimens tested show that they are capable of dissipating energy with a ductility somewhat larger than 2 without any loss in strength. However, for a μ_δ just larger than 3, there is a considerable reduction in strength, it reduces rapidly to a strength somewhat higher than the strength corresponding to the soft story frame. Therefore, it has been estimated that buildings with this type of infilled frames, and considering a $\mu_\delta = 2$ can resist ground motions that have a smoothed response spectra like the one shown in Fig. 92 with the following peak effective acceleration a_{ep}.

Case Where 11 Frames Are Infilled

For $T = 0.39$ secs: $a_{ep} \leq 0.54$ g
$T = 0.30$ secs: $a_{ep} \leq 0.54$ g

Case Where 4 Frames are Infilled

For $T = 0.61$ secs: $a_{ep} \leq 0.31$ g
$T = 0.47$ secs: $a_{ep} \leq 0.25$ g

As indicated above and discussed in detail in Sections 4.2.10, 4.2.11, and 5.2.5, and illustrated in Figs. 26, 27, and 85, the reinforced lightweight concrete infills reach maximum lateral resistance [93 kips (414KN) and 100 kips (445KN) for Specimens 10 and 11 respectively] and at this load level, crushing of the infills starts at a corner and propagates quickly throughout the infilled panel. There is, consequently, a significant reduction in lateral strength until it appears to stabilize to a value of about 42 kips (187KN) for Specimen 10. This value is considerably higher than the 27.4 kips (122KN) which is the maximum lateral resistance of a bare frame soft story (Specimen 9). Although this is a significant reduction, the failure is far from being sudden or brittle and, as pointed out in Section 5.2.5, it occurs with an increase in lateral deformation. For example, considering that for a reduction in strength of 24.5% the $\mu_\delta = 4.3$ leads to the following estimated a_{ep} for the prototype buildings.

Case Where 11 Frames Are Infilled

For $T = 0.39$ secs: $a_{ep} \leq 0.68$ g
$T = 0.30$ secs: $a_{ep} \leq 0.64$ g

Case Where 11 Frames Are Infilled

For $T = 0.61$ sec: $a_{ep} = 0.53$ g
For $T = 0.47$ sec: $a_{ep} = 0.41$ g

Considering that for the reduced lateral strength the value at which this strength appears to be stabilized, i.e., a 54.8% reduction and that the inelastic deformation at this level gives a $\mu_\delta = 6.6$, the following values of a_{ep} can be obtained:

Case Where 11 Frames Are Infilled

For T = 0.39 secs: $a_{ep} \leq 0.64$ g

For T = 0.30 secs: $a_{ep} \leq 0.48$ g

Case Where 4 Frames Are Infilled

For T = 0.61 secs: $a_{ep} \leq 0.37$ g

For T = 0.47 secs: $a_{ep} \leq 0.28$ g

From analysis of the above results it can be concluded that R/C bare frame buildings of the type investigated can be advantageously infilled with reinforced lightweight concrete for even the most severe seismic regions of the US if all the frames are infilled, and for the ATC map areas 1, 2, 3, 4 and 5 if only 4 of the 11 frames are infilled. Again it should be emphasized that the above conclusion is subjected to the same limitations (a) through (c) noted in Section 6.6.3 (1).

6.7 Concluding Remarks Regarding the Use of Infills in the Seismic Resistant Design and Retrofitting of Buildings

After analyzing results obtained throught a series of numerical computations based on experimental results and assumptions regarding the dynamic characteristics of ground motions and structure of the building, a series of main observations have been made. These are summarized in relation to the seismic resistant design of new buildings and retrofitting of existing ones. However, first it is emphasized that the numerical analyses have been conducted to obtain trends or guidelines and not to represent or to obtain accurate predictions of actual behavior. Therefore, while the specific values may be questioned, it is believed that the trends and guidelines, and subsequently the following observations, are valid. It should also be noted that these observations are valid for the type of building (11 stories, 3 bay frame) and types of infills considered in this study.

6.7.1 Seismic Resistant Design of New Buildings

(1) Infilling all frames up to 11 stories with unreinforced masonry can be used advantageously with respect to the use of bare frame in seismic regions in which the peak effective acceleration $a_{ep} \leq 0.12$ g if all frames are infilled. Under these ground motions the infill will behave "elastically" and no danger of shattering of the masonry units will exist. If out-of-plane failure can be restrained and/or the scattering of masonry units contained, unreinforced infills can be used advantageously in seismic regions with $a_{ep} \leq 0.26$ g if all frames are infilled, and 0.22 g if only 4 of the 11 frames are infilled. This conclusion is valid for seismic zones where the ground motions have dynamic characteristics similar to those considered in the derivation of the smoothed elastic response spectra of Fig. 92.

(2) Masonry infills properly reinforced with $\rho \geq 0.4\%$ can be used advantageously for buildings located even in the most severe seismic regions of the U.S. The most promising infill amongst all those tested appears to be that of solid bricks reinforced with two mats of wire welded fabric and covered with thin layers of a cement mortar or concrete. For this type of infill the infilled frames can resist ground motions with an $a_{ep} = 0.59$ g if all the frames are infilled and an $a_{ep} = 0.44$ g if only 4 of the 11 frames are infilled. This conclusion is limited by the conditions discussed in detail in Sec. 6.6.3. Because of the assumptions made in the numerical analysis, particularly those regarding the idealization of the experimentally obtained lateral load-deformation relationship, caution should be taken in applying this conclusion to cases where the ground motions can contain severe (high a_{ep}) acceleration pulses of long duration.

(3) Lightweight concrete infills with $\rho \geq 0.6\%$ can be used advantageously in seismic zones where the ground motions have $a_{ep} \leq 0.54$ g if all the frames are infilled and $a_{ep} \leq 0.25$ g if only 4 of the 11 frames are infilled. It might even be used for seismic zones with an $a_{ep} \leq 0.64$ g if all frames are infilled and an $a_{ep} \leq 0.41$ g if only 4 frames are

infilled, however, the effect that the significant drop in resistance that has been observed to occur after a $\mu_\delta = 2$ can have on the actual dynamic response of the building should be investigated before applying to these later zones, particularly in case of ground motions that can contain long duration acceleration pulses with these high a_{ep}, where it has been shown that any deformation softening can increase ductility demands considerably [16].

6.7.2 Repair and Retrofitting of R/C Bare Frame in Existing Buildings

From the experience gained in repairing the bare frames using the epoxy injection technique and then retrofitting them by means of different infills, it appears that the use of panels of masonry units (solid brick, as well as hollow brick or even concrete blocks), reinforced externally with two mats of welded wire fabric (WWF) and then basketed through the use of cross ties and finally covering each side with a thin layer of cement mortar or concrete, offers great potential to retrofit energy dissipation capacity in existing buildings, provided that the anchorage to the frame is done according to a technique similar to that illustrated in Figs. 77-81. Again it should be emphasized that this conclusion is valid for buildings having a height similar to one considered in this investigation, i.e., up to 11 stories. Application to taller buildings requires further investigation. This type of infill not only increases the stiffness and strength in about 480% and 358% respectively if all the frames are infilled, and in more than 175% and 98% if only 4 frames are infilled, but also allows excellent hysteretic behavior with peak ductility displacement, μ_δ, up to 4.2 with a maximum reduction in strength of only 14%.

The importance in the observed behavior of close quality control of the materials, good workmanship, particularly in the attachment (anchorage) of the panel to the frame, should be emphasized.

VII. SUMMARY: CONCLUSIONS AND RECOMMENDATIONS

Several observations and conclusions have been formulated in evaluating the experimental results and the effects of infills in the design and retrofitting of seismic resistant buildings whose structural systems are based on moment resisting space frames. These observations and conclusions have been grouped and the main ones are presented in this chapter. In view of the relatively small amount of experimental data on which these conclusions are based, and the idealizations, simplifications, and assumptions made in the numerical analysis conducted, it is convenient to clearly recognize the constraints surrounding the validity of the conclusions that have been drawn so that they will not be misused. For clarity these limitations are summarized regarding the following parameters:

1. Type of Frame. A specially designed R/C moment resisting space frame of 3 bays and 11 stories.

2. Type of Infills. Unreinforced and reinforced masonry units (hollow and solid bricks, and concrete blocks) and lightweight reinforced concrete.

3. Quality Control of Materials. In spite of fact that the masonry units used in construction were carefully selected and that the grout, mortar, and concrete were carefully designed, mixed, placed, and cured, considerable variations in the mechanical characteristics of these materials were observed, particularly in the masonry infill materials. The results indicated that the behavior of the infill is very sensitive to variations in the quality of material and therefore good quality control of all material is a must for certain types of infills.

4. Workmanship. Although good workmanship was used throughout construction of the infills, some weaker, stiffer, and premature types of inelastic behavior and pattern of cracking and/or crushing were attributed to lack of uniform workmanship in laying the masonry units

and in the anchorage of the infill to the frame; thus good workmanship is required.

5. Infill Panel Arrangement. The two external bays of the 3 bay frames were fully infilled, i.e., without any opening, and forming what can be called a "coupled infilled frame."

6. Type of Building Considered in the Assessment of the Implications of Results Obtained. Buildings having a rectangular plan consisting of 11 frames of 3 bays and of 11 stories high where the frames are fully infilled as described in item 5, and the locations of these infilled frames are such that no significant torsional forces are induced during the seismic response of the building. The importance of this limitation cannot be overemphasized.

7. Idealization of the Actual Lateral Load-Deformation Relationships of the Bare and Infilled Frames. The analytical assessment of the implications of the experimental results regarding behavior of the building have been made idealizing the actual experimental relationship by a linear elastic-perfectly plastic model using different yielding strengths and ductility levels.

8. Dynamic Characteristics of Building Site and Ground Motions. It has been assumed that: the building is on firm ground and a "rigid foundation" can be constructed; and that all the ground motions that can occur have dynamic characteristics similar to those included in the derivation of the smoothed linear elastic and inelastic design response spectra suggested by Newmark and Hall [6] and illustrated in Figs. 92 and 93. The importance of the limitations imposed by these assumptions in conjunction with the idealization pointed out in item 7, should be emphasized, particularly for the case where significant inelastic behavior is involved in the response. The effects of ground motions containing severe acceleration pulses (high a_{ep}) of long duration should be investigated before the conclusions to be presented herein are applied to the design of new buildings and/or to retrofitting of existing buildings. The interacting effects of the observed significant deformation softening

after reaching peak lateral resistance with long acceleration pulses input can lead to deformation demands considerably higher than those predicted by a linear elastic-perfectly plastic idealization.

9. Reliability of the Analytical Results. In view of all the assumptions, idealizations, and uncertainties involved in the conducted analysis, the numerical values obtained should be considered as approximate and indicating trends, rather than an exact representation of what can be expected in specific cases.

7.1 Conclusions

The main conclusions are presented below, grouped in the four following categories.

7.1.1 Conclusions Regarding Overall Behavior of the Infilled Specimen Tested

(1) The addition of either unreinforced or reinforced infill to moment resisting frame increases significantly the lateral stiffness and lateral resistance of the frame.

(2) As soon as cracking occurs, which happens very early, at service lateral load level, the initial tangential lateral stiffness decreases significantly, up to 80 percent, to a value that remains practically constant for a long range of lateral load. To represent this behavior an effective interstory stiffness at lateral service load has been defined.

(3) The lateral stiffness and strength depends on the history of loading. Under monotonically increasing load these two characteristics depend on the type of infill, the highest being for the lightweight concrete and the lowest for the brick. They do not depend upon how the panel is reinforced but they are sensitive to the quality control of the materials and to how well the infill is made, particularly to the workmanship along the interfaces of the infills and the boundary frame elements.

Under cyclic load the lateral strength and stiffness deteriorates, particularly if deformation reversals are included. The degree of deterioration depends upon the amount and type of reinforcement of the infill panel, and particularly the way that this panel is attached (anchored) to the frame.

(4) Hysteretic behavior depends upon the type of infill, the amount and arrangement of reinforcement and the way that the panel is attached (anchored) to the frame. The cyclic loading of unreinforced infills leads to considerable deterioration in stiffness and strength when compared with the values observed under monotonic loading. The peak strength under cyclic loading, which is somewhat smaller than that obtained under monotonically increasing load, deteriorates as the severity of deformation and number of cycles increases but remains somewhat larger than the strength of a frame with a soft story corresponding to the story in which damage of the infill concentrates. Excellent hysteretic behavior has been obtained with the use of solid brick masonry infills externally reinforced with welded wire fabric covered with cement mortar.

(5) Although the interstory displacement ductility under peak strength is small, about 2, large values are obtained under reduced strength. In the case of solid brick externally reinforced with welded wire fabric, this ductility was 4.2 under 86% of the peak strength, and reached the value of 14 under 68% of peak strength.

(6) Except for one specimen (reported in Ref. 1) whose failure mechanisms involved two stories, in all other specimens the damage concentrates in one story, consequently the final mechanism of failure is what can be defined as "a somewhat strengthened soft story frame." Thus the energy dissipated by an infilled R/C frame should be larger than a bare soft story frame.

(7) Failure of unreinforced masonry infills was accompanied by production of substantial debris containing hazardously large pieces of masonry. The amount of debris in reinforced infills was smaller and most was contained in the plane of the infill, particularly in solid brick

masonry reinforced externally with welded wire fabric.

(8) The effective viscous damping coefficient of the virgin specimens is smaller than 2 percent. As soon as cracking develops the value of this damping coefficient increases up to 12 percent.

7.1.2 Conclusions from Comparison of Behaviors of Infilled Frames and Bare Frame

(1) The initial tangential interstory lateral stiffness of the virgin infilled frames was more than 10 times the similar stiffness of the bare frame.

(2) The effective interstory lateral stiffness of virgin infilled frames was 5.3 to 11.7 times the lateral stiffness of the bare frame depending on the type of infill, the smallest being for the clay brick and the largest for the lightweight concrete infill.

(3) In case of repaired infills and retrofitting of repaired frames, the effective interstory lateral stiffness of the infilled frame was at least 3.4 times that of the virgin bare frame.

(4) The maximum lateral resistance of virgin infilled frames was 4.8 to 5.8 times that obtained for the bare frame. For cases or repaired infills and retrofitting of repaired frames the maximum lateral resistance was 2.8 to 8.0 times that of the bare frame. The maximum increase has been obtained with lightweight concrete infills and the minimum with clay bricks.

(5) The interstory displacement ductility ratio of the infilled frame is smaller than that of a bare frame but larger than that of a bare soft story frame. For what can be considered a maximum acceptable interstory drift index, say 0.02 or even for values of this index up to 0.07, the hysteretic behavior of the solid brick masonry externally reinforced with welded wire fabric was superior (large energy absorption and energy dissipation capacities) to that of the bare frame.

(6) The addition of infills introduces significant changes in

the dynamic characteristic of the bare moment resisting frame. It modifies significantly the periods, modes of vibration, as well as the damping of the specimens. In the linear elastic range the fundamental period is decreased more than 54%, while the mass is increased in not more than 10%. The effective viscous damping coefficient is increased considerably up to 500%. In the inelastic range the pattern of lateral deformations changed fundamentally because most of the significant inelastic deformations concentrate in one, or at the most, in two stories.

7.1.3 Conclusions Drawn from Assessment of the Implication of Experimental Results Obtained Regarding the Seismic Resistant Design of Buildings

(1) The addition of infill into the moment resisting frames of a building introduces significant changes in the dynamic characteristics of the building which should be considered in its design. These changes depend upon the number of frames that are infilled as well as the location of these frames.

(2) The mass is increased, however, even when all the transverse frames of the building under consideration (Fig. 1) are infilled, the increase with respect to a bare frame building is only about 10%. This increase in mass has two main effects. First, it induces a change in the period of the building which is about 5%, therefore it can be considered negligible in front of the uncertainties which exist in estimating the values of other main parameters. Secondly, the increase in mass increases directly, i.e., in 10% at the most, the reactive mass, thus it increases the inertia forces that are developed during the seismic response.

(3) The stiffness of the building is increased significantly. Considering average values obtained for each of the different types of infill, in the case where all the frames are infilled the increase varies from 366% to 994%. If only four of the frames are infilled the increase varies from 136% to 353%.

(4) Because of the relatively large increase in stiffness with respect to mass, the fundamental period of the structure is decreased significantly. If the 11 frames are infilled the decreases in the fundamental period varies from 54% to 70%. If only four frames are infilled the decrease varies from 35% to 53%.

(5) As consequence of the measured increase in the effective viscous damping ratio, ξ, obtained by the addition of the infills, the value of this ratio for the whole building has to increase when compared with a bare frame structure and, therefore, will result in a decrease in its seismic response (a value of ξ = 5% was assumed for the whole building in the analyses conducted).

(6) <u>Strength Supply</u>. The addition of the infills to the frames of the building can increase the available (supplied) strength significantly. If all the 11 frames are infilled the lateral strength in the transverse direction of the building is increased with respect to the strength of the bare frame building in 182% up to 700%, depending upon the type of infills. In the case where only 4 of the 11 frames are infilled, the increase varies from 34% to 255%. The smallest increase corresponds to the unreinforced masonry infills and the largest one is produced by the reinforced lightweight concrete.

(7) <u>Strength Demands</u>. As a consequence of the changes introduced by the addition of infills in the dynamic characteristics of the bare frame building, the demands in strengths for linear elastic behavior when subjected to ground motions similar to those considered in the derivation of the response spectra of Fig. 92 increases in 86% up to 141% when all the frames are infilled, and in 56% to 141% when only 4 of the 11 frames are infilled.

(8) <u>Supplied Strength vs. Demanded Strength in the Case of Elastic Behavior</u>. From comparison of values given in (6) and (7), it can be concluded that, except for cases of unreinforced infills in which only 4 of the 11 frames are infilled, the increase in supplied strength

is larger than the increase in the demanded strength, thus from the view-point of strength it is beneficial to add infills.

(9) Deformation Demands in the Case of Elastic Behavior. The addition of the infills decreases the demands on maximum displacement with respect to that corresponding to the bare frame building. The decreases vary from 56% to 85% in cases where all the frames are infilled, and 33% to 60% in cases where only 4 of the 11 frames are infilled. This decrease in displacement demand is a significant advantage in the use of infills.

(10) From conclusions (8) and (9) it is obvious that if it is possible to design the building to remain in the "elastic" range, then it is advantageous to add any of the types of infills reinforced with $\rho \geq 0.4\%$ that have been considered in this study. While a bare frame building can resist elastically ground motions similar to those considered in the derivation of the response spectra of Fig. 92 with an effective peak acceleration of $a_{ep} = 0.10$ g, the addition of infills of solid bricks reinforced externally with wire welded fabric allows the building to resist an $a_{ep} = 0.22$ g, i.e., an increase in 120% in intensity of ground motions if all the frames are infilled. If only 4 of the 11 frames are infilled it can resist an $a_{ep} = 0.14$ g, i.e., an increase in intensity of 40%. By infilling all the frames with reinforced lightweight concrete it is possible to resist elastically ground motions with an $a_{ep} \leq 0.32$ g, which means that they can be used in all the seismic regions of the U.S. except those classified as area 7 in the ATC map area classification.

(11) For buildings which can resist the extreme ground motion expected at the site through large inelastic deformations, the use of infills like that of solid bricks reinforced externally with welded wire fabric offers considerable advantage over the use of just bare frame. Because these infilled frames can develop an interstory displacement ductility $\mu_\delta = 4.2$ with a reduction in strength of only 14%, the building can resist ground motions with an $a_{ep} \leq 0.44$ g even if only

4 of the 11 frames are infilled. To be able to resist a similar ground motion the bare frame building will need to develop a $\mu_\delta \geq 5.6$ with significantly larger displacement, and consequently more damage throughout the whole structure. In the case of infilled frame the damage will concentrate in just one or two stories.

7.1.4 Conclusions Drawn from Assessment of the Implication of Experimental Results Obtained Regarding the Repair and Retrofitting of Existing Buildings

1. For bare frames that have been damaged (cracking and spalling of unconfined concrete) due to considerable yielding, developing inter-story displacement ductility of four, the following repair technique gives good result: removal of any crushed and loose concrete and re-casting of it, and injection of cracks with epoxy.

2. Undamaged, or damaged bare frames after their repair, can be effectively retrofitted for seismic resistant purposes by the addition of reinforced infills that are properly attached (anchored) to the frame. Of all the infills studied, the best was the one based on use of solid bricks reinforced externally with welded wire fabric covered with cement mortar and anchored to the frame, as illustrated in Figs. 77 through 81.

7.2 Recommendations for Future Research

(1) To investigate further the behavior of masonry infills which are externally reinforced with welded wire fabric and then covered with cement mortar or concrete. The use of soft hollow bricks or concrete blocks and of the shotcrete technique for applying the cover, should be studied.

(2) New methods for attaching (anchoring) the infill panels to the frame in the case of retrofitting these panels to existing bare frames, should be investigated.

(3) The values of the effective viscous damping ratio in bare frame and infilled frame building should be studied. The variation of

this ratio as damage increases in the infills should also be investigated further.

(4) Review the reliability of present analytical methods to predict strength, stiffness, and deformation capacity (energy absorption and energy dissipation capacities) of infilled frames and to develop new, simpler, and more reliable methods .

(5) To conduct integrated analytical and experimental studies (using earthquake simulators) on the seismic response of buildings with infilled frames when they are subjected to different types of ground motions, particularly those including severe acceleration pulses of long duration.

(6) To study effects of partial infilling as well as infill with openings.

(7) To investigate the feasibility of using infills for taller buildings by studying ways of infilling that will permit the spread of significant inelastic deformations to more than one story.

REFERENCES

[1] Klingner, R. E. and Bertero, V. V., "Infilled Frames in Earthquake Resistant Construction," Report No. EERC 76-32, Earthquake Engineering Research Center, University of California, Berkeley, December 1976.

[2] Biggs, J. M. and Grace, P. H., "Seismic Response of Buildings Designed by Code for Different Earthquake Intensities," MIT Structural Publicaiton No. 358, Massachusetts Institute of Technology, Cambridge, January 1973.

[3] Uniform Building Code, 1970 Edition, Vol. 1, International Conference of Building Officials, Whittier, California, 1970.

[4] Wilson, E. L. and Dovey, H. H., "Static and Earthquake Analysis of Three Dimensional Frame and Shear Wall Buildings," Report No. EERC 72-1, Earthquake Engineering Research Center, University of California, Berkeley, May 1972.

[5] Building Code Requirements for Reinforced Concrete (ACI 318-71), American Concrete Institute, 1971.

[6] Newmark, N. M. and Hall, W. I., "Procedures and Criteria for Earthquake Resistant Design," Building Standards for Disaster Mitigation, National Bureau of Standards, Building Science Series 46, February 1973.

[7] Newmark, N. M., "Current Trends in the Seismic Analysis and Design of High Rise Structures," Earthquake Engineering, Prentice-Hall, Inc., Englewood Cliffs, N.J., 1970.

[8] El-Hafez, M. B. and Powell, G. H., "Computer Aided Ultimate Load Design of Unbraced Multistory Steel Frames," Report No. EERC 73-3, Earthquake Engineering Research Center, University of California, Berkeley, 1973.

[9] Kent, D. C. and Park, R., "Flexural Members with Confined Concrete," Journal of the Structural Division, ASCE, Vol. 97, No. ST 7, July 1971.

[10] Mahin, S. A. and Bertero, V. V., "An Evaluation of Some Methods for Predicting Seismic Response of Reinforced Concrete Buildings," Report No. EERC 75-5, Earthquake Engineering Research Center, University of California, Berkeley, 1975.

[11] Mattock, A. H., "Rotational Capacity of Hinging Regions in Reinforced Concrete Beams," Proceedings of The International Symposium on the Flexural Mechanics of Reinforced Concrete, ACE Special Publication 12, November 1964.

[12] Corley, W. G., "Rotational Capacity of Reinforced Concrete Beams," Journal of the Structural Division, ASCE, Vol. 92, No. ST5, October 1966.

[13] ATC Publication ATC 3-06, "Tentative Provisions for the Development of Seismic Regulations for Buildings," National Bureau of Standards, June 1978.

[14] Park, R. and Paulay, T., "Reinforced Concrete Structures," John Wiley and Sons, 1975.

[15] Bertero, V. V., "Establishment of Design Earthquakes: Evaluation of Present Methods," Proceedings of The International Symposium on Earthquake Structural Engineering, University of Missouri, Rolla, Vol. 1, pp. 551-580, August 1976.

[16] Mahin, S. A. and Bertero, V. V., "An Evaluation of Inelastic Seismic Design Spectra," Proceedings, ASCE, Vol. 107, No. ST9, September 1981.

T A B L E S

TABLE 1 SUMMARY OF SPECIMENS TESTED AND THEIR MAXIMUM RESISTANCE

TEST SPECIMEN NO.	MODEL NO.	LOADING PROGRAM	FIRST-STORY PANEL	SECOND-STORY PANEL	THIRD-STORY PANEL	MAX LOAD (KIPS)*	LOCATION OF FAILURE
1	1	Monotonic	Clay Brick ρ=0%	Clay Brick ρ=0.6%	Clay Brick ρ=0.6%	55.2	First Story
2	1,R1	Cyclic	Clay Brick ρ=0%	Clay Brick ρ=0.6%	Clay Brick ρ=0.6%	35.3	First Story
3	3	Monotonic	Concrete Brick ρ=0.6%	LWC ρ=0.6%	LWC ρ=0.6%	67.9	First Story
4	2	Cyclic	Clay Brick ρ=0.6%	Clay Brick ρ=0.6%	Clay Brick ρ=0.6%	54.5	First Story
5	1,R2	Monotonic	6in. R/C	Clay Brick ρ=0.6%	Clay Brick ρ=0.6%	68.6	Third Story
6	1,R3	Cyclic	6in. R/C	Clay Brick ρ=0.6%	RC ρ=0.6%	80.0	Second Story
7	2,R1	Cyclic	Clay Brick ρ=0.15%	Clay Brick ρ=0.6%	Clay Brick ρ=0.6%	39.2	First Story
8	3,R1	Cyclic	Concrete Brick ρ=0.6%	LWC ρ=0.6%	LWC ρ=0.6%	46.7	First Story
9	3,R2	Cyclic	No Panel	LWC ρ=0.6%	LWC ρ=0.6%	27.4	First Story
10	3,R3	Cyclic	6in. R/C	LWC ρ=0.6%	LWC ρ=0.6%	92.7	Second Story
11	3,R4	Monotonic	6in. R/C	LWC ρ=0.6%	LWC ρ=0.6%	100.0	Second Story
12	1,R4	Monotonic	6in. R/C	Clay Brick ρ=.15%	RC ρ=0.6%	63.2	Second Story
13	2,R2	Cyclic	6in. R/C	Clay Brick ρ=0.6%	Clay Brick ρ=0.6%	76.0	Third Story
14	2,R3	Monotonic	6in. R/C	Clay Brick ρ=0.6%	RC ρ=0.6%	83.0	Second Story
15	4	Cyclic	No Panel	No Panel	No Panel	12.6	Total Mechanism
16	5	Cyclic	Split Brick 90° =0.4%	Split Brick 90° =0.4%	Split Brick 90° =0.4%	70.7 56.6**	First Story
17	5,R1	Monotonic	Split Brick 90° =0.4%	Split Brick 90° =0.4%	Split Brick 90° =0.4%	61.3 49.0**	First Story
18	4,R1	Cyclic	Split Brick 45° =0.4%	Split Brick 45° =0.4%	Split Brick 45° =0.4%	57.3 45.8**	Combined Mechanism

*1 Kip = 4.45 KN

** Factored by $\frac{2.0 \text{ in}}{2.5 \text{ in}}$

TABLE 2 MECHANICAL CHARACTERISTICS OF MATERIALS

(a) FRAME CONCRETE AND INFILL MATERIALS

SPECIMEN NO.	COMPRESSIVE STRENGTH OF			
	FRAME CONCRETE (ksi)*	INFILL MATERIALS		
		MASONRY UNITS (ksi)*	GROUT (ksi)*	MORTAR (ksi)*
1	3.78	Clay 6.11	1.47	2.00
2	3.78	Clay 6.11	1.95	0.46
3	4.00	Concrete 2.10-3.90	3.21	5.45
4	3.19	Clay 6.11	2.63	2.50
5	3.78	Clay 6.11	3.55	4.41
6	3.78	Clay 6.11	3.53	3.66
7	3.19	Clay 6.11	No data	No data
8	4.00	Concrete 2.1-3.9	3.20	5.45
9	4.00	No panel	No panel	No panel
10	4.00	LWC 6.02	---	---
11	4.00	LWC 5.73	---	---
12	3.78	Clay 6.11	No data	No data
13	3.19	Clay 6.11	3.18	4.38
14	3.19	Clay 6.11	4.15	4.19
15	4.51	No panel	No panel	No panel
16	5.16	Solid 1.90	5.39**	2.78
17	5.75	Solid 1.90	3.26**	No data
18	5.00	Solid 1.90	5.13**	1.61

* 1 ksi = 0.145 MPa

** Cement Mortar Cover. See Construction Details, Fig. 79

(b) REINFORCING STEEL

TYPE	YIELDING STRENGTH f_y (ksi)*	TENSILE STRENGTH f_{ult} (ksi)*
#7 BAR	72.6	100.3
#4 BAR	74.2	107.5
#3 BAR	68.2	94.5
#2 BAR	73.4	105.8
#5 GA. WIRE	97.0	98.4
#11 GA. WIRE	102.0	110.0
2 x 2 MESH	55.0	72.7

* 1 ksi = 0.145 MPa

TABLE 3 MAXIMUM INTERSTORY LATERAL STIFFNESS OF TEST SPECIMENS

TEST SPECIMEN	MAXIMUM INTERSTORY LATERAL STIFFNESS		
	INITIAL TANGENT (K/in)*	EFFECTIVE STIFFNESS AT SERVICE LOAD LEVEL, K_I^s (K/in)*	RELATIVE STIFFNESS K_I^s/K_{bf}^s
1	1090	206	5.89
2	1090	236	6.74
3	585	212	6.06
4	920	187	5.34
5	195	195	5.57
6	271	238	6.80
7	780	195	5.57
8	725	250	7.14
9	103	60	1.71
10	990	358	10.23
11	1500	409	11.69
12	494	167	4.77
13	178	176	5.03
14	203	210	6.00
15	65	35	1.00
16	1250	292(234)	8.34(6.69)**
17	834	118(94)	3.37(2.69)**
18	960	203(162)	5.80(4.63)**

*1 K/in = 0.175 KN/mm ** Factored by $\frac{2.0\text{ in}}{2.5\text{ in}}$

TABLE 4 EFFECTS OF INFILLS ON THE PERIOD, T_{if}, OF THE PROTOTYPE BUILDING

DEGREE OF CHANGES AND TYPE OF INFILL	UPPER BOUND ALL 11 FRAMES ARE INFILLED				LOWER BOUND ONLY 4 OF THE 11 FRAMES ARE INFILLED			
	SAME MASS			INFILL ADD MASS	SAME MASS			INFILL ADD MASS
	T^{+}_{if}/T_{bf}*	T^{+}_{if} in secs for T_{bf} (secs)		T^{+}_{if}/T_{bf}	T^{-}_{if}/T_{bf}	T^{-}_{if} in secs for T_{bf} (secs)		T^{-}_{if}/T_{bf}
		1.30	1.01			1.30	1.01	
LOWEST (Solid Brick with WWF)	0.46	0.60	0.46	0.49	0.65	0.84	0.66	0.66
AVERAGE (Hollow Massonry)	0.40	0.52	0.40	0.42	0.58	0.75	0.59	0.59
HIGHEST (Lightweight Concrete)	0.30	0.39	0.30	0.32	0.47	0.61	0.47	0.48

*T_{bf} is the Period of the Prototype Building with Bare Frame Structure

TABLE 5 EFFECTS OF INFILLS ON SUPPLIED MAXIMUM STRENGTH OF THE PROTOTYPE BUILDING, $(V_n)_{if}$

COMPARISON OF $(V_n)_{if}$ WITH THE SUPPLIED MAXIMUM STRENGTH OF THE BUILDING BARE FRAME $(V_n)_{bf}$ BASED ON THE MEASURED STRENGTH OF THE SPECIMENS, i.e., $\frac{(V_n)^s_{if}}{(V_n)^s_{bf}}$ BEING $(V_n)^s_{bf} = 12.5$ kips

TYPE OF INFILL AND REINFORCEMENT	(ρ in%)	UPPER BOUND ALL 11 FRAMES ARE INFILLED: $(V_n)^s_{if}$ (kips)*	$(V_n)^s_{if}/(V_n)^s_{bf}$	$(V_n)_{if}$ kips	Increase of Strength in %	LOWER BOUND ONLY 4 OF 11 FRAMES ARE INFILLED: $\frac{7(V_n)^s_{bf}+4(V_n)^s_{if}}{11(V_n)^s_{bf}}$	$(V_n)_{if}$ kips	Increase of Strength in %
UNREINFORCED MASONRY	0.	Lower 35.3	2.82	6989	182	Highest 1.66	4117	66
						Lowest 1.34	3329	34
REINFORCED HOLLOW MASONRY	0.15	Lower 39.0	3.14	7722	214	Highest 1.78	4383	78
	0.60					Lowest 1.46	3596	46
		Lowest 46.7	3.74	9247	274	Highest 2.00	4937	100
						Lowest 1.68	4150	68
		Average 65.0	5.20	12870	420	Highest 2.53	6255	153
						Lowest 2.21	5468	121
		Highest 83.0	6.64	16434	564	Highest 3.05	7551	205
						Lowest 2.73	6764	173
SOLID BRICK REINFORCED WITH WWF	0.40	Lowest 57.3	4.58	11345	358	Highest 2.30	5701	130
						Lowest 1.39	4914	98
		Average 63.1	5.05	12494	405	Highest 2.47	6118	147
						Lowest 2.15	5330	115
		Highest 70.7	5.65	13999	465	Highest 2.69	6665	169
						Lowest 2.37	5878	137
REINFORCED LIGHTWEIGHT CONCRETE	0.60	Lower 92.7	7.42	18355	642	Higest 3.34	8249	234
						Lowest 3.02	7452	202
		Higher 100.0	8.00	19800	700	Highest 3.55	8775	255
						Lowest 3.23	7988	223

*1 K = 4.45 KN

TABLE 6 INCREASE IN LINEAR ELASTIC SEISMIC FORCE DEMANDS, V_{if}^{D}, DUE TO CONSIDERATION OF INFILLS AS STRUCTURAL ELEMENTS

COMPARISON OF V_{if}^{D} WITH SEISMIC FORCE DEMANDS BASED ON THE BUILDING BARE FRAME STRUCTURE, V_{bf}^{D}, AND FOR SAME MASS

DEGREES OF CHANGE IN T, AND TYPE OF INFILL	T_{bf} in secs	UPPER BOUND ALL 11 FRAMES ARE INFILLED			LOWER BOUND ONLY 4 OF THE 11 FRAMES ARE INFILLED		
		T_{if}^{+} in secs	V_{in}^{D} / V_{bf}^{D}	Increase in %	T_{if}^{-} in secs	V_{in}^{D} / V_{bf}^{D}	Increase in %
LOWEST (Solid Brick with WWF)	$\frac{1.30}{1.01}$	$\frac{0.60}{0.46}$	$\frac{2.41}{1.86}$	$\frac{141}{86}$	$\frac{0.84}{0.66}$	$\frac{1.56}{1.57}$	$\frac{56}{57}$
AVERAGE (Hollow Masonry)	$\frac{1.30}{1.01}$	$\frac{0.52}{0.40}$	$\frac{2.41}{1.86}$	$\frac{141}{86}$	$\frac{0.75}{0.54}$	$\frac{1.76}{1.86}$	$\frac{76}{86}$
HIGHEST (Lightweight Concrete)	$\frac{1.30}{1.01}$	$\frac{0.39}{0.30}$	$\frac{2.41}{1.86}$	$\frac{141}{86}$	$\frac{0.61}{0.47}$	$\frac{2.41}{1.86}$	$\frac{141}{86}$

TABLE 7 DECREASE IN LINEAR ELASTIC DISPLACEMENT DEMANDS, δ_{if}^{D}, DUE TO CONSIDERATION OF INFILLS AS STRUCTURAL ELEMENTS

COMPARISON OF δ_{if}^{D} WITH THE DISPLACEMENT DEMANDS BASED ON THE BUILDING BARE FRAME STRUCTURE, δ_{bf}^{D}

DEGREES OF CHANGE IN T, AND TYPE OF INFILLS	T_{bf}^{p} in secs	UPPER BOUND ALL 11 FRAMES ARE INFILLED			LOWER BOUND ONLY 4 OF THE 11 FRAMES ARE INFILLED		
		T_{if} in secs	$\delta_{in}^{D} / \delta_{bf}^{D}$	Decrease in %	T_{if} in secs	$\delta_{in}^{D} / \delta_{bf}^{D}$	Decrease in %
LOWEST (Solid Brick with WWF)	$\frac{1.30}{1.01}$	$\frac{0.60}{0.46}$	$\frac{0.44}{0.34}$	$\frac{56}{66}$	$\frac{0.84}{0.60}$	$\frac{0.66}{0.67}$	$\frac{34}{33}$
AVERAGE (Hollow Masonry)	$\frac{1.30}{1.01}$	$\frac{0.52}{0.40}$	$\frac{0.34}{0.24}$	$\frac{66}{76}$	$\frac{0.75}{0.54}$	$\frac{0.60}{0.49}$	$\frac{40}{51}$
HIGHEST (Lightweight Concrete)	$\frac{1.30}{1.01}$	$\frac{0.39}{0.30}$	$\frac{0.18}{0.15}$	$\frac{82}{85}$	$\frac{0.61}{0.47}$	$\frac{0.46}{0.40}$	$\frac{54}{60}$

TABLE 8 BUILDING SEISMIC RESISTANT COEFFICIENT, $C = \frac{(V_n)}{W}$

AND EFFECTIVE PEAK ACCELERATION, a_{ep}, THAT IT CAN RESIST ELASTICALLY

TYPE OF INFILL AND REINFORCEMENT	(ρ in %)	UPPER BOUND ALL 11 FRAMES ARE INFILLED				LOWER BOUND ONLY 4 OF 11 FRAMES ARE INFILLED			
		V_n (kips)*	C	T (secs)	a_{ep}/g	V_n (kips)*	C	T (secs)	a_{ep}/g
NONE BARE FRAME		2475	0.11	1.30	0.10	2475	0.11	1.30	0.10
UNREINFORCED MASONRY	0.%	6989 (L)	0.30	0.52	0.12	3329	0.14	0.75	0.07
REINFORCED HOLLOW MASONRY	0.15%	7762 (L)	0.34	0.52	0.13	3610	0.16	0.75	0.08
	0.6%	12870 (Av)	0.56	0.52	0.22	5468	0.24	0.75	0.13
SOLID BRICK REINFORCED WITH WWF	0.4%	12494 (Av)	0.54	0.60	0.21	5330	0.23	0.84	0.14
REINFORCED LIGHTWEIGHT CONCRETE	0.6%	19107 (Av)	0.83	0.39	0.32	7735	0.33	0.61	0.17

*1 kip = 4.45 KN

F I G U R E S

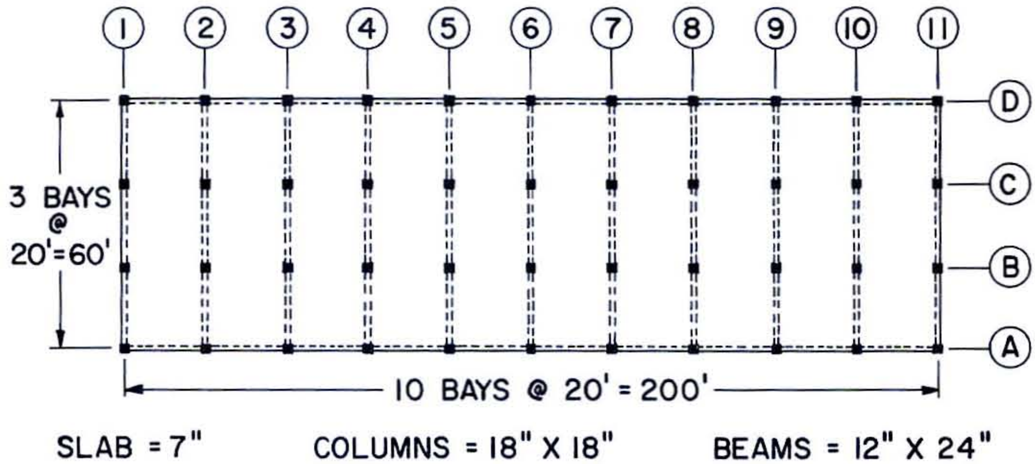

FIG. 1 FLOOR FRAMING PLAN, PROTOTYPE BUILDING

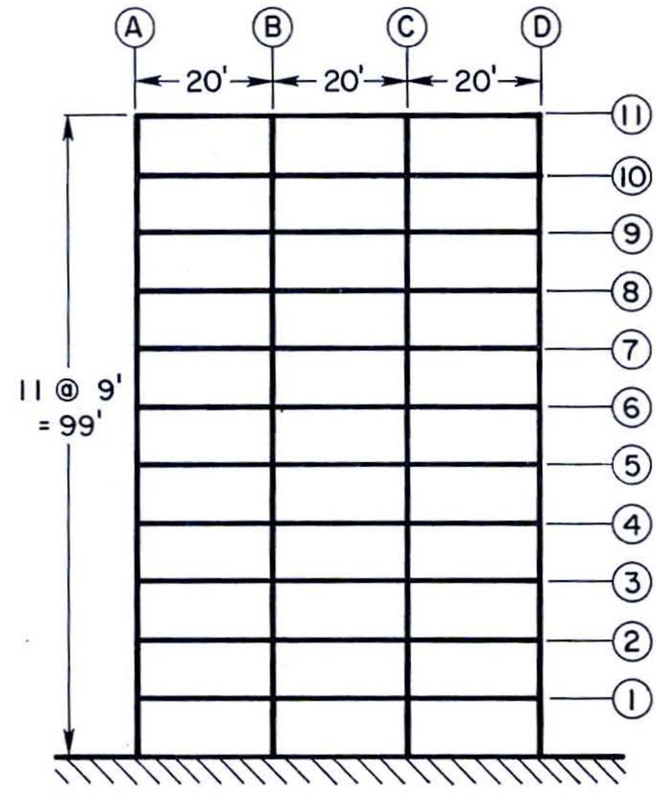

FIG. 2 ELEVATION OF PROTOTYPE END FRAME

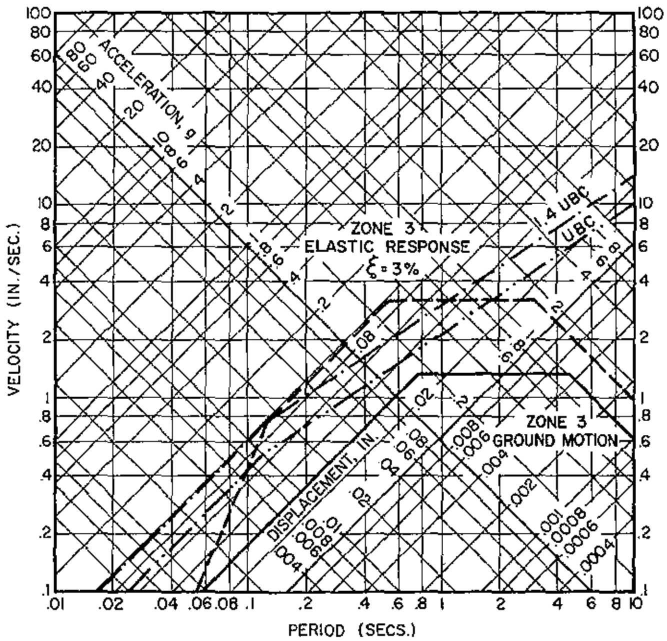

FIG. 3 ELASTIC DESIGN SPECTRA

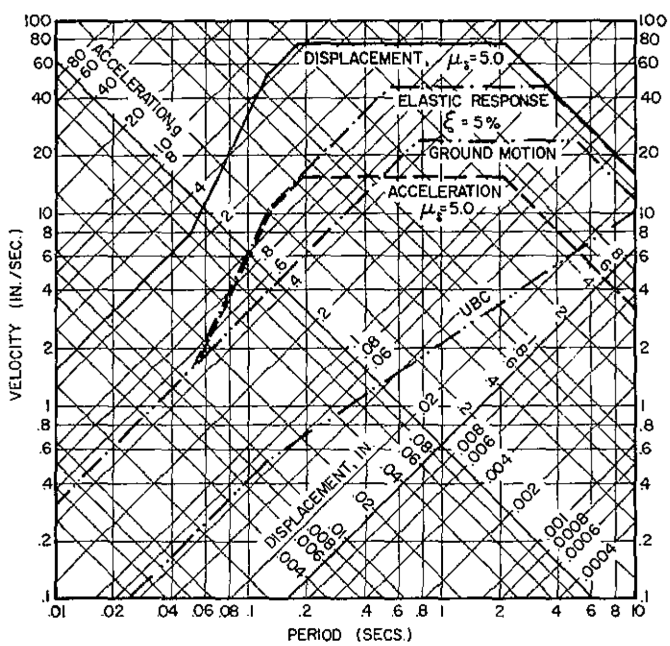

FIG. 4 ELASTO-PLASTIC DESIGN SPECTRA

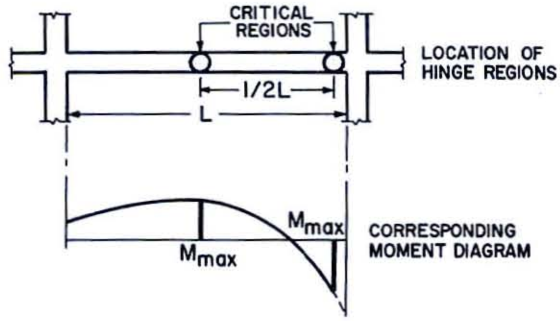

FIG. 5 LOCATION OF CRITICAL REGIONS FOR DESIGN OF BEAMS AGAINST SHEAR

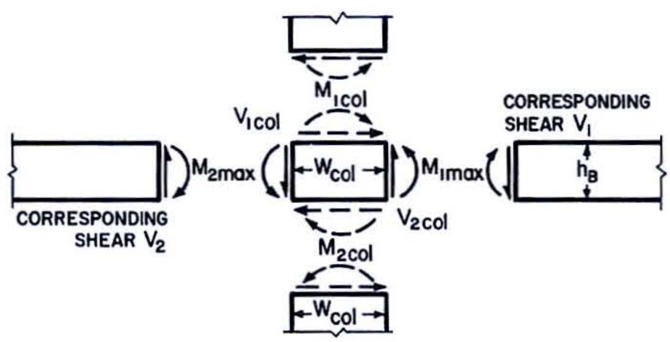

$$M_{1col} + M_{2col} = \left[M_{1max} + M_{2max} + \frac{W_{col}}{2}(V_1 + V_2) - \frac{h_B}{2}(V_{1col} + V_{2col})\right]$$

FIG. 6 CRITERIA USED FOR STRONG-COLUMN, WEAK-BEAM DESIGN

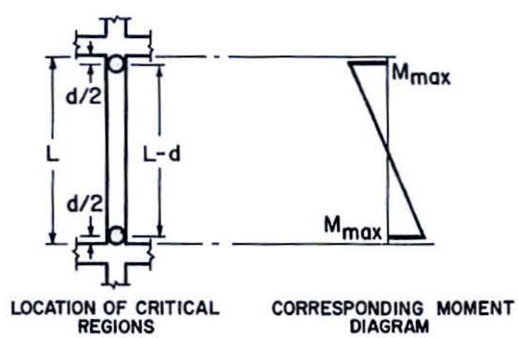

FIG. 7 LOCATION OF CRITICAL REGIONS FOR DESIGN OF COLUMNS AGAINST SHEAR

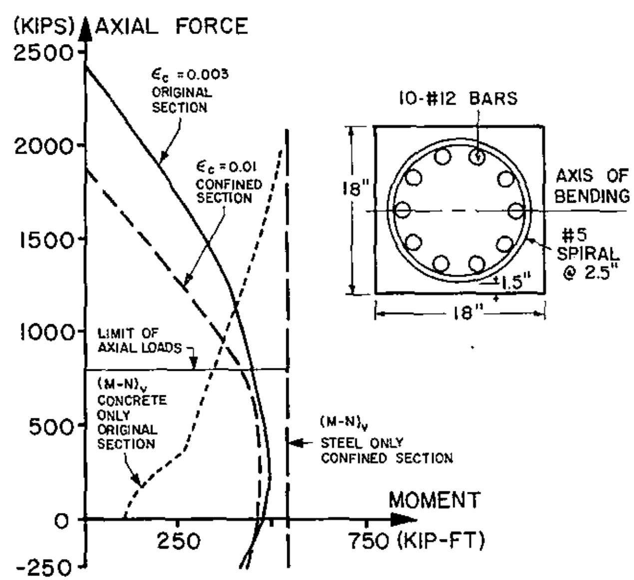

FIG. 8 MOMENT-AXIAL FORCE INTERACTION DIAGRAM, PROTOTYPE COLUMN

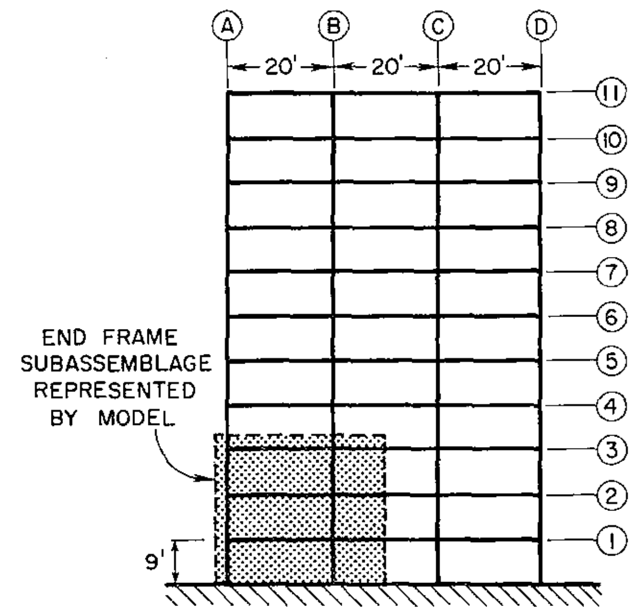

FIG. 9 END FRAME ELEVATION SHOWING LOCATION OF SUBASSEMBLAGE

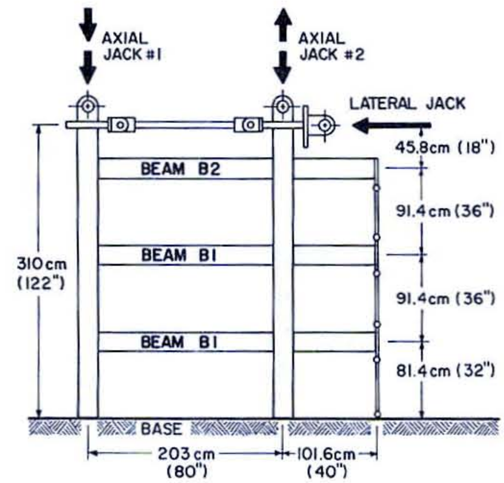

FIG. 10(a) STRUCTURAL SUBASSEMBLAGE TEST SPECIMEN

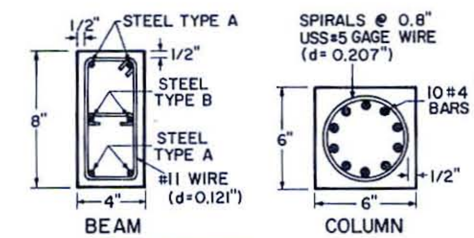

BEAM TYPE*	STEEL TYPE A	STEEL TYPE B	TRANSVERSE REINFORCEMENT
B1	#3	#2 DEFORMED	HOOPS AND CROSSTIES @ 1"
B2	#3	USS #11 GAGE WIRE	USS #11 GAGE WIRE (d = 0.121")

*REFER TO FIG. 10a

GRADE 60 STEEL
NOMINAL f_y= 60 KSI

FIG. 10(b) DESIGN DETAILS OF FRAME MEMBERS

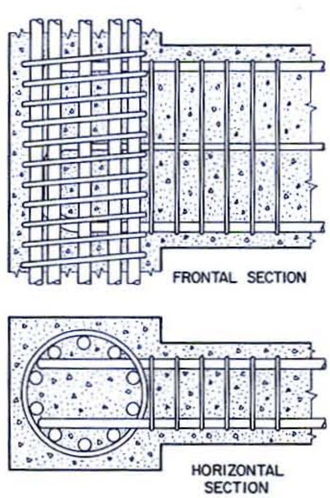

FIG. 10(c) DETAIL OF FIRST-STORY EXTERIOR BEAM COLUMN CONNECTION

FIG. 10 TEST SPECIMEN AND DESIGN DETAILS

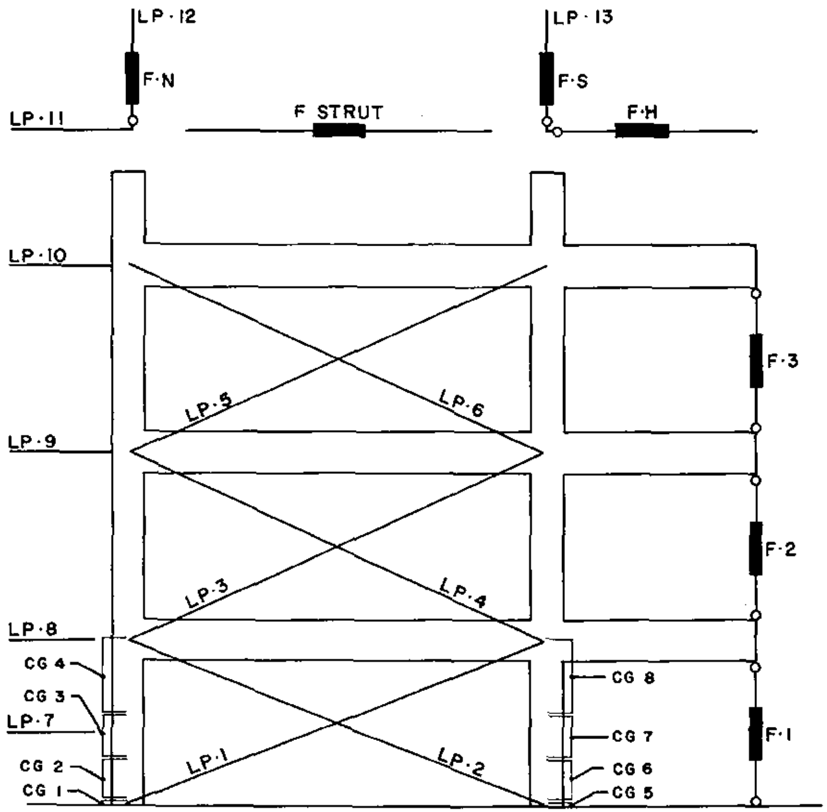

LP = LINEAR POTENTIOMETER, MEASURES DISPLACEMENT
CG = CLIP GAGE, MEASURES DISPLACEMENT
WG = WELDABLE MICRODOT GAGE, MEASURES STEEL STRAIN
F·1,F·2,F·3 = CONNECTING STRUT FORCES
F·N,F·S,F·H = HYDRAULIC JACK LOADS

FIG. 11 TYPICAL EXTERNAL INSTRUMENTATION

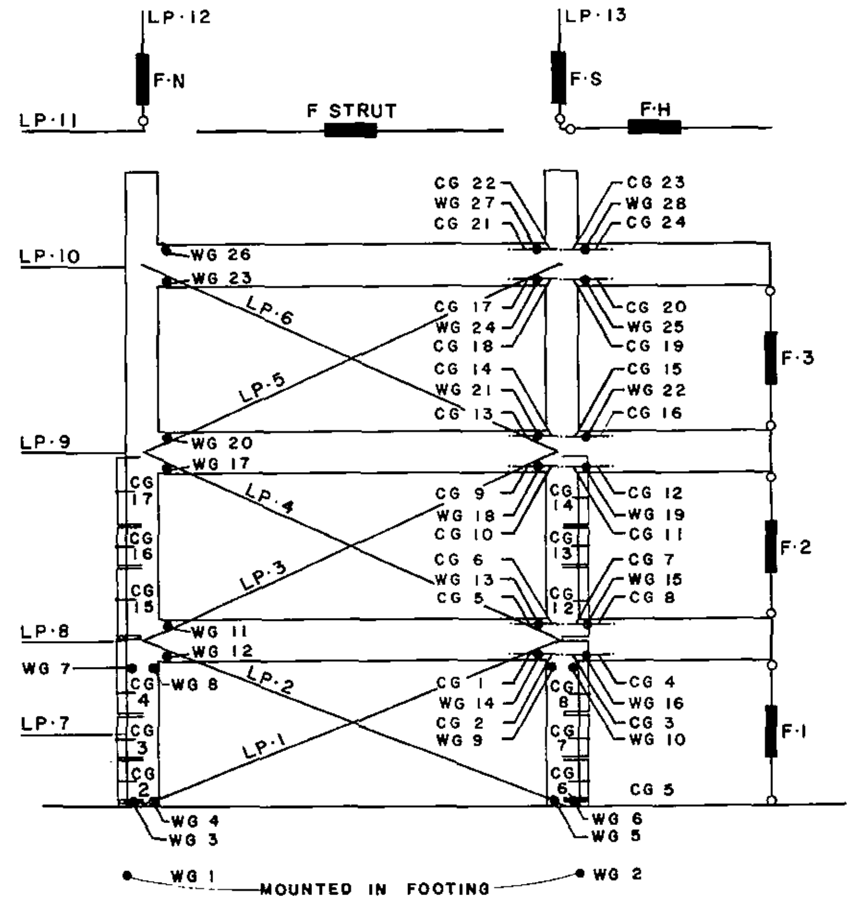

FIG. 12 INSTRUMENTATION, TEST SPECIMEN 15

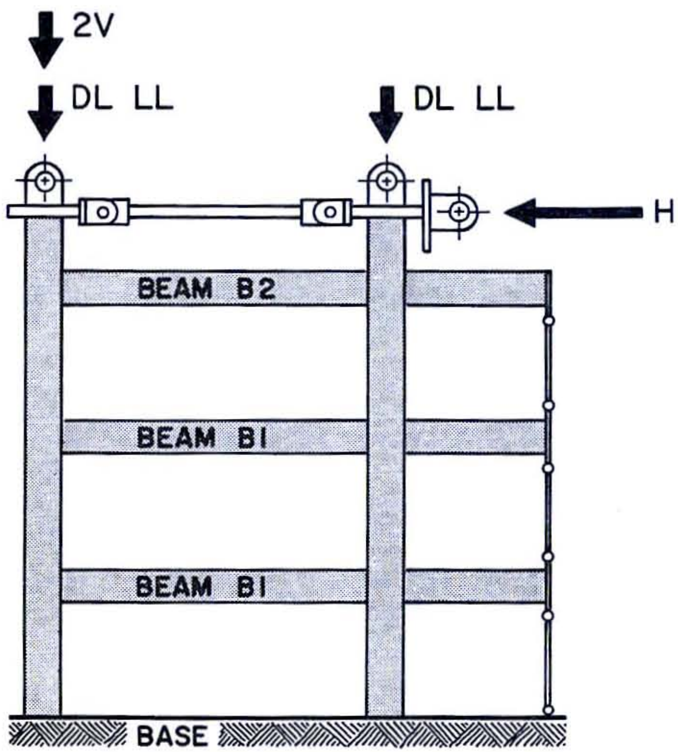

FIG. 13 LOADING PATTERN FOR BARE FRAME

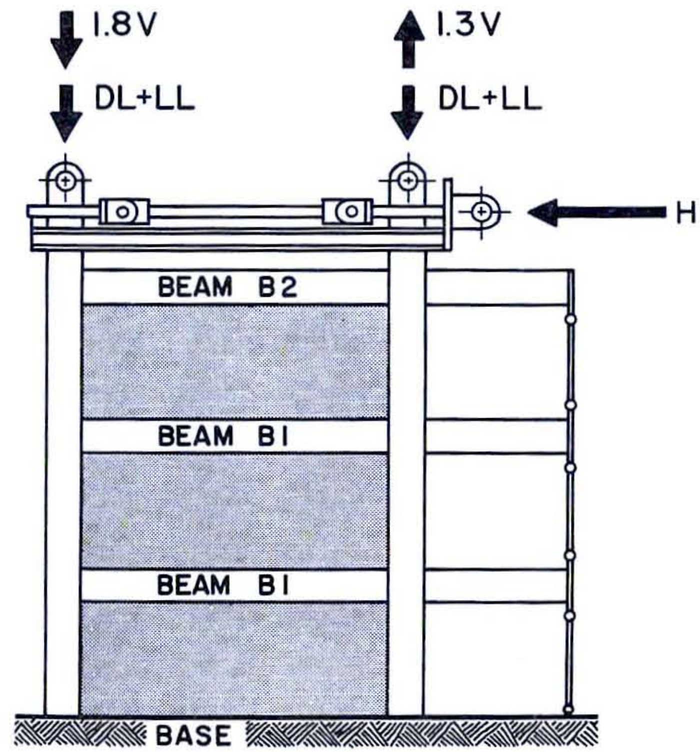

FIG. 14 LOADING PATTERN FOR INFILLED FRAME

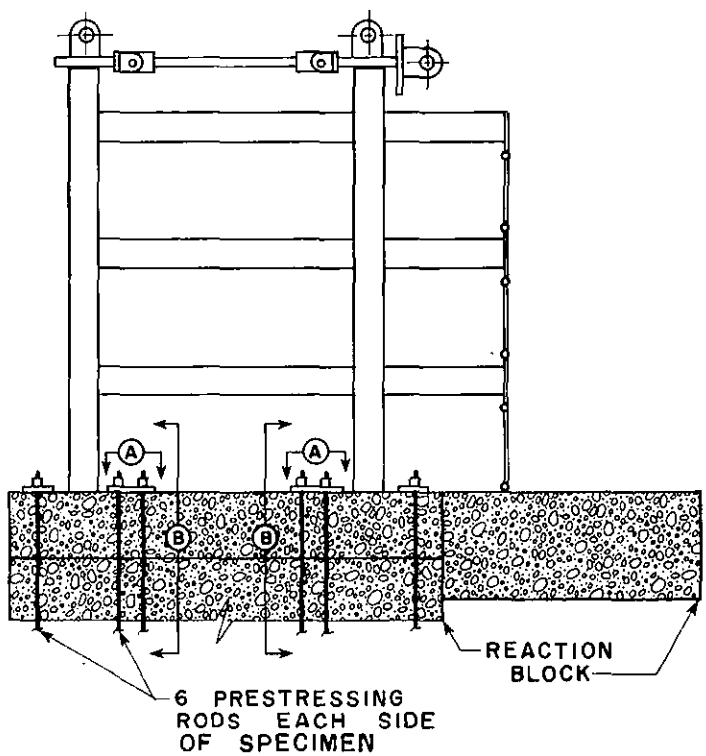

FIG. 15 SPECIMEN WITH STRENGTHENED FIRST-STORY PANEL

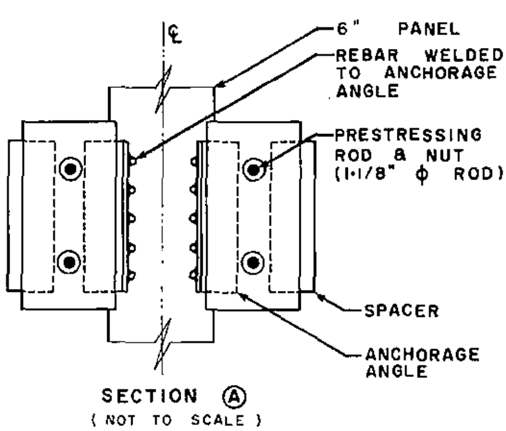

(a)

FIG. 16 DETAILS OF SPECIMEN OF STRENGTHED FIRST-STORY PANEL (SEE FIG. 15)

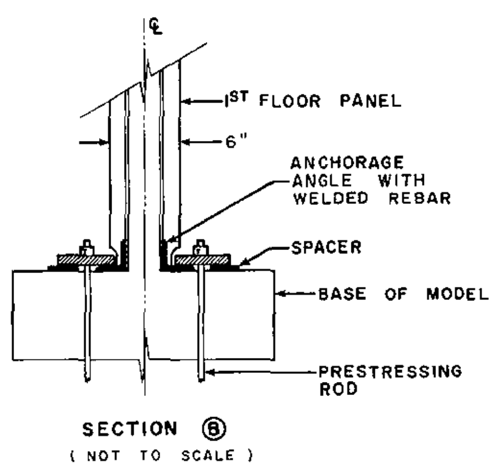

(b)

FIG. 16 DETAILS OF SPECIMEN OF STRENGTHENED FIRST-STORY PANEL (SEE FIG. 15)

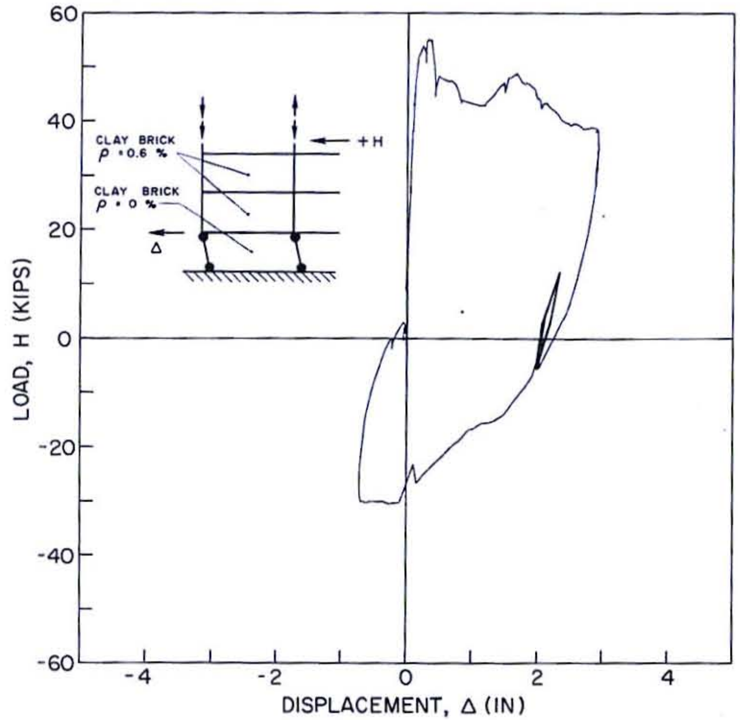

FIG. 17 LOAD-DEFLECTION RELATIONSHIP, TEST SPECIMEN 1

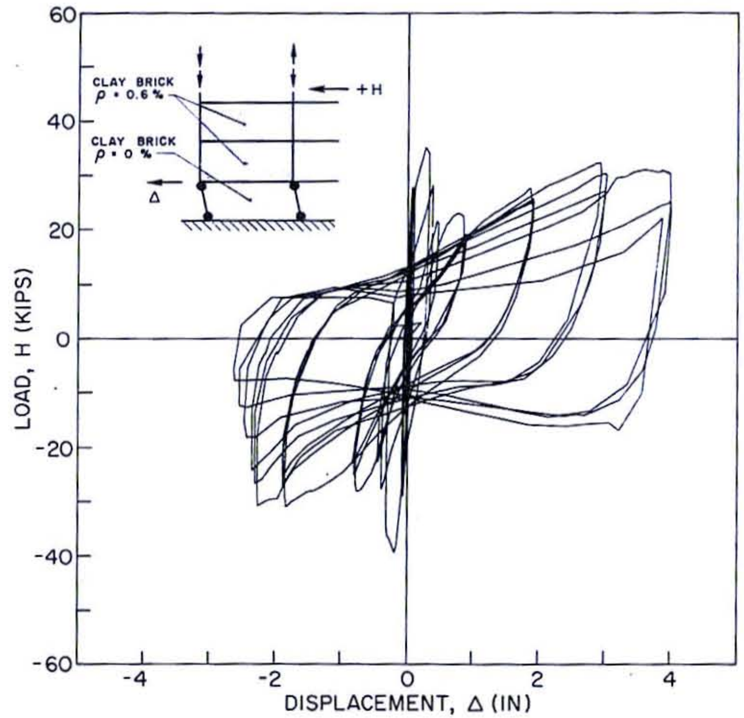

FIG. 18 LOAD-DEFLECTION RELATIONSHIP, TEST SPECIMEN 2

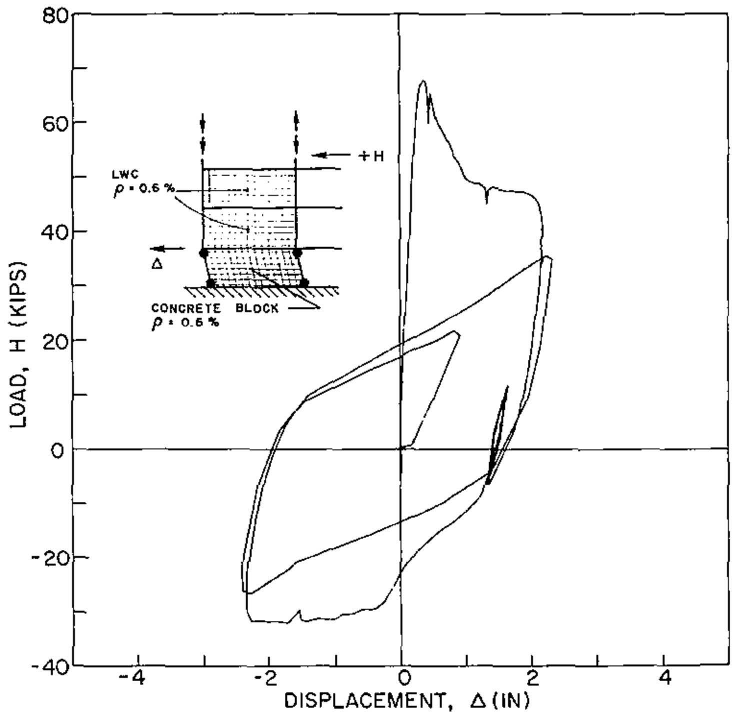

FIG. 19 LOAD-DEFLECTION RELATIONSHIP, TEST SPECIMEN 3

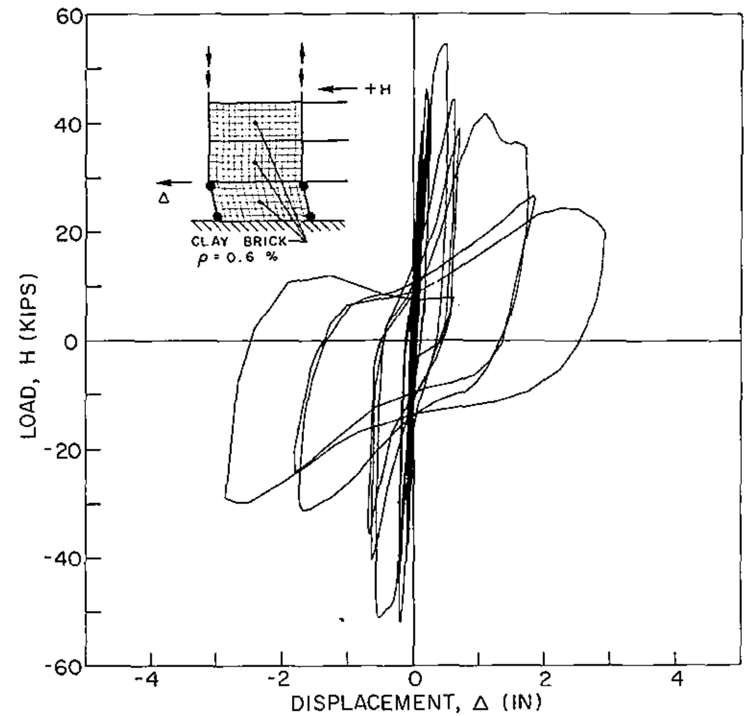

FIG. 20 LOAD-DEFLECTION RELATIONSHIP, TEST SPECIMEN 4

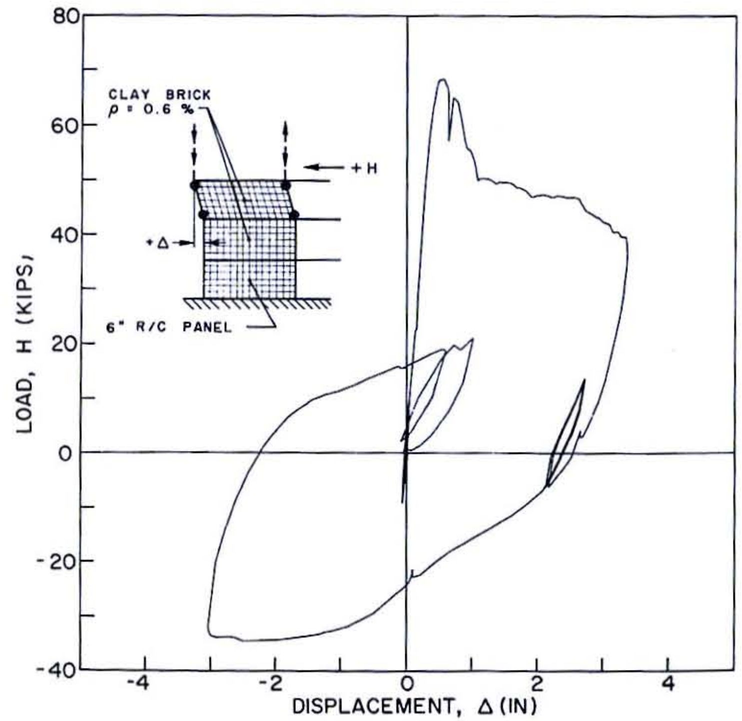

FIG. 21 LOAD-DEFLECTION RELATIONSHIP, TEST SPECIMEN 5

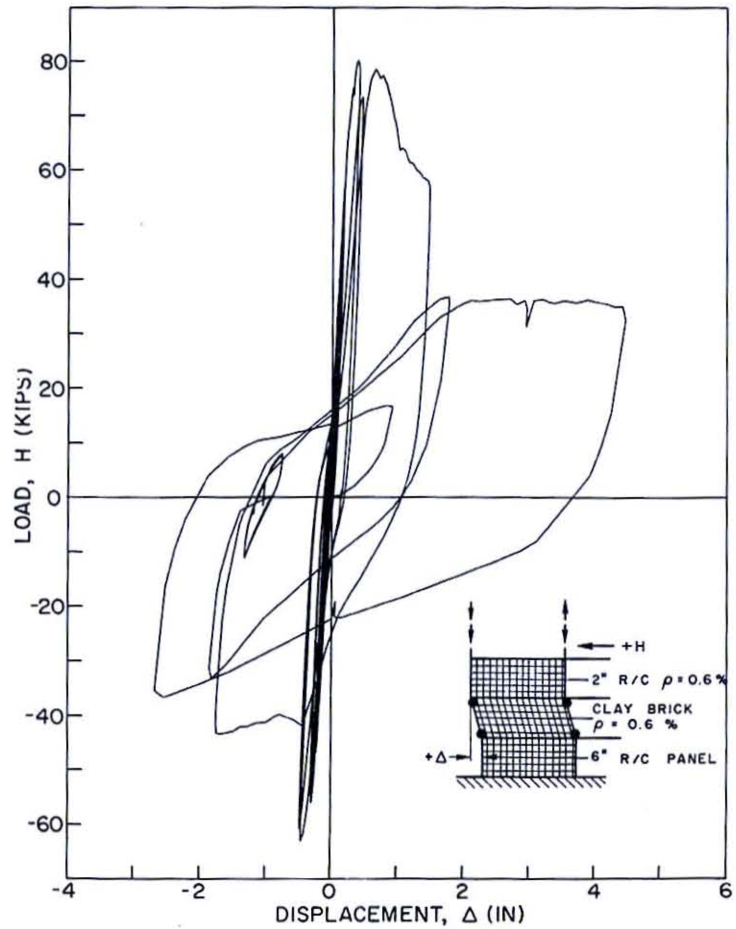

FIG. 22 LOAD-DEFLECTION RELATIONSHIP, TEST SPECIMEN 6

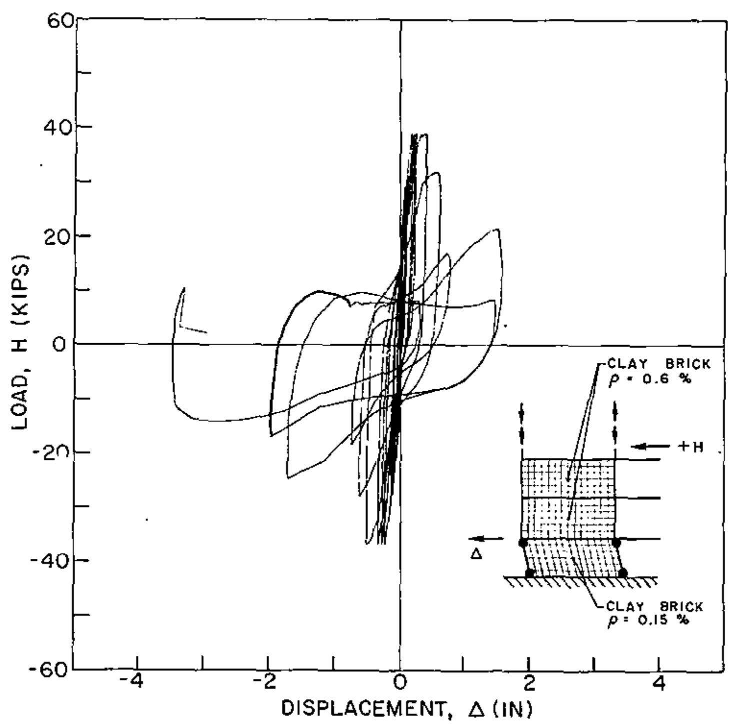

FIG. 23 LOAD-DEFLECTION RELATIONSHIP,
TEST SPECIMEN 7

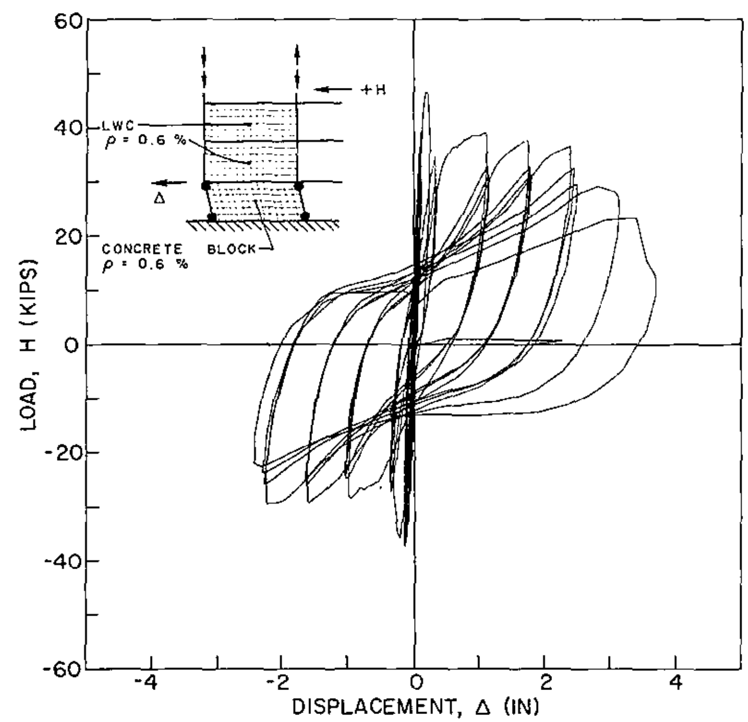

FIG. 24 LOAD-DEFLECTION RELATIONSHIP,
TEST SPECIMEN 8

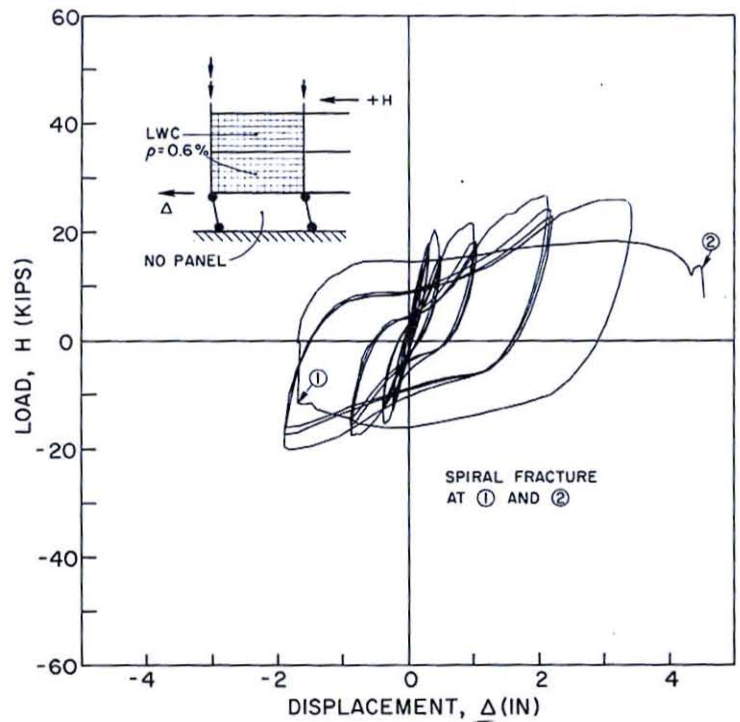

FIG. 25 LOAD-DEFLECTION RELATIONSHIP, TEST SPECIMEN 9

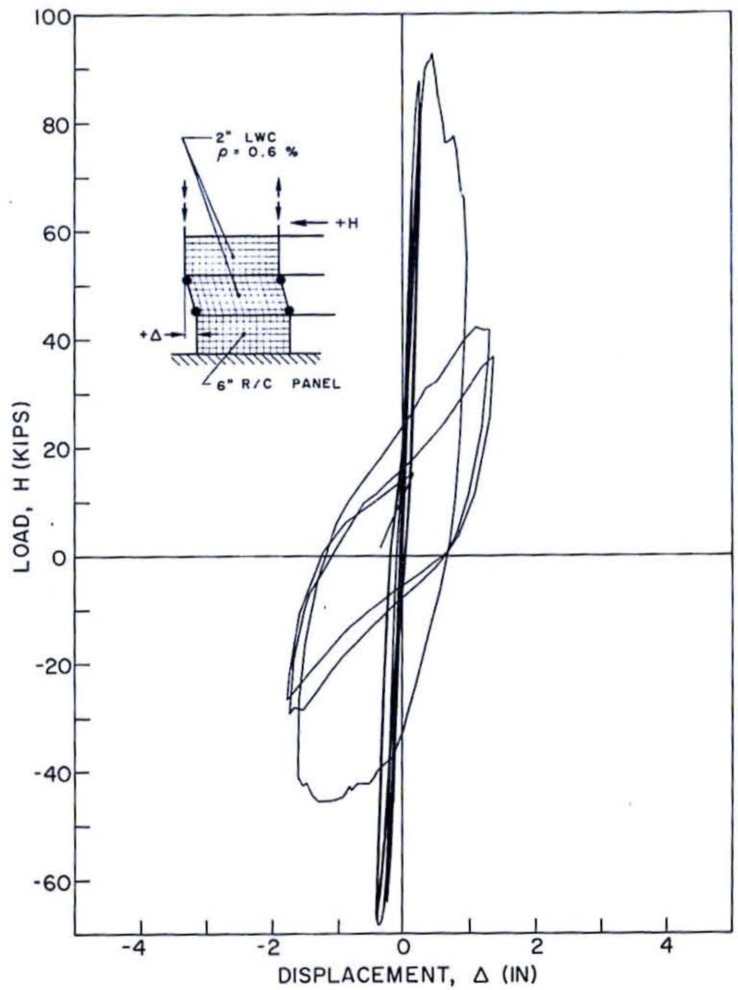

FIG. 26 LOAD-DEFLECTION RELATIONSHIP, TEST SPECIMEN 10

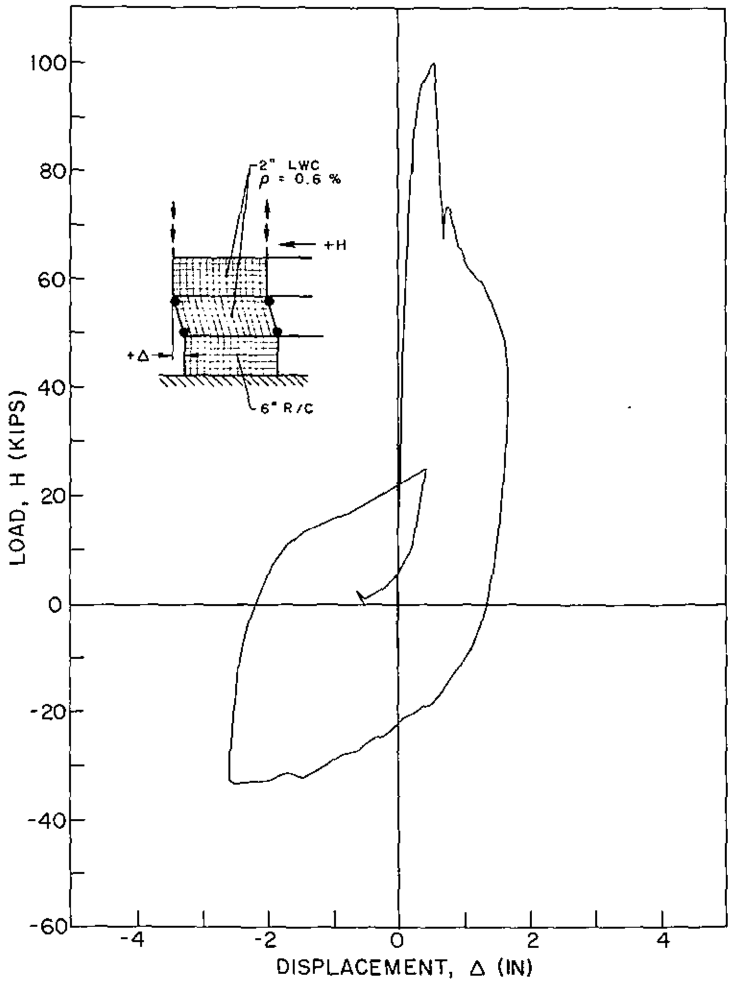

FIG. 27 LOAD-DEFLECTION RELATIONSHIP, TEST SPECIMEN 11

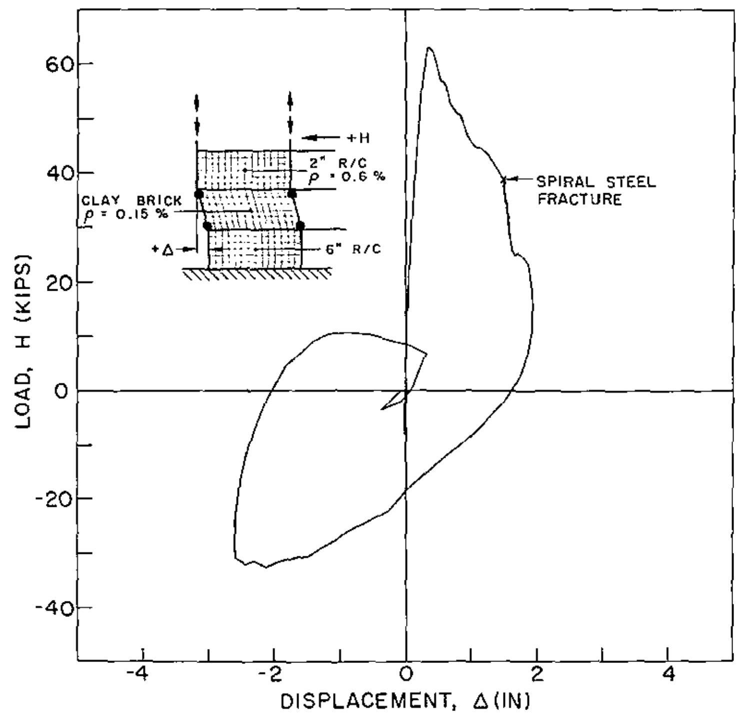

FIG. 28 LOAD-DEFLECTION RELATIONSHIP, TEST SPECIMEN 12

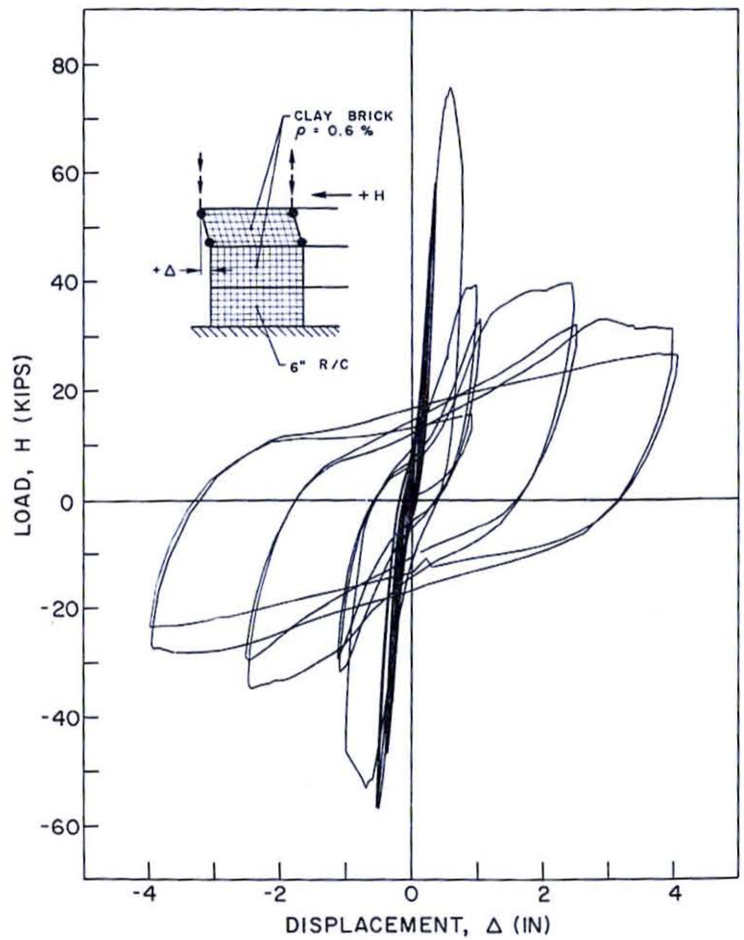

FIG. 29 LOAD-DEFLECTION RELATIONSHIP, TEST SPECIMEN 13

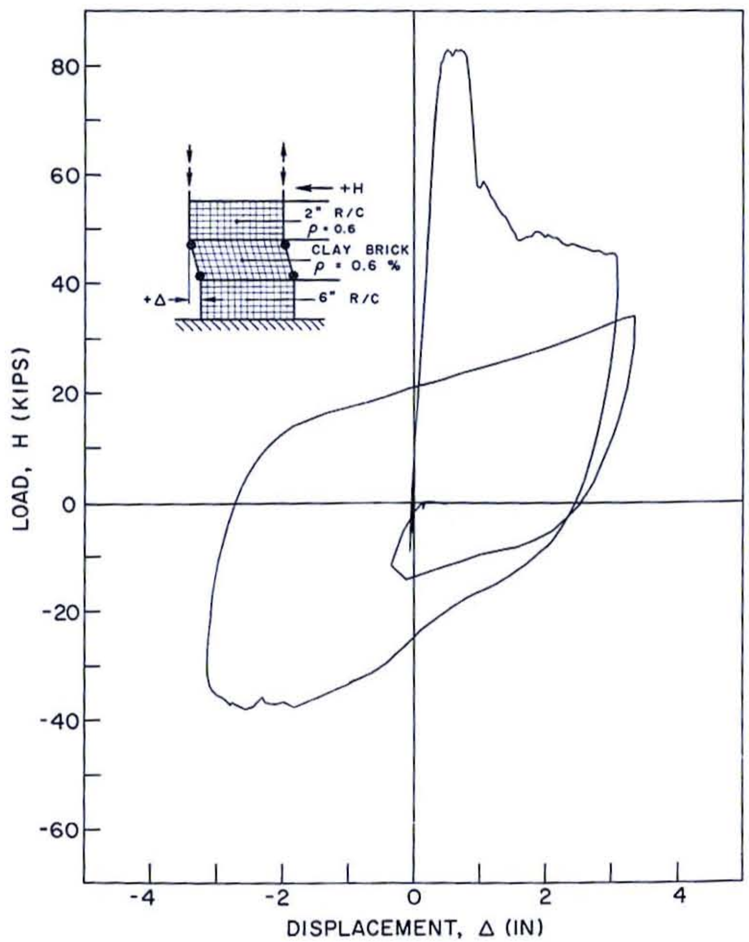

FIG. 30 LOAD-DEFLECTION RELATIONSHIP TEST SPECIMEN 14

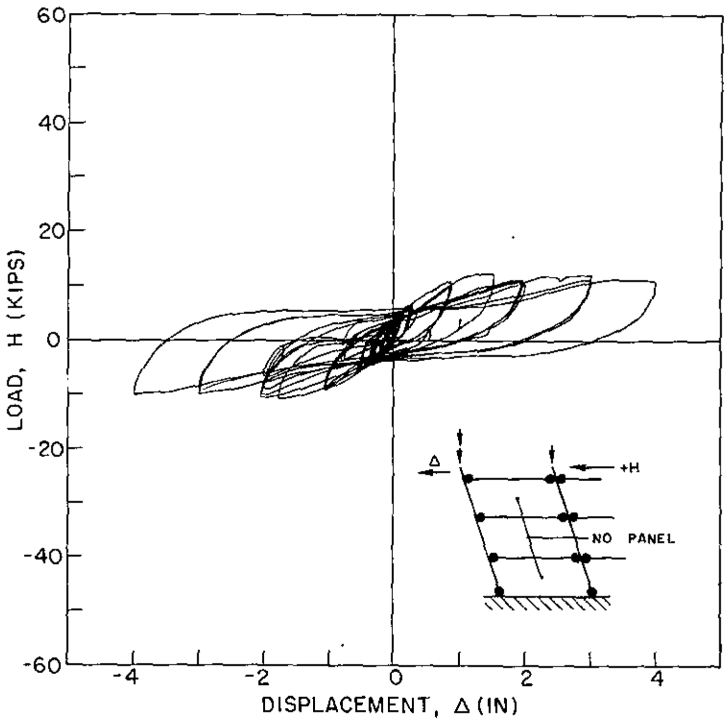

FIG. 31 LOAD-DEFLECTION RELATIONSHIP, TEST SPECIMEN 15

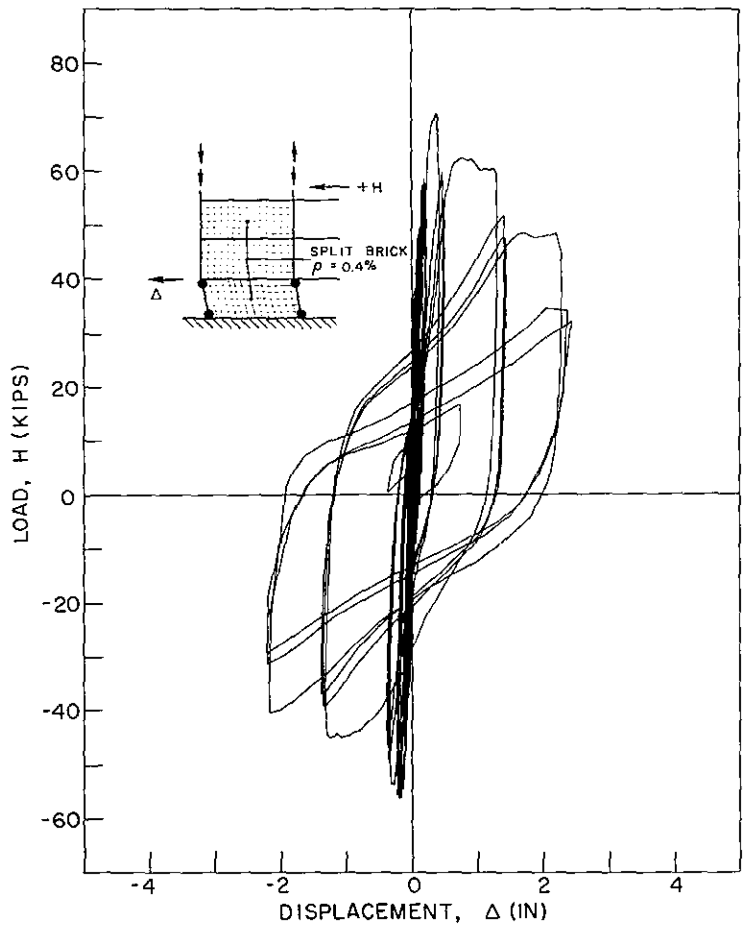

FIG. 32 LOAD-DEFLECTION RELATIONSHIP, TEST SPECIMEN 16

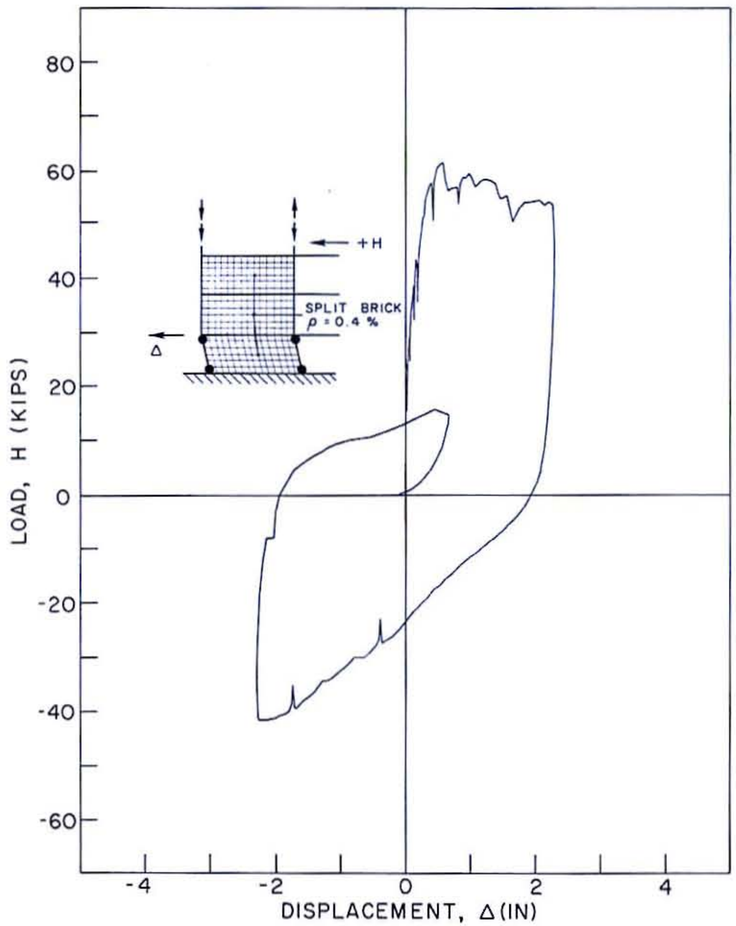

FIG. 33 LOAD-DEFLECTION RELATIONSHIP, TEST SPECIMEN 17

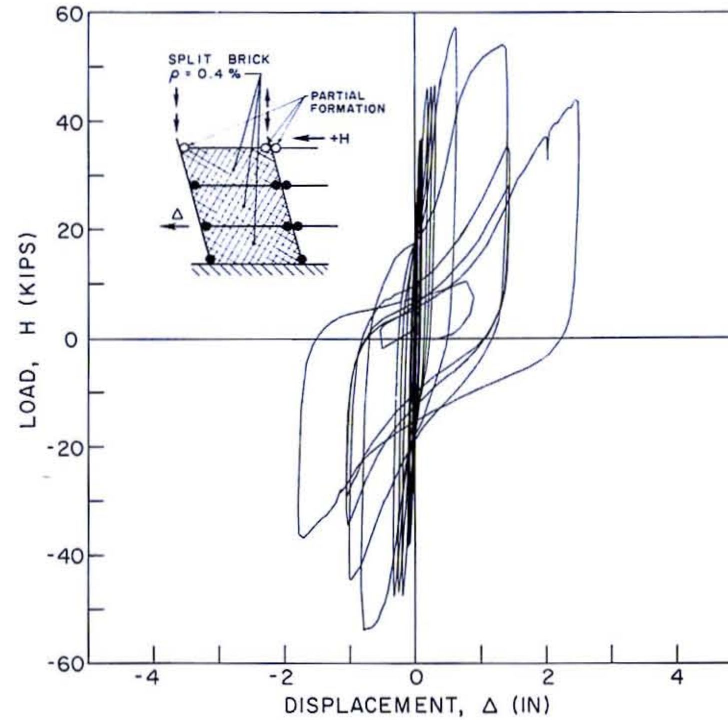

FIG. 34 LOAD-DEFLECTION RELATIONSHIP, TEST SPECIMEN 18

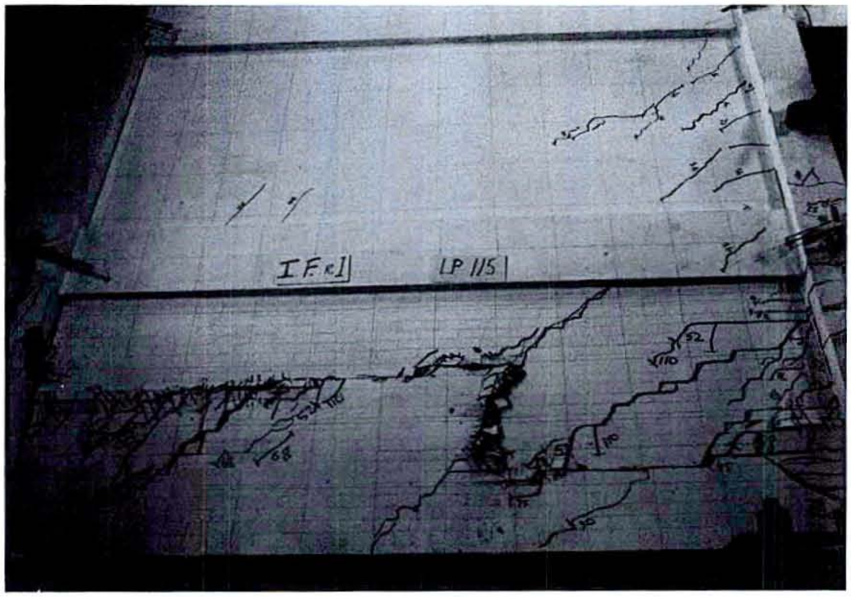

FIG. 35 TEST SPECIMEN 1, CRUSHING AND SLIDING SHEAR OCCURRING IN FIRST-STORY PANEL

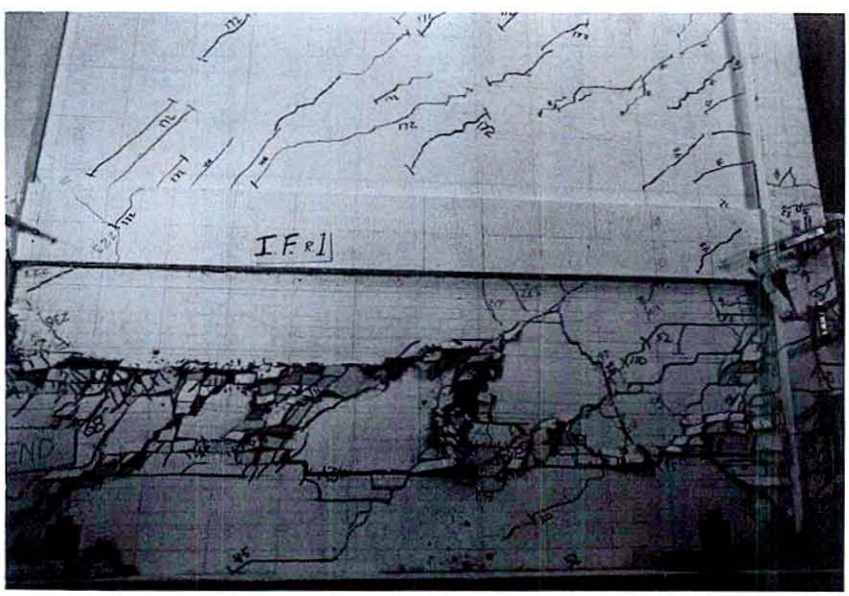

FIG. 36 TEST SPECIMEN 1, OVERVIEW OF FIRST-STORY PANEL DAMAGE AT TEST COMPLETION

FIG. 37 TEST SPECIMEN 2, PANEL CRUSHING AND SLIDING TO ACCOMMODATE FRAME DISPLACEMENT

FIG. 38 TEST SPECIMEN 2, PANEL CRUSHING AND SLIDING TO ACCOMMODATE FRAME DISPLACEMENT

FIG. 39 TEST SPECIMEN 3, BEFORE DISPLACEMENT REVERSAL

FIG. 40 TEST SPECIMEN 3, AFTER PARTIAL DISPLACEMENT REVERSAL

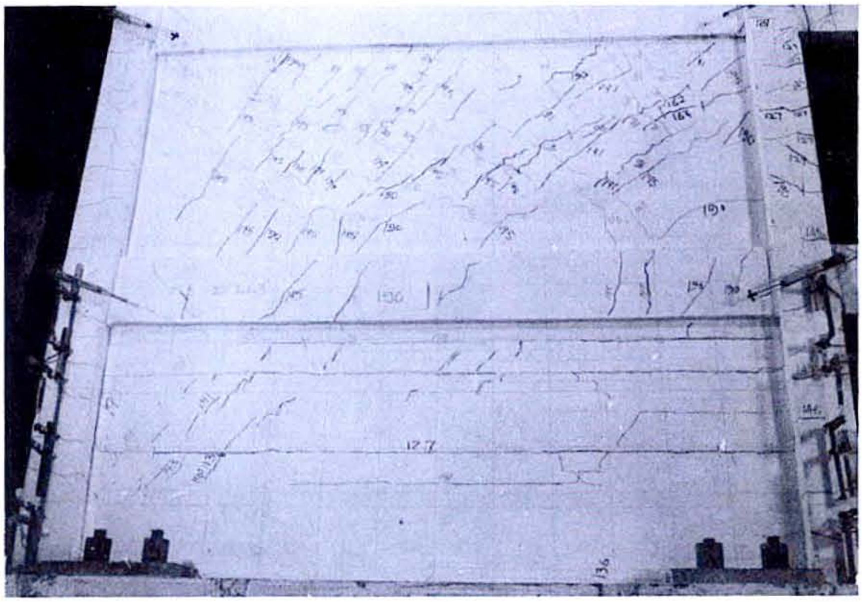

FIG. 41 TEST SPECIMEN 4, HORIZONTAL CRACKING IN MORTAR BEDS, BOTTOM STORY PANEL

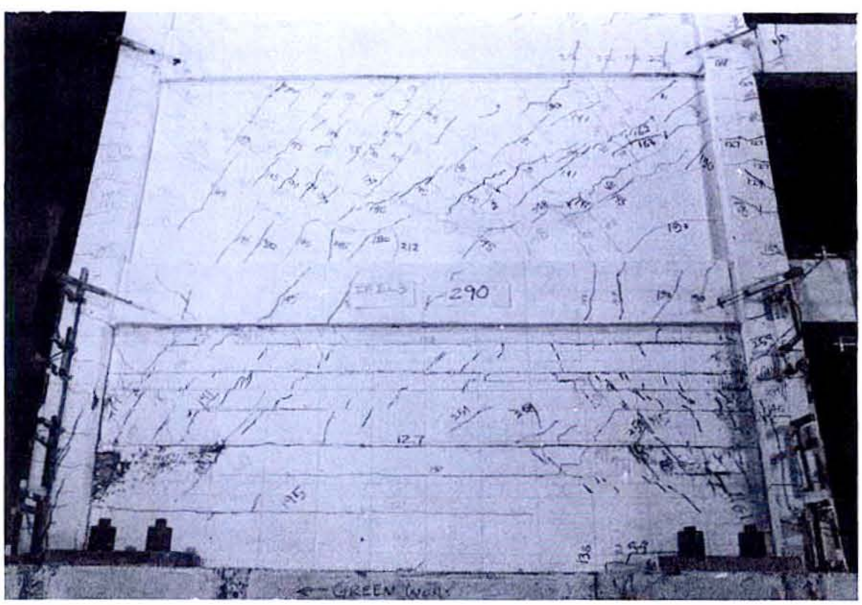

FIG. 42 TEST SPECIMEN 4, INITIAL CRUSHING AT RIGHT

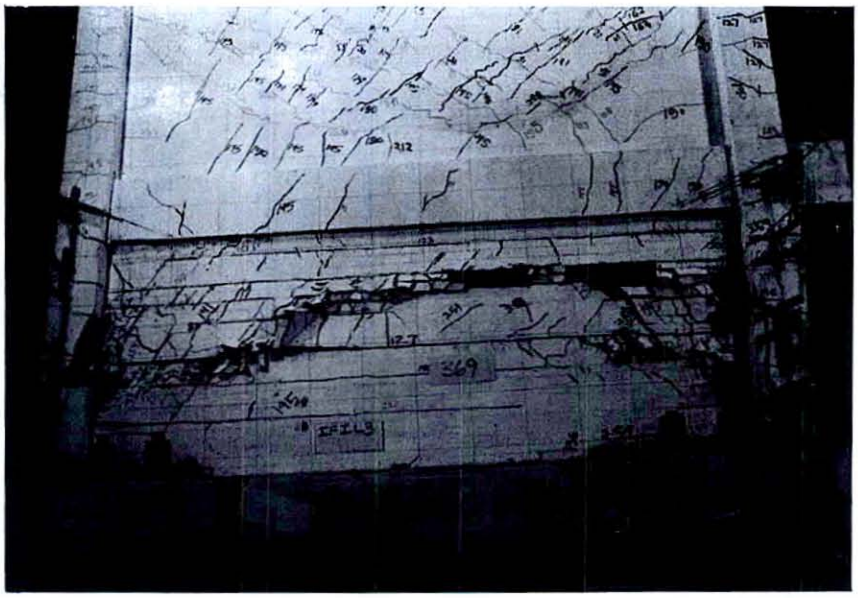

FIG. 43 TEST SPECIMEN 4, CRUSHED ZONE PROPAGATING THROUGH FIRST-STORY PANEL

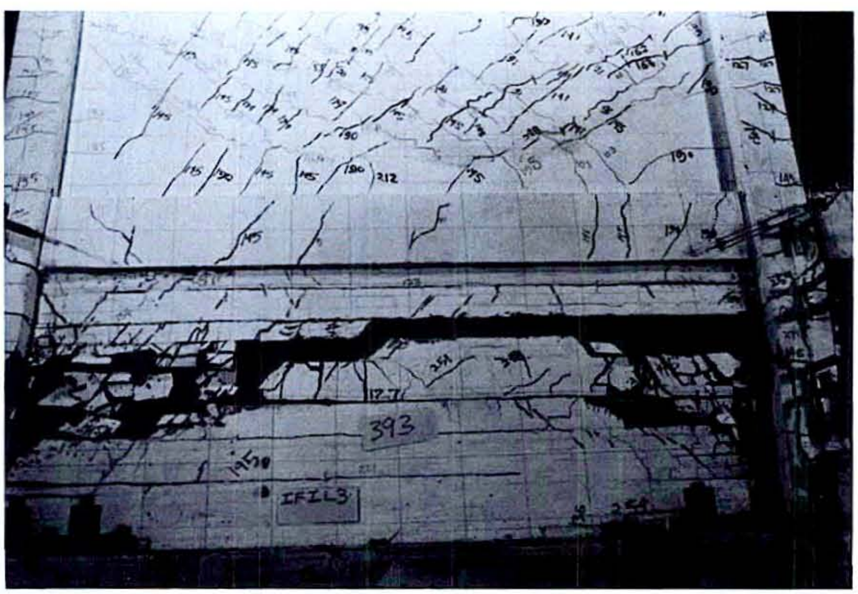

FIG. 44 TEST SPECIMEN 4, AFTER SPALLING OF MASONRY MATERIAL IN CRUSHED ZONE

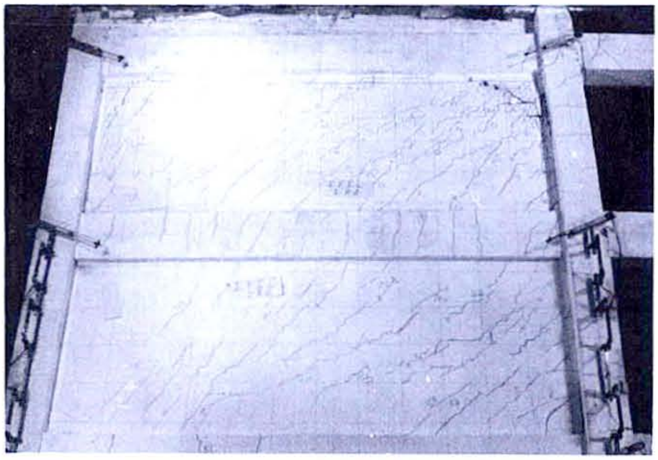

FIG. 45 TEST SPECIMEN 5, HORIZONTAL CRACK COMPLETELY ACROSS TOP OF THIRD-STORY PANEL

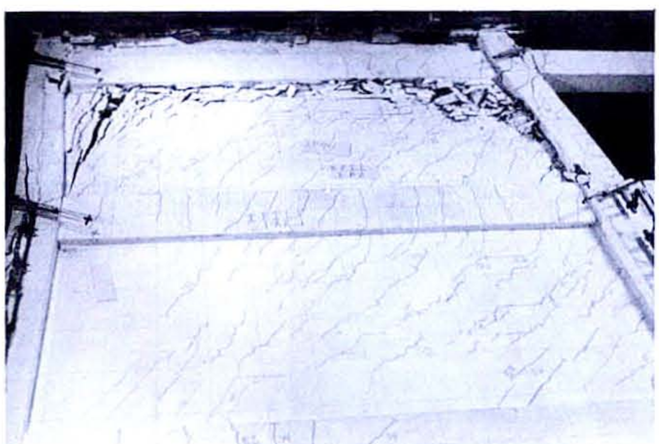

FIG. 46 TEST SPECIMEN 5, CRUSHING AND SLIDING SHEAR AT TOP OF THIRD-STORY PANEL

FIG. 47 TEST SPECIMEN 5, DETAIL OF CORNER FROM FIG. 46

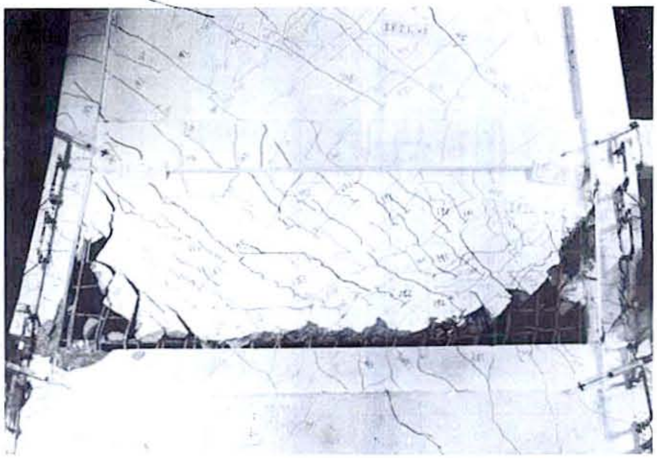

FIG. 48 TEST SPECIMEN 6, CONTINUOUS SPALLED PANEL BONE EXPANDS DUE TO INTERACTION WITH COLUMNS

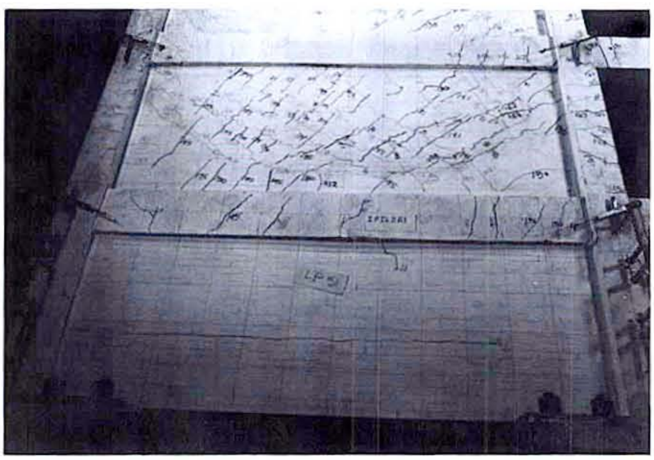

FIG. 49 TEST SPECIMEN 7, HORIZONTAL CRACK FIRST-STORY PANEL

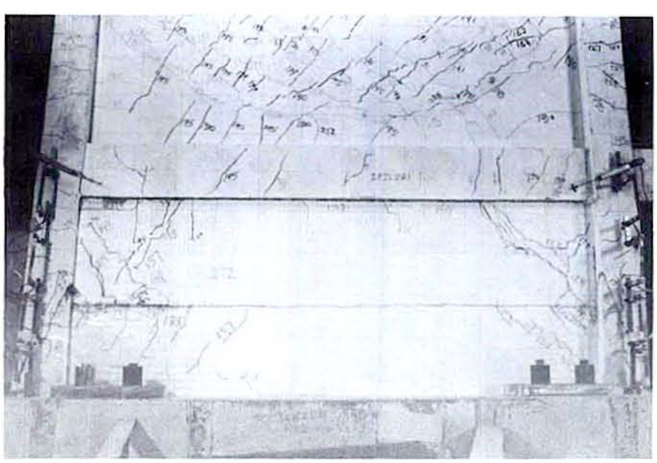

FIG. 50 TEST SPECIMEN 7, RELATIVE DISPLACEMENTS ACROSS HORIZONTAL CRACK IN THE FIRST-STORY PANEL

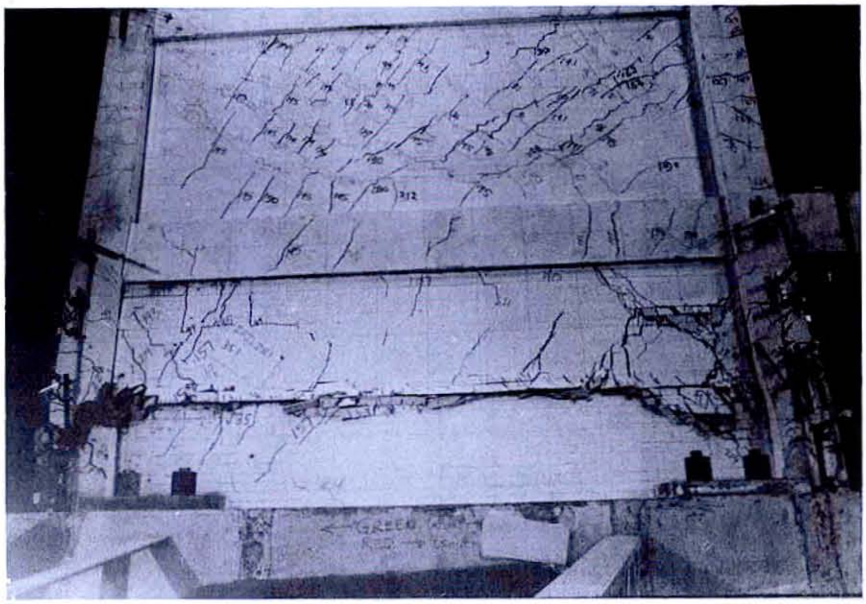

FIG. 51 TEST SPECIMEN 7, COLUMN SPIRAL FRACTURE

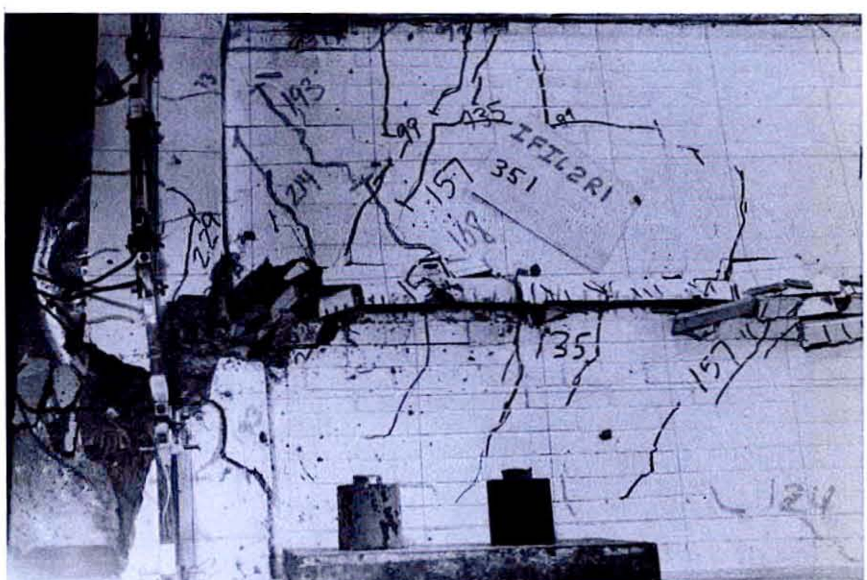

FIG. 52 TEST SPECIMEN 7, COLUMN SPIRAL FRACTURE

FIG. 53 TEST SPECIMEN 8, HORIZONTAL CRACK BEGINS TO FORM

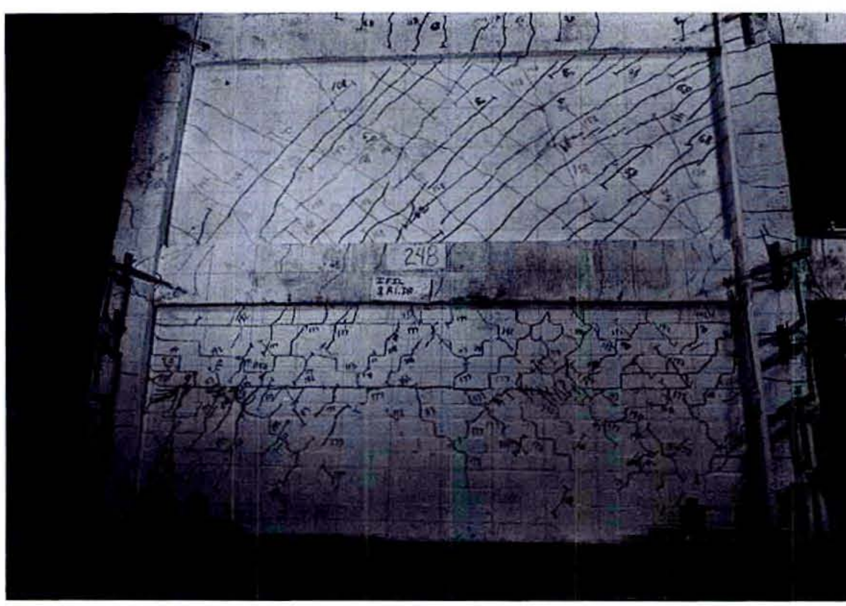

FIG. 54 TEST SPECIMEN 8, HORIZONTAL CRACK COMPLETELY ACROSS PANEL

FIG. 55 TEST SPECIMEN 8, LARGE RELATIVE DISPLACEMENT ACROSS HORIZONTAL CRACK

FIG. 56 TEST SPECIMEN 8, SIGNIFICANT SPALLING ALONG CRACK, MATERIAL BEGINS TO FALL OUT OF PANEL

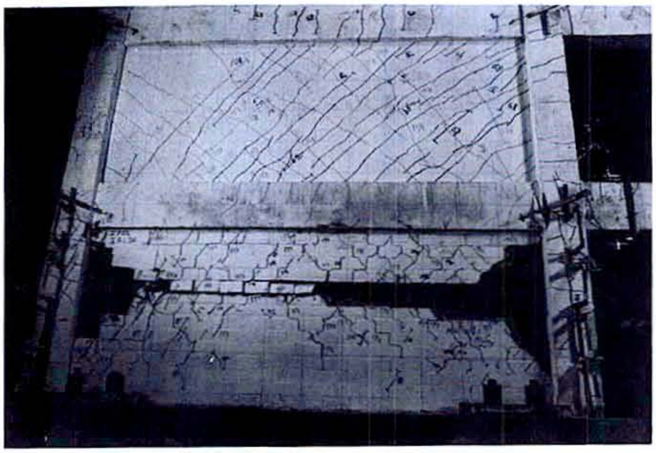

FIG. 57 TEST SPECIMEN 8, SPALLING CONTINUES

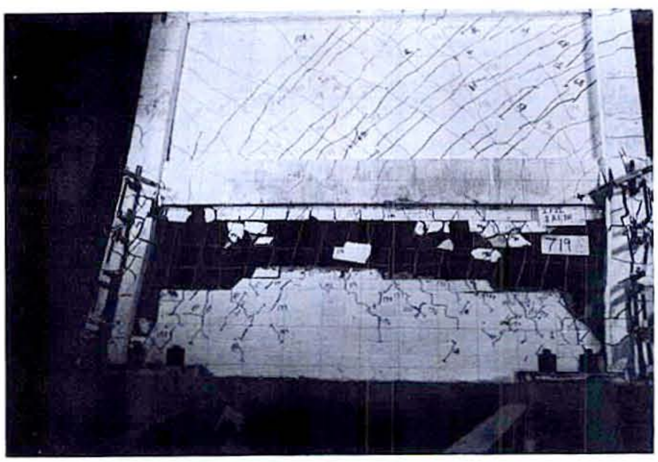

FIG. 58 TEST SPECIMEN 8, VERY LARGE HORIZONTAL GAP COMPLETELY ACROSS PANEL

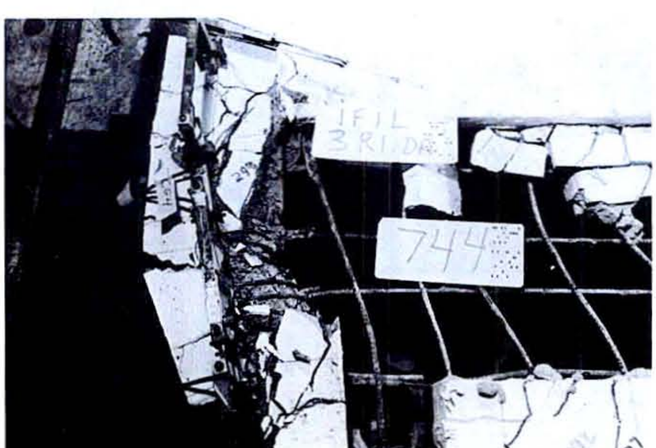

FIG. 59 TEST SPECIMEN 8, SPIRAL STEEL FAILS, LEFT COLUMN

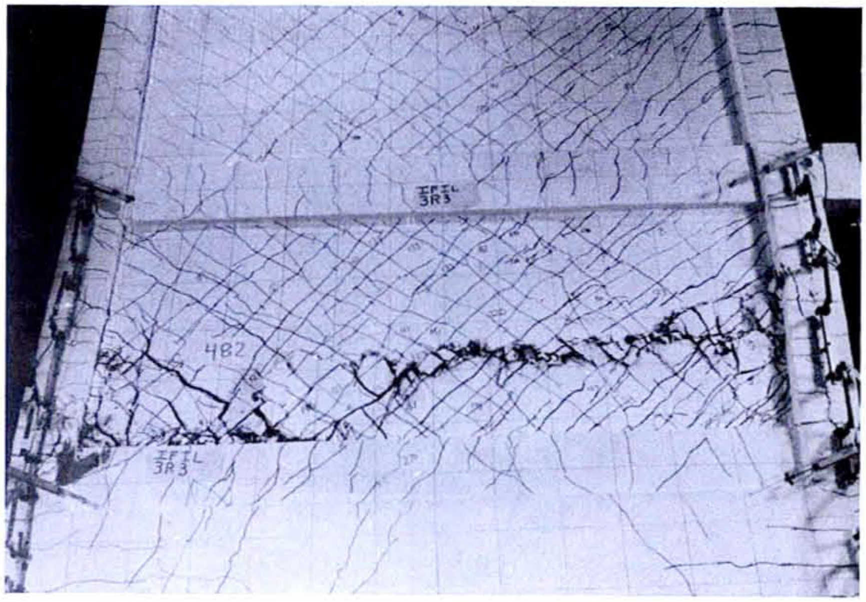

FIG. 60 TEST SPECIMEN 10, DAMAGE PROPAGATES HORIZONTALLY ACROSS TO THE RIGHT COLUMN

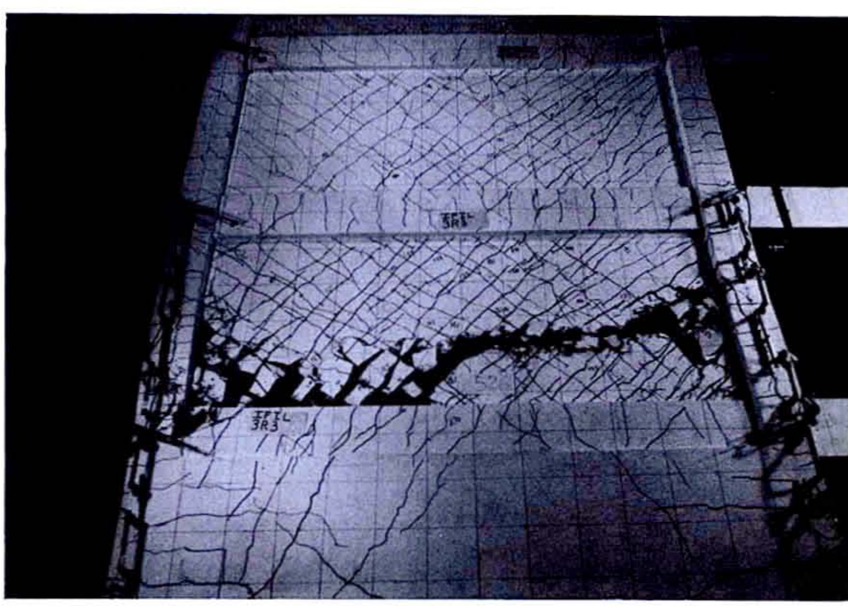

FIG. 61 TEST SPECIMEN 10, REMAINING PORTION OF SECOND-STORY PANEL AFFECTS LOCATION OF COLUMN PLASTIC HINGES

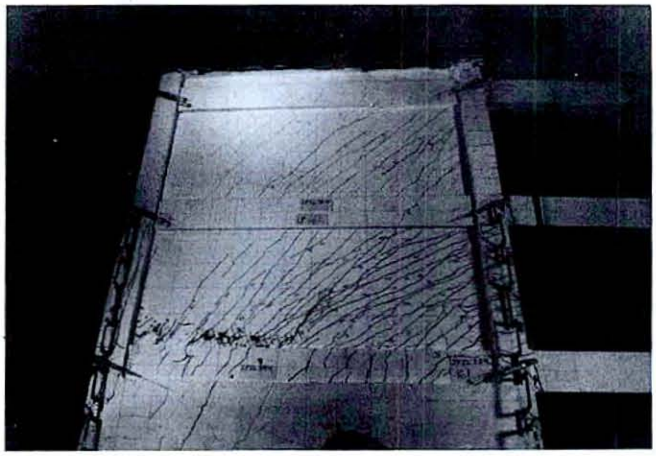

FIG. 62 TEST SPECIMEN 11, INITIAL CRUSHING IN LOWER LEFT PORTION OF SECOND-STORY PANEL

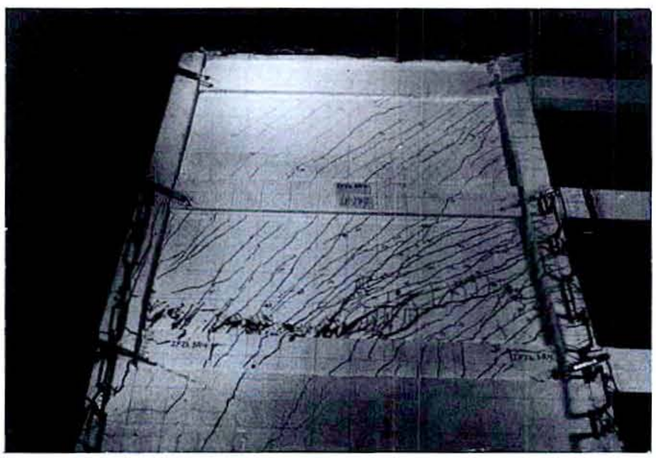

FIG. 63 TEST SPECIMEN 11, DAMAGE PROPAGATING CROSS PANEL

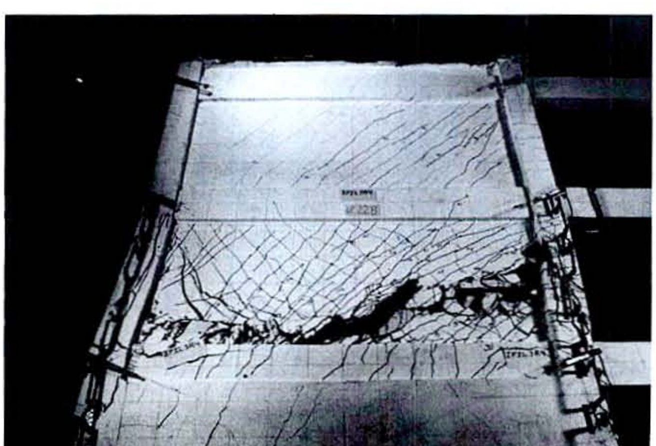

FIG. 64 TEST SPECIMEN 11, FOLLOWING DISPLACEMENT REVERSAL

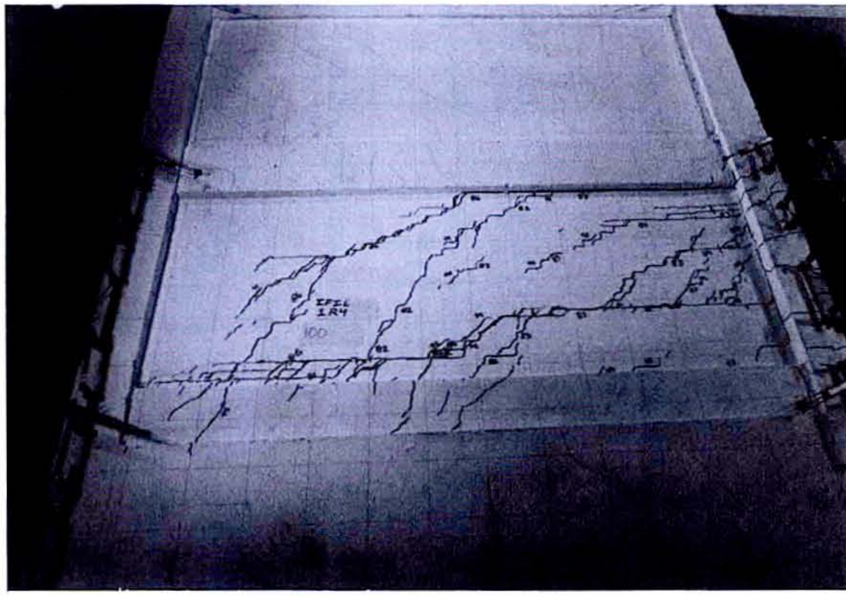

FIG. 65 TEST SPECIMEN 12, CRUSHING OF SECOND-STORY PANEL BEGINS IN LOWER LEFT CORNER A

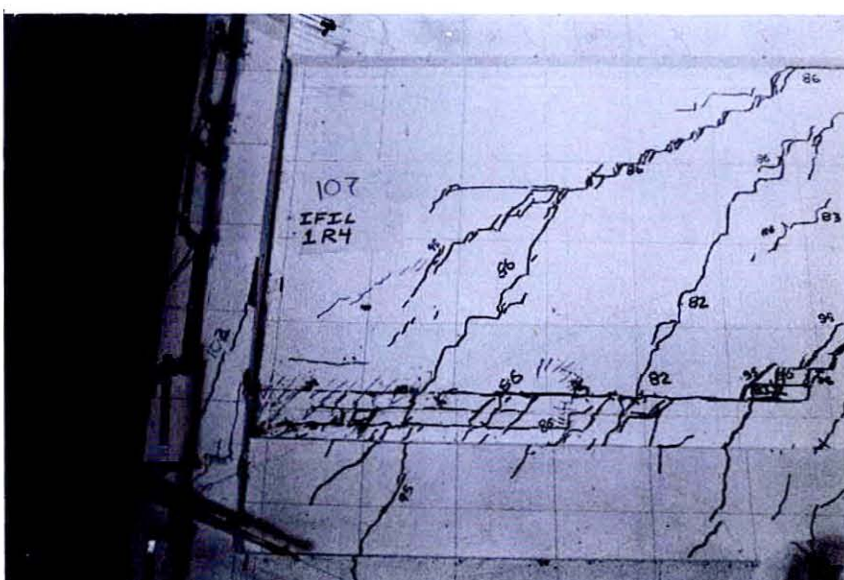

FIG. 66 TEST SPECIMEN 12, COLUMN SUBJECTED TO SEVERE SHEAR AND SHEAR DISTORTION

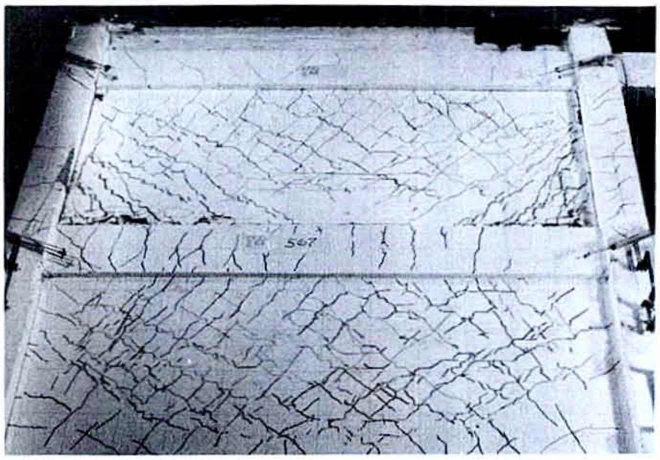

FIG. 67 TEST SPECIMEN 13, CRUSHING BEGINS ON THIRD-STORY PANEL ADJACENT TO COLUMNS

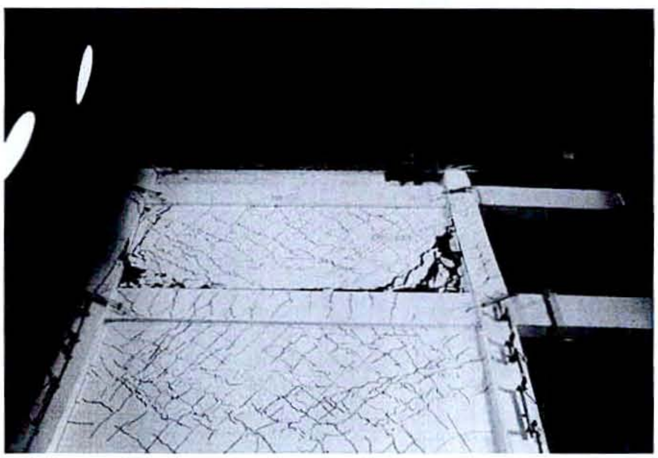

FIG. 68 TEST SPECIMEN 13, DAMAGE CONTINUES, SHEAR CRACK IN LEFT COLUMN

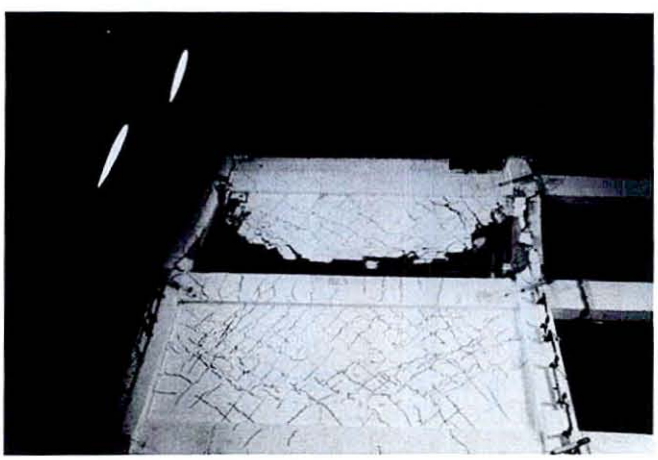

FIG. 69 TEST SPECIMEN 13, PANEL MATERIAL ADJACENT TO COLUMNS COMPLETELY SPALLED

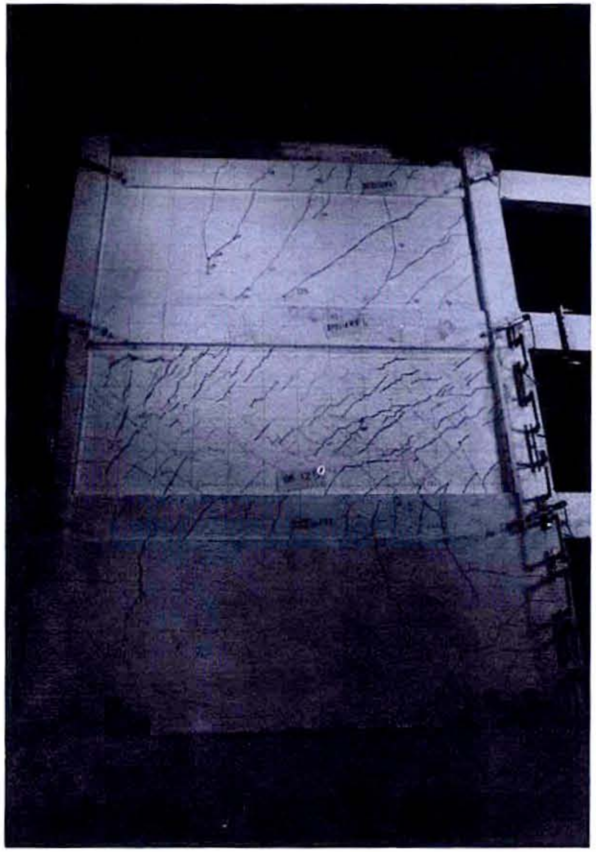

FIG. 70 TEST SPECIMEN 14, SLIDING SHEAR BEGINS FAILURE AT TOP LEFT CORNER OF SECOND-STORY PANEL

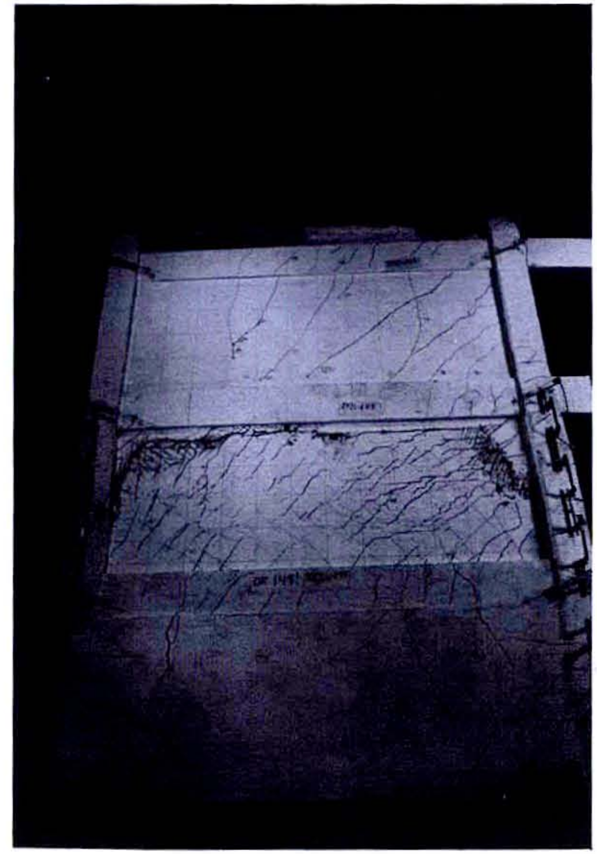

FIG. 71 TEST SPECIMEN 14, HORIZONTAL FAILURE SURFACE EXTENDS COMPLETELY ACROSS TOP OF SECOND-STORY PANEL, WITH CRUSHING OF THE PANEL OCCURRING IN TOP RIGHT CORNER

FIG. 72 TEST SPECIMEN 16, INTERCONNECTING SHEAR CRACKS BEGIN TO FORM HORIZONTAL FAILURE SURFACE

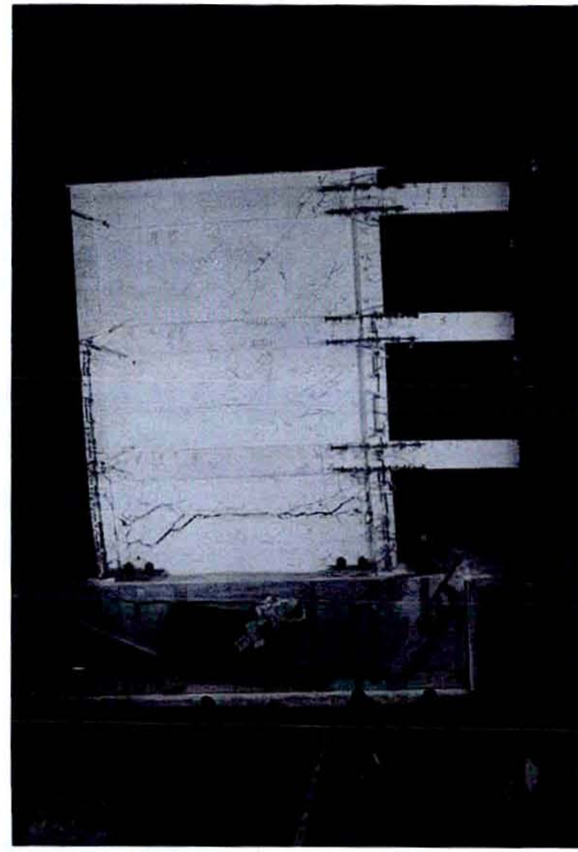

FIG. 73 TEST SPECIMEN 16, WITH FULLY DEVELOPED FAILURE SURFACE

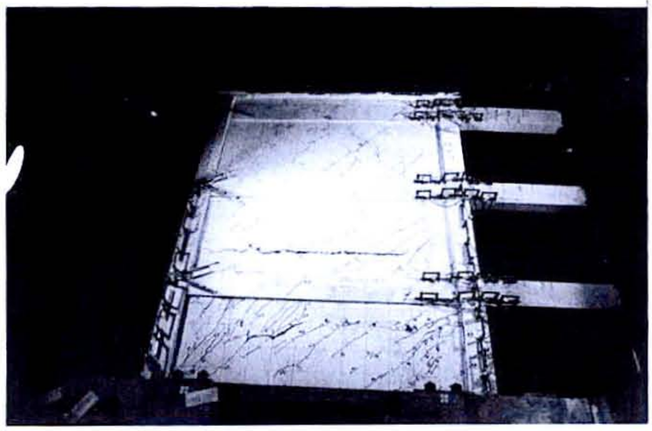

FIG. 74 TEST SPECIMEN 17, HORIZONTAL FAILURE SURFACE IN SECOND-STORY PANEL, SHEAR CRUSHING FAILURE BEGINNING IN THE FIRST-STORY PANEL

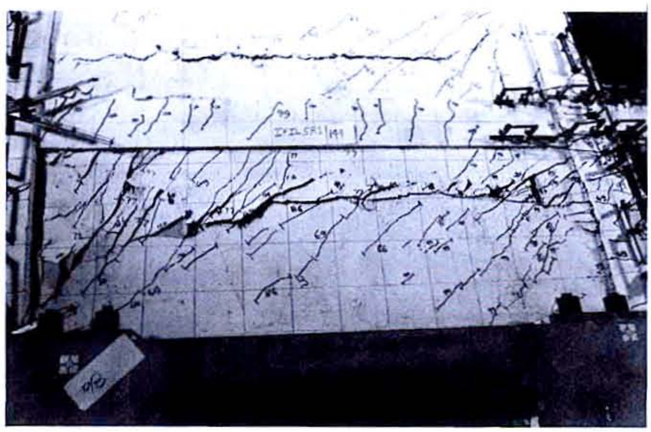

FIG. 75 TEST SPECIMEN 17, SHEAR CRUSHING, FIRST-STORY PANEL

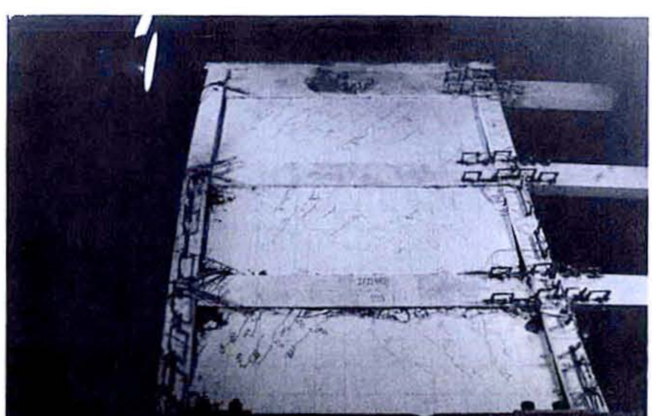

FIG. 76 TEST SPECIMEN 18, BOUNDARY SEPARATION, PANEL DAMAGE MINIMAL

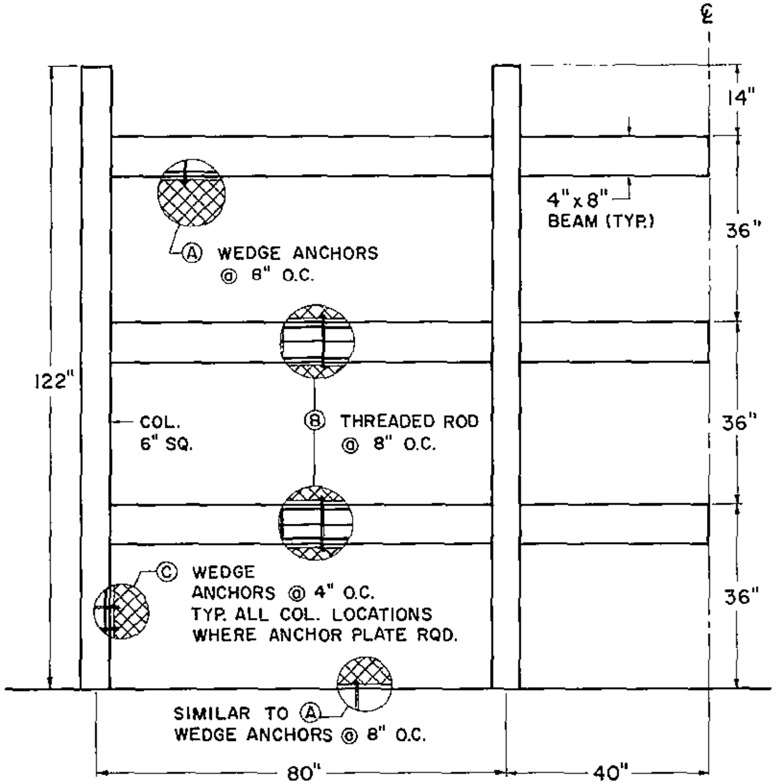

FIG. 77 FRAME-PANEL ANCHORAGE SYSTEM FOR TEST SPECIMEN 18

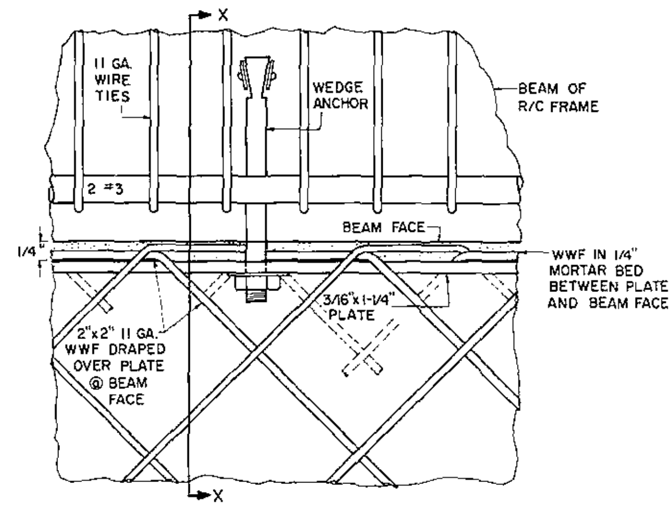

MASONRY INFILLED R/C FRAME: CONNECTION DETAIL Ⓐ
USING A PERIPHERAL STEEL PLATE

FIG. 78 DETAIL A, WEDGE ANCHOR FASTENING WWF TO BEAM

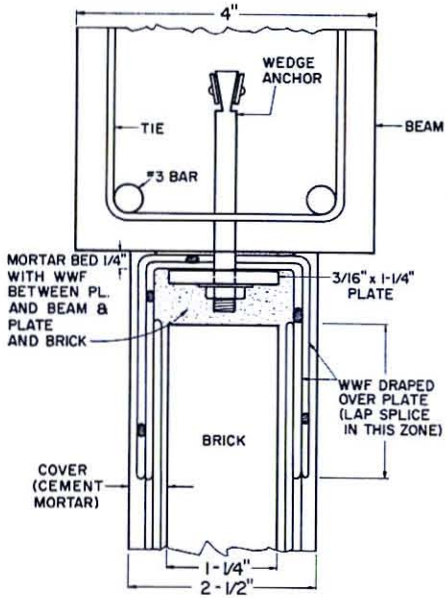

MASONRY INFILLED R/C FRAME:
CONNECTION DETAIL Ⓐ (SECTION X-X)
BETWEEN INFILL AND FRAME BEAM

FIG. 79 SECTION X-X THROUGH BEAM AND PANEL

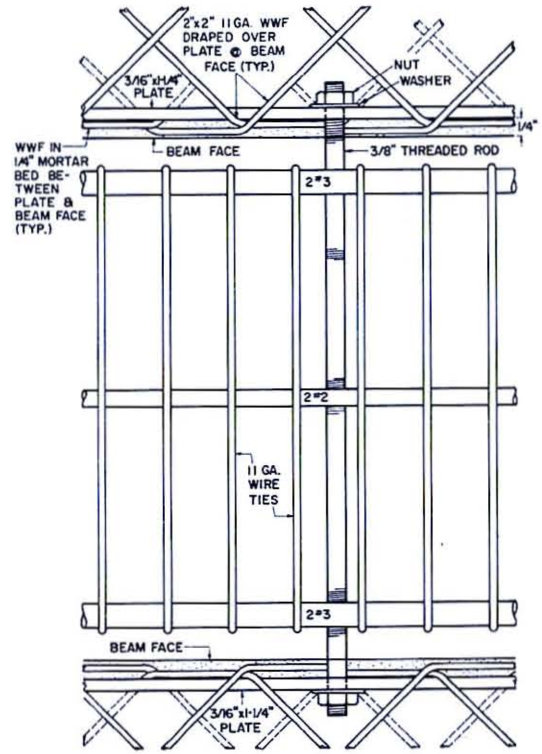

FIG. 80 DETAIL B, THREADED ROD PROVIDING POSITIVE ANCHORAGE BOLTING COMPLETELY THROUGH BEAM

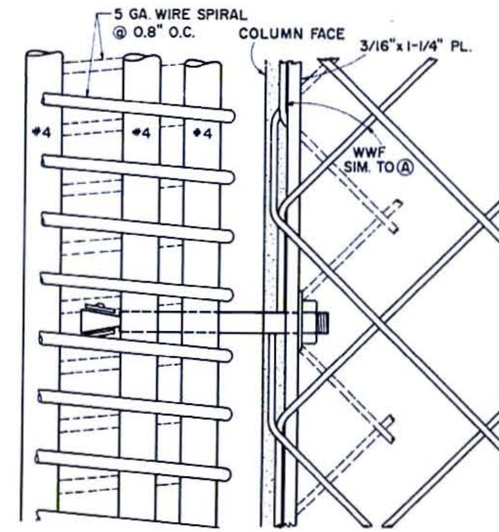

FIG. 81 DETAIL C, WEDGE ANCHOR FASTENING WWF TO COLUMN

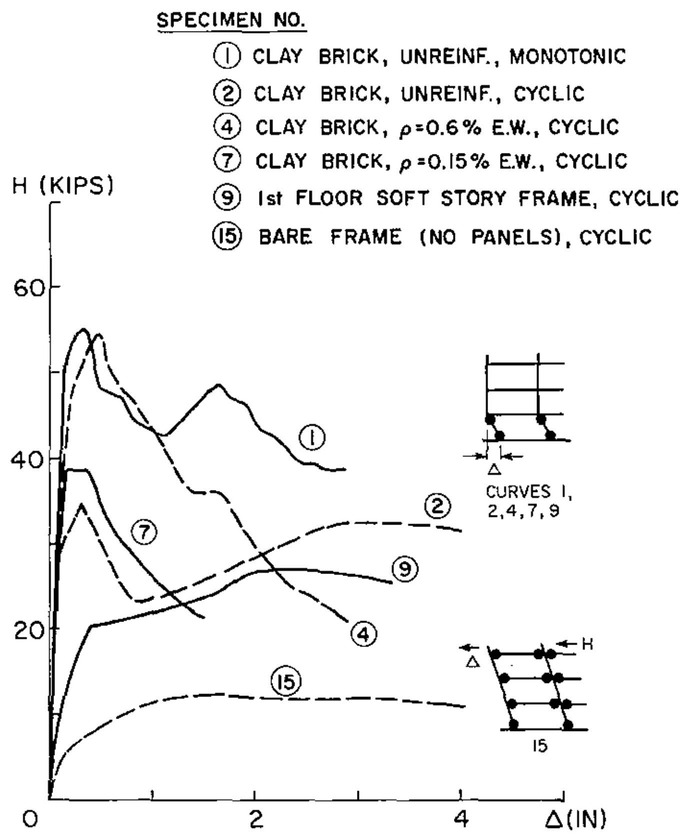

FIG. 82 RESPONSE ENVELOPE 1, TEST SPECIMENS 1, 2, 4, 7, 9, 15

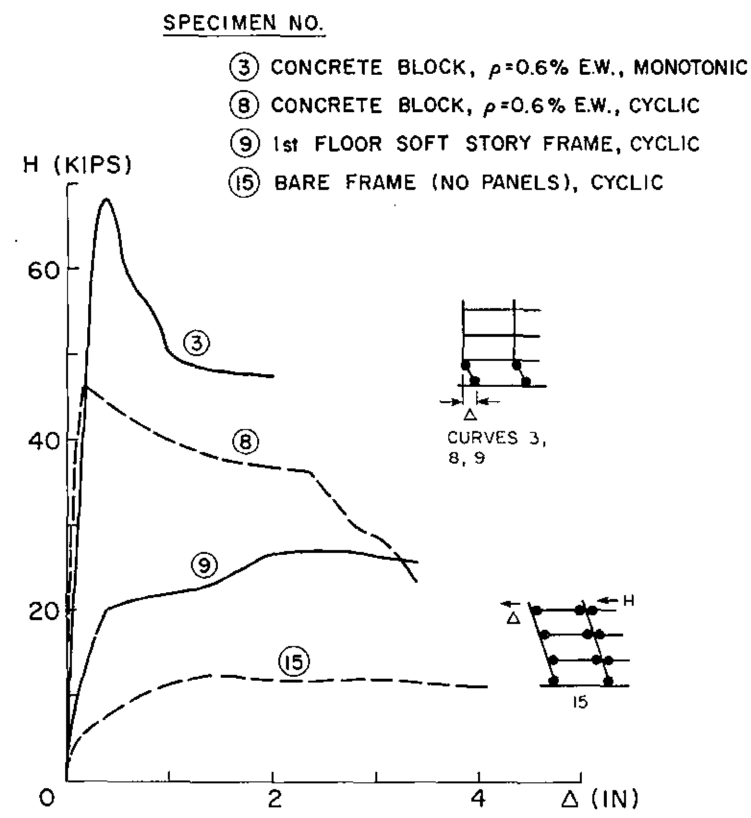

FIG. 83 RESPONSE ENVELOPE 2, TEST SPECIMENS 3, 8, 9, 15

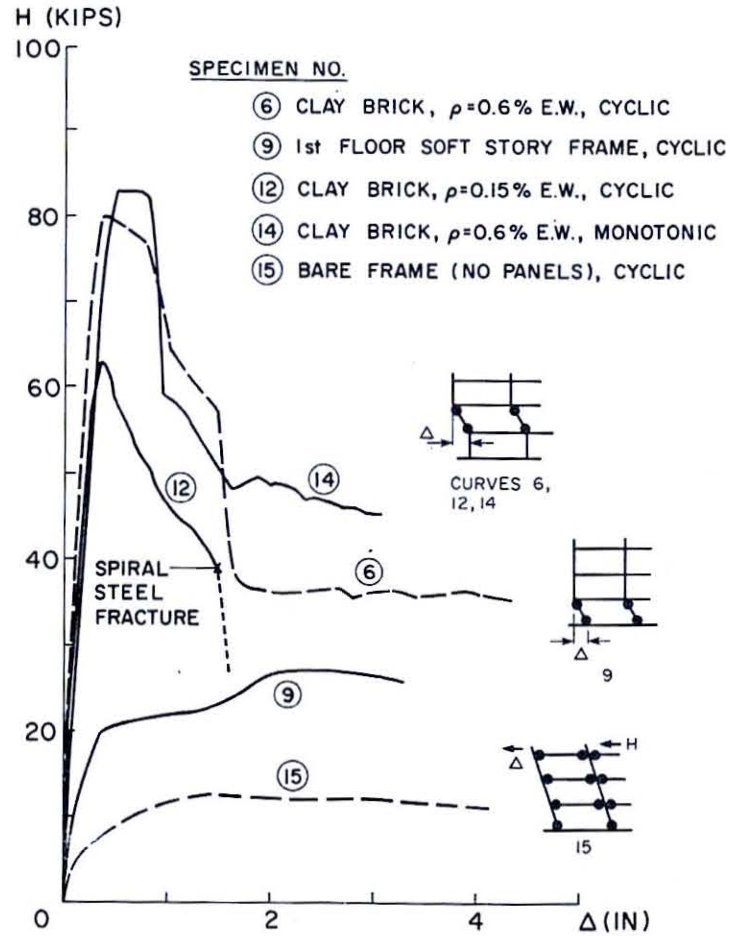

FIG. 84 RESPONSE ENVELOPE 3, TEST SPECIMENS 6, 9, 12, 14, 15

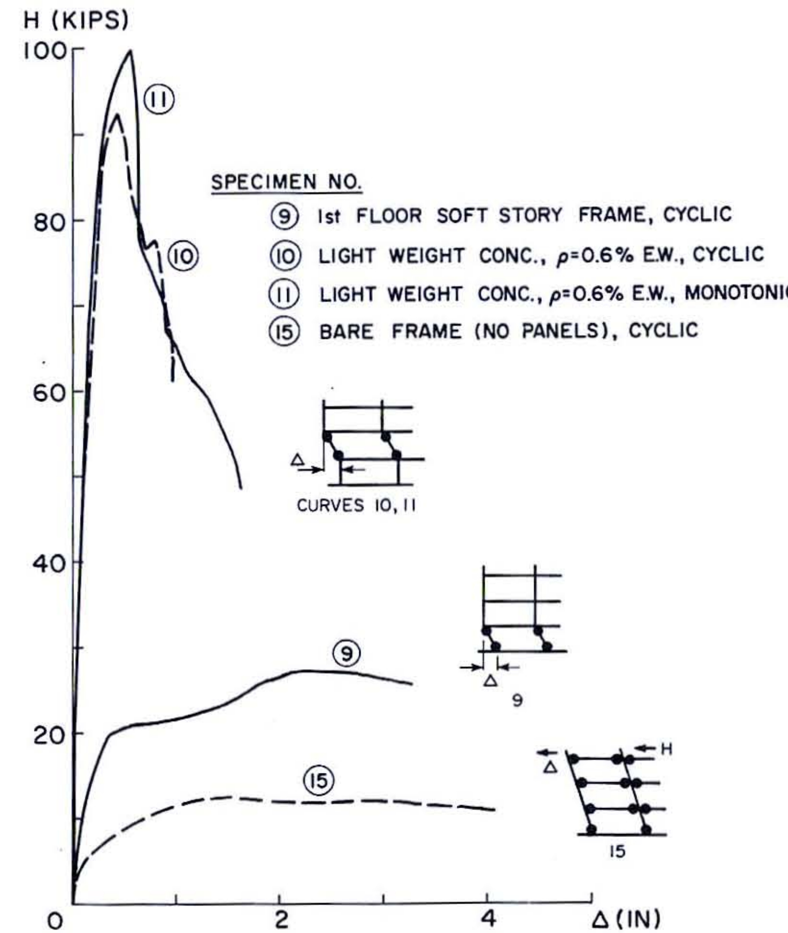

FIG. 85 RESPONSE ENVELOPE 4, TEST SPECIMENS 9, 10, 11, 15

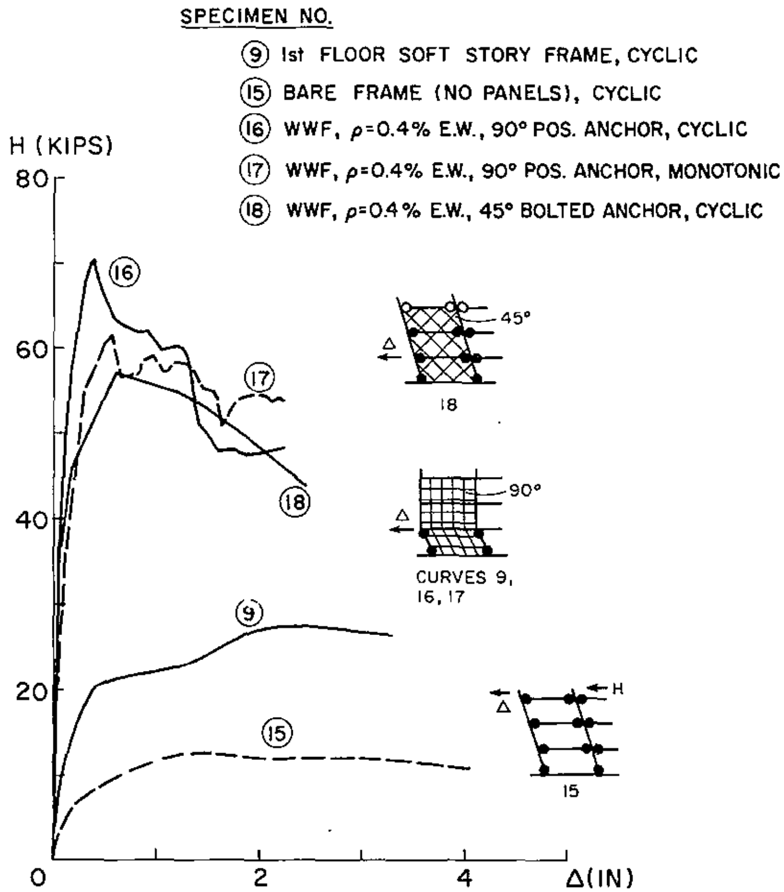

FIG. 86 RESPONSE ENVELOPE 5 (UNFACTORED), TEST SPECIMENS 9, 15, 16, 17, 18

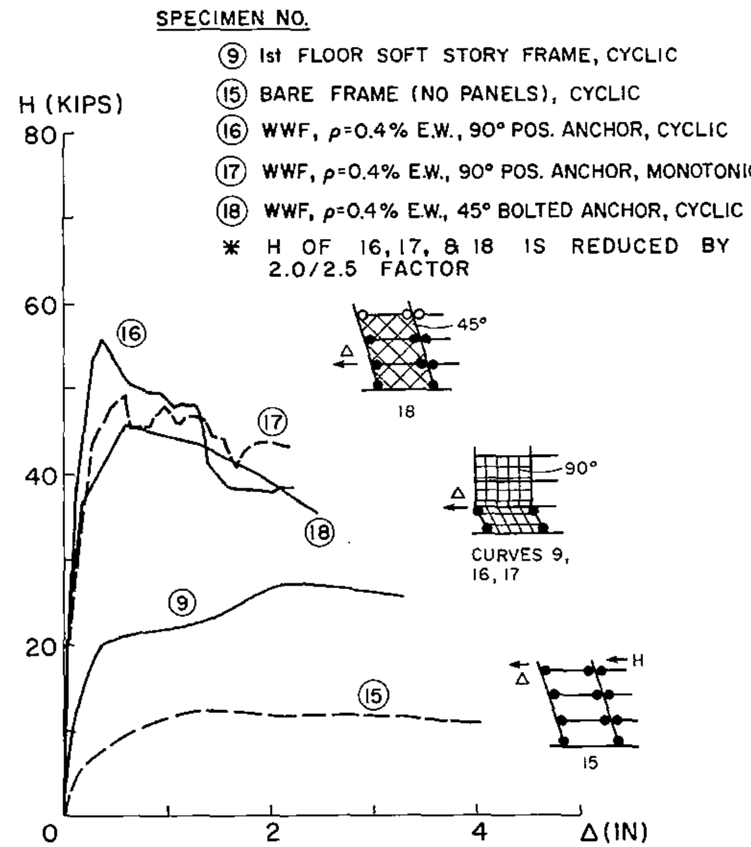

FIG. 87 RESPONSE ENVELOPE 6 (FACTORED), TEST SPECIMENS 9, 15, 16, 17, 18

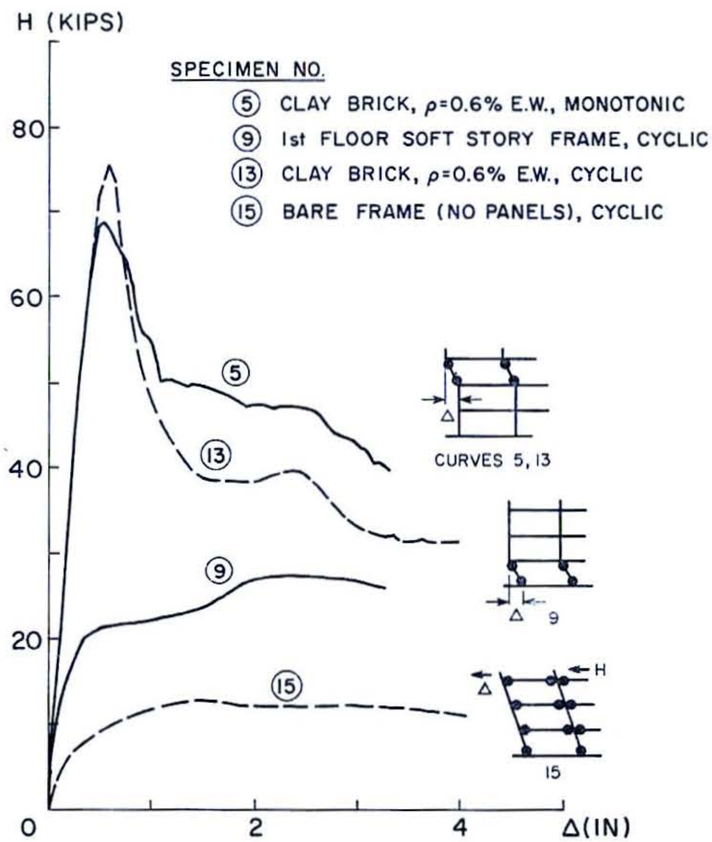

FIG. 88 RESPONSE ENVELOPE 7, TEST SPECIMENS 5, 9, 13, 15

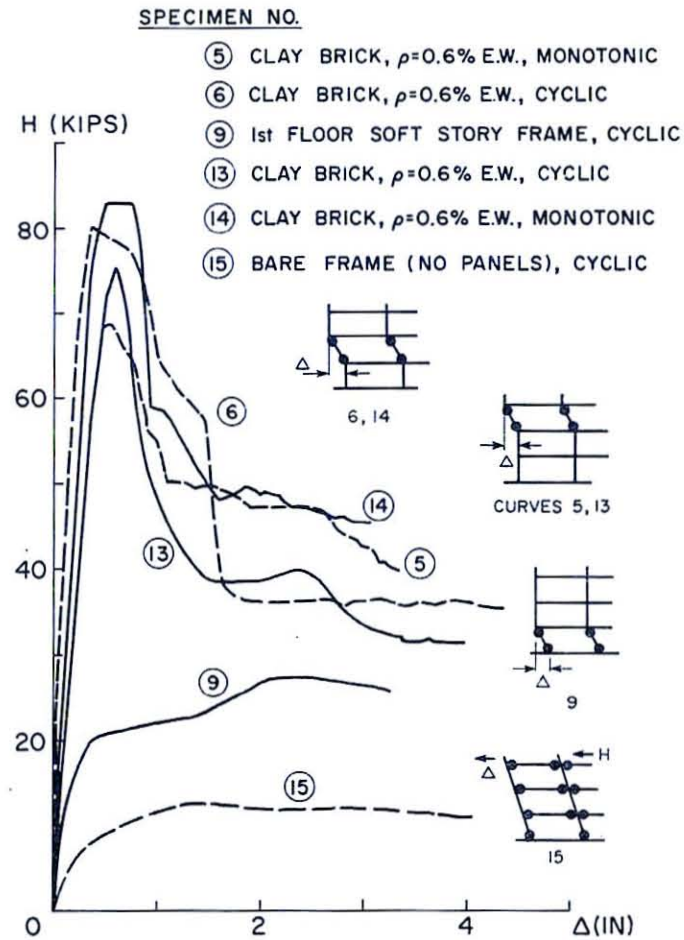

FIG. 89 RESPONSE ENVELOPE 8, TEST SPECIMENS 5, 6, 9, 13, 14, 15

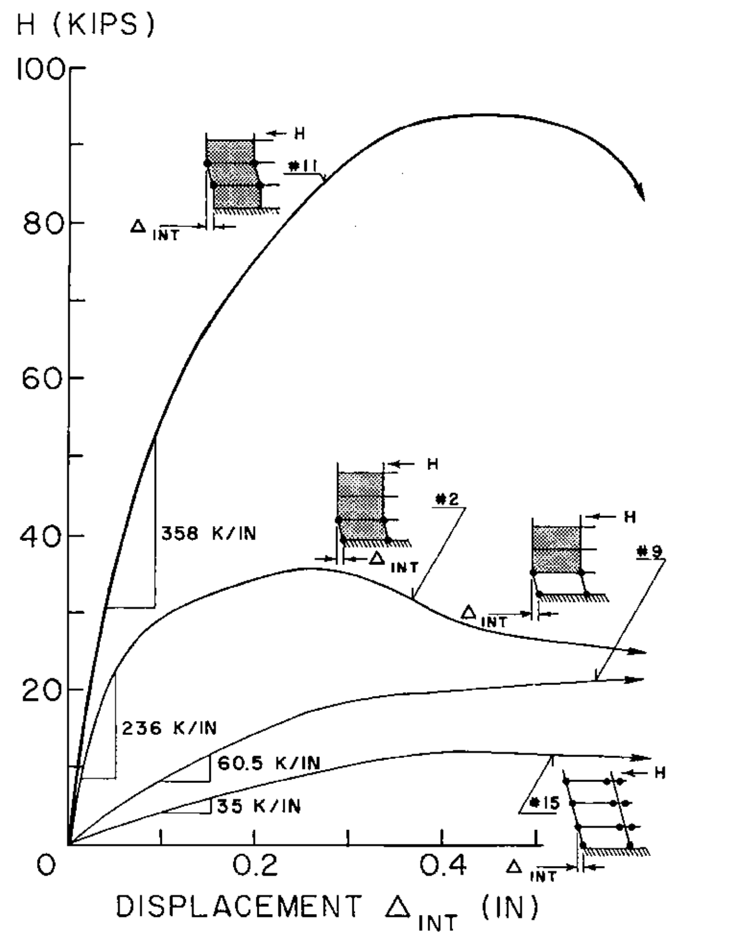

FIG. 90 COMPARISON OF INITIAL PARTS OF LATERAL LOAD-INTERSTORY DRIFT DIAGRAMS OF SOME SPECIMENS TESTED ILLUSTRATING LATERAL STIFFNESS

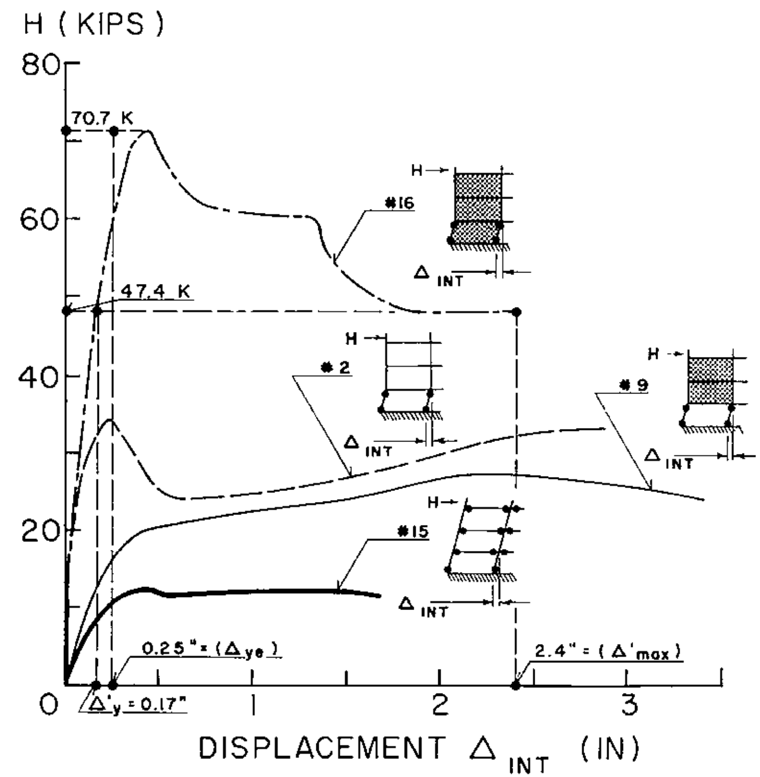

FIG. 91 COMPARISON OF LATERAL LOAD-INTERSTORY DRIFT DIAGRAMS OF SOME SPECIMENS TESTED

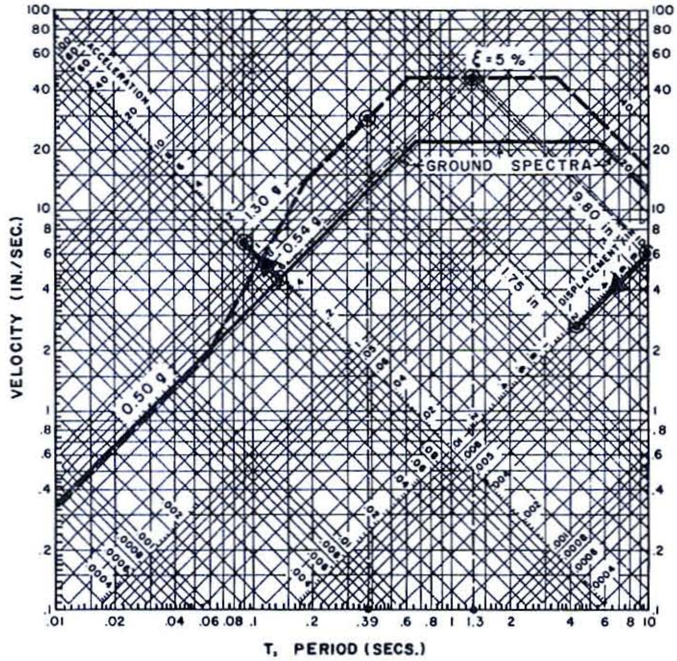

FIG. 92 SMOOTHED LINEAR ELASTIC RESPONSE SPECTRA FOR AN EFFECTIVE PEAK GROUND ACCELERATION OF 0.5g AND A DAMPING RATIO ξ = 5% AFTER NEWMARK AND HALL [6]

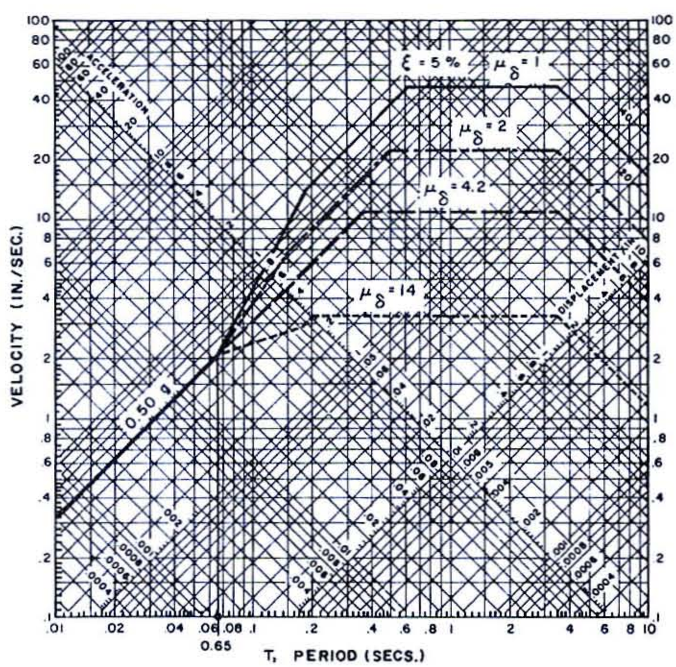

FIG. 93 SMOOTHED INELASTIC DESIGN RESPONSE SPECTRA FOR DIFFERENT VALUES OF THE DISPLACEMENT DUCTILITY, μ_δ, DERIVED FROM THE LINEAR DESIGN SPECTRA OF FIG. 92

EARTHQUAKE ENGINEERING RESEARCH CENTER REPORTS

NOTE: Numbers in parenthesis are Accession Numbers assigned by the National Technical Information Service; these are followed by a price code. Copies of the reports may be ordered from the National Technical Information Service, 5285 Port Royal Road, Springfield, Virginia, 22161. Accession Numbers should be quoted on orders for reports (PB --- ---) and remittance must accompany each order. Reports without this information were not available at time of printing. Upon request, EERC will mail inquirers this information when it becomes available.

EERC 67-1 "Feasibility Study Large-Scale Earthquake Simulator Facility," by J. Penzien, J.G. Bouwkamp, R.W. Clough and D. Rea - 1967 (PB 187 905)A07

EERC 68-1 Unassigned

EERC 68-2 "Inelastic Behavior of Beam-to-Column Subassemblages Under Repeated Loading," by V.V. Bertero - 1968 (PB 184 888)A05

EERC 68-3 "A Graphical Method for Solving the Wave Reflection-Refraction Problem," by H.D. McNiven and Y. Mengi - 1968 (PB 187 943)A03

EERC 68-4 "Dynamic Properties of McKinley School Buildings," by D. Rea, J.G. Bouwkamp and R.W. Clough - 1968 (PB 187 902)A07

EERC 68-5 "Characteristics of Rock Motions During Earthquakes," by H.B. Seed, I.M. Idriss and F.W. Kiefer - 1968 (PB 188 338)A03

EERC 69-1 "Earthquake Engineering Research at Berkeley," - 1969 (PB 187 906)A11

EERC 69-2 "Nonlinear Seismic Response of Earth Structures," by M. Dibaj and J. Penzien - 1969 (PB 187 904)A08

EERC 69-3 "Probabilistic Study of the Behavior of Structures During Earthquakes," by R. Ruiz and J. Penzien - 1969 (PB 187 886)A06

EERC 69-4 "Numerical Solution of Boundary Value Problems in Structural Mechanics by Reduction to an Initial Value Formulation," by N. Distefano and J. Schujman - 1969 (PB 187 942)A02

EERC 69-5 "Dynamic Programming and the Solution of the Biharmonic Equation," by N. Distefano - 1969 (PB 187 941)A03

EERC 69-6 "Stochastic Analysis of Offshore Tower Structures," by A.K. Malhotra and J. Penzien - 1969 (PB 187 903)A09

EERC 69-7 "Rock Motion Accelerograms for High Magnitude Earthquakes," by H.B. Seed and I.M. Idriss - 1969 (PB 187 940)A02

EERC 69-8 "Structural Dynamics Testing Facilities at the University of California, Berkeley," by R.M. Stephen, J.G. Bouwkamp, R.W. Clough and J. Penzien - 1969 (PB 189 111)A04

EERC 69-9 "Seismic Response of Soil Deposits Underlain by Sloping Rock Boundaries," by H. Dezfulian and H.B. Seed 1969 (PB 189 114)A03

EERC 69-10 "Dynamic Stress Analysis of Axisymmetric Structures Under Arbitrary Loading," by S. Ghosh and E.L. Wilson 1969 (PB 189 026)A10

EERC 69-11 "Seismic Behavior of Multistory Frames Designed by Different Philosophies," by J.C. Anderson and V. V. Bertero - 1969 (PB 190 662)A10

EERC 69-12 "Stiffness Degradation of Reinforcing Concrete Members Subjected to Cyclic Flexural Moments," by V.V. Bertero, B. Bresler and H. Ming Liao - 1969 (PB 202 942)A07

EERC 69-13 "Response of Non-Uniform Soil Deposits to Travelling Seismic Waves," by H. Dezfulian and H.B. Seed - 1969 (PB 191 023)A03

EERC 69-14 "Damping Capacity of a Model Steel Structure," by D. Rea, R.W. Clough and J.G. Bouwkamp - 1969 (PB 190 663)A06

EERC 69-15 "Influence of Local Soil Conditions on Building Damage Potential during Earthquakes," by H.B. Seed and I.M. Idriss - 1969 (PB 191 036)A03

EERC 69-16 "The Behavior of Sands Under Seismic Loading Conditions," by M.L. Silver and H.B. Seed - 1969 (AD 714 982)A07

EERC 70-1 "Earthquake Response of Gravity Dams," by A.K. Chopra - 1970 (AD 709 640)A03

EERC 70-2 "Relationships between Soil Conditions and Building Damage in the Caracas Earthquake of July 29, 1967," by H.B. Seed, I.M. Idriss and H. Dezfulian - 1970 (PB 195 762)A05

EERC 70-3 "Cyclic Loading of Full Size Steel Connections," by E.P. Popov and R.M. Stephen - 1970 (PB 213 545)A04

EERC 70-4 "Seismic Analysis of the Charaima Building, Caraballeda, Venezuela," by Subcommittee of the SEAONC Research Committee: V.V. Bertero, P.F. Fratessa, S.A. Mahin, J.H. Sexton, A.C. Scordelis, E.L. Wilson, L.A. Wyllie, H.B. Seed and J. Penzien, Chairman - 1970 (PB 201 455)A06

EERC 70-5 "A Computer Program for Earthquake Analysis of Dams," by A.K. Chopra and P. Chakrabarti - 1970 (AD 723 994)A05

EERC 70-6 "The Propagation of Love Waves Across Non-Horizontally Layered Structures," by J. Lysmer and L.A. Drake 1970 (PB 197 896)A03

EERC 70-7 "Influence of Base Rock Characteristics on Ground Response," by J. Lysmer, H.B. Seed and P.B. Schnabel 1970 (PB 197 897)A03

EERC 70-8 "Applicability of Laboratory Test Procedures for Measuring Soil Liquefaction Characteristics under Cyclic Loading," by H.B. Seed and W.H. Peacock - 1970 (PB 198 016)A03

EERC 70-9 "A Simplified Procedure for Evaluating Soil Liquefaction Potential," by H.B. Seed and I.M. Idriss - 1970 (PB 198 009)A03

EERC 70-10 "Soil Moduli and Damping Factors for Dynamic Response Analysis," by H.B. Seed and I.M. Idriss - 1970 (PB 197 869)A03

EERC 71-1 "Koyna Earthquake of December 11, 1967 and the Performance of Koyna Dam," by A.K. Chopra and P. Chakrabarti 1971 (AD 731 496)A06

EERC 71-2 "Preliminary In-Situ Measurements of Anelastic Absorption in Soils Using a Prototype Earthquake Simulator," by R.D. Borcherdt and P.W. Rodgers - 1971 (PB 201 454)A03

EERC 71-3 "Static and Dynamic Analysis of Inelastic Frame Structures," by F.L. Porter and G.H. Powell - 1971 (PB 210 135)A06

EERC 71-4 "Research Needs in Limit Design of Reinforced Concrete Structures," by V.V. Bertero - 1971 (PB 202 943)A04

EERC 71-5 "Dynamic Behavior of a High-Rise Diagonally Braced Steel Building," by D. Rea, A.A. Shah and J.G. Bouwkamp 1971 (PB 203 584)A06

EERC 71-6 "Dynamic Stress Analysis of Porous Elastic Solids Saturated with Compressible Fluids," by J. Ghaboussi and E. L. Wilson - 1971 (PB 211 396)A06

EERC 71-7 "Inelastic Behavior of Steel Beam-to-Column Subassemblages," by H. Krawinkler, V.V. Bertero and E.P. Popov 1971 (PB 211 335)A14

EERC 71-8 "Modification of Seismograph Records for Effects of Local Soil Conditions," by P. Schnabel, H.B. Seed and J. Lysmer - 1971 (PB 214 450)A03

EERC 72-1 "Static and Earthquake Analysis of Three Dimensional Frame and Shear Wall Buildings," by E.L. Wilson and H.H. Dovey - 1972 (PB 212 904)A05

EERC 72-2 "Accelerations in Rock for Earthquakes in the Western United States," by P.B. Schnabel and H.B. Seed - 1972 (PB 213 100)A03

EERC 72-3 "Elastic-Plastic Earthquake Response of Soil-Building Systems," by T. Minami - 1972 (PB 214 868)A08

EERC 72-4 "Stochastic Inelastic Response of Offshore Towers to Strong Motion Earthquakes," by M.K. Kaul - 1972 (PB 215 713)A05

EERC 72-5 "Cyclic Behavior of Three Reinforced Concrete Flexural Members with High Shear," by E.P. Popov, V.V. Bertero and H. Krawinkler - 1972 (PB 214 555)A05

EERC 72-6 "Earthquake Response of Gravity Dams Including Reservoir Interaction Effects," by P. Chakrabarti and A.K. Chopra - 1972 (AD 762 330)A08

EERC 72-7 "Dynamic Properties of Pine Flat Dam," by D. Rea, C.Y. Liaw and A.K. Chopra - 1972 (AD 763 928)A05

EERC 72-8 "Three Dimensional Analysis of Building Systems," by E.L. Wilson and H.H. Dovey - 1972 (PB 222 438)A06

EERC 72-9 "Rate of Loading Effects on Uncracked and Repaired Reinforced Concrete Members," by S. Mahin, V.V. Bertero, D. Rea and M. Atalay - 1972 (PB 224 520)A08

EERC 72-10 "Computer Program for Static and Dynamic Analysis of Linear Structural Systems," by E.L. Wilson, K.-J. Bathe, J.E. Peterson and H.H.Dovey - 1972 (PB 220 437)A04

EERC 72-11 "Literature Survey - Seismic Effects on Highway Bridges," by T. Iwasaki, J. Penzien and R.W. Clough - 1972 (PB 215 613)A19

EERC 72-12 "SHAKE-A Computer Program for Earthquake Response Analysis of Horizontally Layered Sites," by P.B. Schnabel and J. Lysmer - 1972 (PB 220 207)A06

EERC 73-1 Unassigned

EERC 73-2 "Analysis of the Slides in the San Fernando Dams During the Earthquake of February 9, 1971," by H.B. Seed, K.L. Lee, I.M. Idriss and F. Makdisi - 1973 (PB 223 402)A14

EERC 73-3 "Computer Aided Ultimate Load Design of Unbraced Multistory Steel Frames," by M.B. El-Hafez and G.H. Powell 1973 (PB 248 315)A09

EERC 73-4 "Experimental Investigation into the Seismic Behavior of Critical Regions of Reinforced Concrete Components as Influenced by Moment and Shear," by M. Celebi and J. Penzien - 1973 (PB 215 884)A09

EERC 73-5 "Hysteretic Behavior of Epoxy-Repaired Reinforced Concrete Beams," by M. Celebi and J. Penzien - 1973 (PB 239 568)A03

EERC 73-6 "General Purpose Computer Program for Inelastic Dynamic Response of Plane Structures," by A. Kanaan and G.H. Powell - 1973 (PB 221 260)A08

EERC 73-7 "A Computer Program for Earthquake Analysis of Gravity Dams Including Reservoir Interaction," by P. Chakrabarti and A.K. Chopra - 1973 (AD 766 271)A04

EERC 73-8 "Behavior of Reinforced Concrete Deep Beam-Column Subassemblages Under Cyclic Loads," by O. Küstü and J.G. Bouwkamp - 1973 (PB 246 117)A12

EERC 73-9 "Earthquake Analysis of Structure-Foundation Systems," by A.K. Vaish and A.K. Chopra - 1973 (AD 766 272)A07

EERC 73-10 "Deconvolution of Seismic Response for Linear Systems," by R.B. Reimer - 1973 (PB 227 179)A08

EERC 73-11 "SAP IV: A Structural Analysis Program for Static and Dynamic Response of Linear Systems," by K.-J. Bathe, E.L. Wilson and F.E. Peterson - 1973 (PB 221 967)A09

EERC 73-12 "Analytical Investigations of the Seismic Response of Long, Multiple Span Highway Bridges," by W.S. Tseng and J. Penzien - 1973 (PB 227 816)A10

EERC 73-13 "Earthquake Analysis of Multi-Story Buildings Including Foundation Interaction," by A.K. Chopra and J.A. Gutierrez - 1973 (PB 222 970)A03

EERC 73-14 "ADAP: A Computer Program for Static and Dynamic Analysis of Arch Dams," by R.W. Clough, J.M. Raphael and S. Mojtahedi - 1973 (PB 223 763)A09

EERC 73-15 "Cyclic Plastic Analysis of Structural Steel Joints," by R.B. Pinkney and R.W. Clough - 1973 (PB 226 843)A08

EERC 73-16 "QUAD-4: A Computer Program for Evaluating the Seismic Response of Soil Structures by Variable Damping Finite Element Procedures," by I.M. Idriss, J. Lysmer, R. Hwang and H.B. Seed - 1973 (PB 229 424)A05

EERC 73-17 "Dynamic Behavior of a Multi-Story Pyramid Shaped Building," by R.M. Stephen, J.P. Hollings and J.G. Bouwkamp - 1973 (PB 240 718)A06

EERC 73-18 Unassigned

EERC 73-19 "Olive View Medical Center Materials Studies, Phase I," by B. Bresler and V.V. Bertero - 1973 (PB 235 986)A06

EERC 73-20 Unassigned

EERC 73-21 "Constitutive Models for Cyclic Plastic Deformation of Engineering Materials," by J.M. Kelly and P.P. Gillis 1973 (PB 226 024)A03

EERC 73-22 "DRAIN - 2D User's Guide," by G.H. Powell - 1973 (PB 227 016)A05

EERC 73-23 "Earthquake Engineering at Berkeley - 1973," (PB 226 033)A11

EERC 73-24 Unassigned

EERC 73-25 "Earthquake Response of Axisymmetric Tower Structures Surrounded by Water," by C.Y. Liaw and A.K. Chopra 1973 (AD 773 052)A09

EERC 73-26 "Investigation of the Failures of the Olive View Stairtowers During the San Fernando Earthquake and Their Implications on Seismic Design," by V.V. Bertero and R.G. Collins - 1973 (PB 235 106)A13

EERC 73-27 "Further Studies on Seismic Behavior of Steel Beam-Column Subassemblages," by V.V. Bertero, H. Krawinkler and E.P. Popov - 1973 (PB 234 172)A06

EERC 74-1 "Seismic Risk Analysis," by C.S. Oliveira - 1974 (PB 235 920)A06

EERC 74-2 "Settlement and Liquefaction of Sands Under Multi-Directional Shaking," by R. Pyke, C.K. Chan and H.B. Seed 1974

EERC 74-3 "Optimum Design of Earthquake Resistant Shear Buildings," by D. Ray, K.S. Pister and A.K. Chopra - 1974 (PB 231 172)A06

EERC 74-4 "LUSH - A Computer Program for Complex Response Analysis of Soil-Structure Systems," by J. Lysmer, T. Udaka, H.B. Seed and R. Hwang - 1974 (PB 236 796)A05

EERC 74-5 "Sensitivity Analysis for Hysteretic Dynamic Systems: Applications to Earthquake Engineering," by D. Ray 1974 (PB 233 213)A06

EERC 74-6 "Soil Structure Interaction Analyses for Evaluating Seismic Response," by H.B. Seed, J. Lysmer and R. Hwang 1974 (PB 236 519)A04

EERC 74-7 Unassigned

EERC 74-8 "Shaking Table Tests of a Steel Frame - A Progress Report," by R.W. Clough and D. Tang - 1974 (PB 240 869)A03

EERC 74-9 "Hysteretic Behavior of Reinforced Concrete Flexural Members with Special Web Reinforcement," by V.V. Bertero, E.P. Popov and T.Y. Wang - 1974 (PB 236 797)A07

EERC 74-10 "Applications of Reliability-Based, Global Cost Optimization to Design of Earthquake Resistant Structures," by E. Vitiello and K.S. Pister - 1974 (PB 237 231)A06

EERC 74-11 "Liquefaction of Gravelly Soils Under Cyclic Loading Conditions," by R.T. Wong, H.B. Seed and C.K. Chan 1974 (PB 242 042)A03

EERC 74-12 "Site-Dependent Spectra for Earthquake-Resistant Design," by H.B. Seed, C. Ugas and J. Lysmer - 1974 (PB 240 953)A03

EERC 74-13 "Earthquake Simulator Study of a Reinforced Concrete Frame," by P. Hidalgo and R.W. Clough - 1974 (PB 241 944)A13

EERC 74-14 "Nonlinear Earthquake Response of Concrete Gravity Dams," by N. Pal - 1974 (AD/A 006 583)A06

EERC 74-15 "Modeling and Identification in Nonlinear Structural Dynamics - I. One Degree of Freedom Models," by N. Distefano and A. Rath - 1974 (PB 241 548)A06

EERC 75-1 "Determination of Seismic Design Criteria for the Dumbarton Bridge Replacement Structure, Vol. I: Description, Theory and Analytical Modeling of Bridge and Parameters," by F. Baron and S.-H. Pang - 1975 (PB 259 407)A15

EERC 75-2 "Determination of Seismic Design Criteria for the Dumbarton Bridge Replacement Structure, Vol. II: Numerical Studies and Establishment of Seismic Design Criteria," by F. Baron and S.-H. Pang - 1975 (PB 259 408)A11 (For set of EERC 75-1 and 75-2 (PB 259 406))A25

EERC 75-3 "Seismic Risk Analysis for a Site and a Metropolitan Area," by C.S. Oliveira - 1975 (PB 248 134)A09

EERC 75-4 "Analytical Investigations of Seismic Response of Short, Single or Multiple-Span Highway Bridges," by M.-C. Chen and J. Penzien - 1975 (PB 241 454)A09

EERC 75-5 "An Evaluation of Some Methods for Predicting Seismic Behavior of Reinforced Concrete Buildings," by S.A. Mahin and V.V. Bertero - 1975 (PB 246 306)A16

EERC 75-6 "Earthquake Simulator Study of a Steel Frame Structure, Vol. I: Experimental Results," by R.W. Clough and D.T. Tang - 1975 (PB 243 981)A13

EERC 75-7 "Dynamic Properties of San Bernardino Intake Tower," by D. Rea, C.-Y. Liaw and A.K. Chopra - 1975 (AD/A008 406) A05

EERC 75-8 "Seismic Studies of the Articulation for the Dumbarton Bridge Replacement Structure, Vol. I: Description, Theory and Analytical Modeling of Bridge Components," by F. Baron and R.E. Hamati - 1975 (PB 251 539)A07

EERC 75-9 "Seismic Studies of the Articulation for the Dumbarton Bridge Replacement Structure, Vol. 2: Numerical Studies of Steel and Concrete Girder Alternates," by F. Baron and R.E. Hamati - 1975 (PB 251 540)A10

EERC 75-10 "Static and Dynamic Analysis of Nonlinear Structures," by D.P. Mondkar and G.H. Powell - 1975 (PB 242 434)A08

EERC 75-11 "Hysteretic Behavior of Steel Columns," by E.P. Popov, V.V. Bertero and S. Chandramouli - 1975 (PB 252 365)A11

EERC 75-12 "Earthquake Engineering Research Center Library Printed Catalog," - 1975 (PB 243 711)A26

EERC 75-13 "Three Dimensional Analysis of Building Systems (Extended Version)," by E.L. Wilson, J.P. Hollings and H.H. Dovey - 1975 (PB 243 989)A07

EERC 75-14 "Determination of Soil Liquefaction Characteristics by Large-Scale Laboratory Tests," by P. De Alba, C.K. Chan and H.B. Seed - 1975 (NUREG 0027)A08

EERC 75-15 "A Literature Survey - Compressive, Tensile, Bond and Shear Strength of Masonry," by R.L. Mayes and R.W. Clough - 1975 (PB 246 292)A10

EERC 75-16 "Hysteretic Behavior of Ductile Moment Resisting Reinforced Concrete Frame Components," by V.V. Bertero and E.P. Popov - 1975 (PB 246 388)A05

EERC 75-17 "Relationships Between Maximum Acceleration, Maximum Velocity, Distance from Source, Local Site Conditions for Moderately Strong Earthquakes," by H.B. Seed, R. Murarka, J. Lysmer and I.M. Idriss - 1975 (PB 248 172)A03

EERC 75-18 "The Effects of Method of Sample Preparation on the Cyclic Stress-Strain Behavior of Sands," by J. Mulilis, C.K. Chan and H.B. Seed - 1975 (Summarized in EERC 75-28)

EERC 75-19 "The Seismic Behavior of Critical Regions of Reinforced Concrete Components as Influenced by Moment, Shear and Axial Force," by M.B. Atalay and J. Penzien - 1975 (PB 258 842)A11

EERC 75-20 "Dynamic Properties of an Eleven Story Masonry Building," by R.M. Stephen, J.P. Hollings, J.G. Bouwkamp and D. Jurukovski - 1975 (PB 246 945)A04

EERC 75-21 "State-of-the-Art in Seismic Strength of Masonry - An Evaluation and Review," by R.L. Mayes and R.W. Clough 1975 (PB 249 040)A07

EERC 75-22 "Frequency Dependent Stiffness Matrices for Viscoelastic Half-Plane Foundations," by A.K. Chopra, P. Chakrabarti and G. Dasgupta - 1975 (PB 248 121)A07

EERC 75-23 "Hysteretic Behavior of Reinforced Concrete Framed Walls," by T.Y. Wang, V.V. Bertero and E.P. Popov - 1975 (PB 267 298)A17

EERC 75-24 Unassigned

EERC 75-25 "Influence of Seismic History on the Liquefaction Characteristics of Sands," by H.B. Seed, K. Mori and C.K. Chan - 1975 (Summarized in EERC 75-28)

EERC 75-26 "The Generation and Dissipation of Pore Water Pressures during Soil Liquefaction," by H.B. Seed, P.P. Martin and J. Lysmer - 1975 (PB 252 648)A03

EERC 75-27 "Identification of Research Needs for Improving Aseismic Design of Building Structures," by V.V. Bertero 1975 (PB 248 136)A05

EERC 75-28 "Evaluation of Soil Liquefaction Potential during Earthquakes," by H.B. Seed, I. Arango and C.K. Chan - 1975 (NUREG 0026)A13

EERC 75-29 "Representation of Irregular Stress Time Histories by Equivalent Uniform Stress Series in Liquefaction Analyses," by H.B. Seed, I.M. Idriss, F. Makdisi and N. Banerjee - 1975 (PB 252 635)A03

EERC 75-30 "FLUSH - A Computer Program for Approximate 3-D Analysis of Soil-Structure Interaction Problems," by J. Lysmer, T. Udaka, C.-F. Tsai and H.B. Seed - 1975 (PB 259 332)A07

EERC 75-31 Unassigned

EERC 75-32 Unassigned

EERC 75-33 "Predicting the Performance of Structures in Regions of High Seismicity," by J. Penzien - 1975 (PB 248 130)A03

EERC 75-34 "Efficient Finite Element Analysis of Seismic Structure - Soil - Direction," by J. Lysmer, H.B. Seed, T. Udaka, R.N. Hwang and C.-F. Tsai - 1975 (PB 253 570)A03

EERC 75-35 "The Dynamic Behavior of a First Story Girder of a Three-Story Steel Frame Subjected to Earthquake Loading," by R.W. Clough and L.-Y. Li - 1975 (PB 248 841)A05

EERC 75-36 "Earthquake Simulator Study of a Steel Frame Structure, Volume II - Analytical Results," by D.T. Tang - 1975 (PB 252 926)A10

EERC 75-37 "ANSR-I General Purpose Computer Program for Analysis of Non-Linear Structural Response," by D.P. Mondkar and G.H. Powell - 1975 (PB 252 386)A08

EERC 75-38 "Nonlinear Response Spectra for Probabilistic Seismic Design and Damage Assessment of Reinforced Concrete Structures," by M. Murakami and J. Penzien - 1975 (PB 259 530)A05

EERC 75-39 "Study of a Method of Feasible Directions for Optimal Elastic Design of Frame Structures Subjected to Earthquake Loading," by N.D. Walker and K.S. Pister - 1975 (PB 257 781)A06

EERC 75-40 "An Alternative Representation of the Elastic-Viscoelastic Analogy," by G. Dasgupta and J.L. Sackman - 1975 (PB 252 173)A03

EERC 75-41 "Effect of Multi-Directional Shaking on Liquefaction of Sands," by H.B. Seed, R. Pyke and G.R. Martin - 1975 (PB 258 781)A03

EERC 76-1 "Strength and Ductility Evaluation of Existing Low-Rise Reinforced Concrete Buildings - Screening Method," by T. Okada and B. Bresler - 1976 (PB 257 906)A11

EERC 76-2 "Experimental and Analytical Studies on the Hysteretic Behavior of Reinforced Concrete Rectangular and T-Beams," by S.-Y.M. Ma, E.P. Popov and V.V. Bertero - 1976 (PB 260 843)A12

EERC 76-3 "Dynamic Behavior of a Multistory Triangular-Shaped Building," by J. Petrovski, R.M. Stephen, E. Gartenbaum and J.G. Bouwkamp - 1976 (PB 273 279)A07

EERC 76-4 "Earthquake Induced Deformations of Earth Dams," by N. Serff, H.B. Seed, F.I. Makdisi & C.-Y. Chang - 1976 (PB 292 065)A08

EERC 76-5 "Analysis and Design of Tube-Type Tall Building Structures," by H. de Clercq and G.H. Powell - 1976 (PB 252 220) A10

EERC 76-6 "Time and Frequency Domain Analysis of Three-Dimensional Ground Motions, San Fernando Earthquake," by T. Kubo and J. Penzien (PB 260 556)A11

EERC 76-7 "Expected Performance of Uniform Building Code Design Masonry Structures," by R.L. Mayes, Y. Omote, S.W. Chen and R.W. Clough - 1976 (PB 270 098)A05

EERC 76-8 "Cyclic Shear Tests of Masonry Piers, Volume 1 - Test Results," by R.L. Mayes, Y. Omote, R.W. Clough - 1976 (PB 264 424)A06

EERC 76-9 "A Substructure Method for Earthquake Analysis of Structure - Soil Interaction," by J.A. Gutierrez and A.K. Chopra - 1976 (PB 257 783)A08

EERC 76-10 "Stabilization of Potentially Liquefiable Sand Deposits using Gravel Drain Systems," by H.B. Seed and J.R. Booker - 1976 (PB 258 820)A04

EERC 76-11 "Influence of Design and Analysis Assumptions on Computed Inelastic Response of Moderately Tall Frames," by G.H. Powell and D.G. Row - 1976 (PB 271 409)A06

EERC 76-12 "Sensitivity Analysis for Hysteretic Dynamic Systems: Theory and Applications," by D. Ray, K.S. Pister and E. Polak - 1976 (PB 262 859)A04

EERC 76-13 "Coupled Lateral Torsional Response of Buildings to Ground Shaking," by C.L. Kan and A.K. Chopra - 1976 (PB 257 907)A09

EERC 76-14 Unassigned

EERC 76-15 "Reinforced Concrete Frame 2: Seismic Testing and Analytical Correlation," by R.W. Clough and J. Gidwani - 1976 (PB 261 323)A08

EERC 76-16 "Cyclic Shear Tests of Masonry Piers, Volume 2 - Analysis of Test Results," by R.L. Mayes, Y. Omote and R.W. Clough - 1976 (PB 297 158)A05

EERC 76-17 "Structural Steel Bracing Systems: Behavior Under Cyclic Loading," by E.P. Popov, K. Takanashi and C.W. Roeder - 1976 (PB 260 715)A05

EERC 76-18 "Experimental Model Studies on Seismic Response of High Curved Overcrossings," by D. Williams and W.G. Godden - 1976 (PB 269 548)A08

EERC 76-19 "Effects of Non-Uniform Seismic Disturbances on the Dumbarton Bridge Replacement Structure," by F. Baron and R.E. Hamati - 1976 (PB 282 981)A16

EERC 76-20 "Investigation of the Inelastic Characteristics of a Single Story Steel Structure Using System Identification and Shaking Table Experiments," by V.C. Matzen and H.D. McNiven - 1976 (PB 258 453)A07

EERC 76-21 "Capacity of Columns with Splice Imperfections," by E.P. Popov, R.M. Stephen and R. Philbrick - 1976 (PB 260 378)A04

EERC 76-22 "Response of the Olive View Hospital Main Building during the San Fernando Earthquake," by S. A. Mahin, V.V. Bertero, A.K. Chopra and R. Collins - 1976 (PB 271 425)A14

EERC 76-23 "A Study on the Major Factors Influencing the Strength of Masonry Prisms," by N.M. Mostaghel, R.L. Mayes, R. W. Clough and S.W. Chen - 1976 (Not published)

EERC 76-24 "GADFLEA - A Computer Program for the Analysis of Pore Pressure Generation and Dissipation during Cyclic or Earthquake Loading," by J.R. Booker, M.S. Rahman and H.B. Seed - 1976 (PB 263 947)A04

EERC 76-25 "Seismic Safety Evaluation of a R/C School Building," by B. Bresler and J. Axley - 1976

EERC 76-26 "Correlative Investigations on Theoretical and Experimental Dynamic Behavior of a Model Bridge Structure," by K. Kawashima and J. Penzien - 1976 (PB 263 388)A11

EERC 76-27 "Earthquake Response of Coupled Shear Wall Buildings," by T. Srichatrapimuk - 1976 (PB 265 157)A07

EERC 76-28 "Tensile Capacity of Partial Penetration Welds," by E.P. Popov and R.M. Stephen - 1976 (PB 262 899)A03

EERC 76-29 "Analysis and Design of Numerical Integration Methods in Structural Dynamics," by H.M. Hilber - 1976 (PB 264 410)A06

EERC 76-30 "Contribution of a Floor System to the Dynamic Characteristics of Reinforced Concrete Buildings," by L.E. Malik and V.V. Bertero - 1976 (PB 272 247)A13

EERC 76-31 "The Effects of Seismic Disturbances on the Golden Gate Bridge," by F. Baron, M. Arikan and R.E. Hamati - 1976 (PB 272 279)A09

EERC 76-32 "Infilled Frames in Earthquake Resistant Construction," by R.E. Klingner and V.V. Bertero - 1976 (PB 265 892)A13

UCB/EERC-77/01 "PLUSH - A Computer Program for Probabilistic Finite Element Analysis of Seismic Soil-Structure Interaction," by M.P. Romo Organista, J. Lysmer and H.B. Seed - 1977 (PB81 177 651)A05

UCB/EERC-77/02 "Soil-Structure Interaction Effects at the Humboldt Bay Power Plant in the Ferndale Earthquake of June 7, 1975," by J.E. Valera, H.B. Seed, C.F. Tsai and J. Lysmer - 1977 (PB 265 795)A04

UCB/EERC-77/03 "Influence of Sample Disturbance on Sand Response to Cyclic Loading," by K. Mori, H.B. Seed and C.K. Chan - 1977 (PB 267 352)A04

UCB/EERC-77/04 "Seismological Studies of Strong Motion Records," by J. Shoja-Taheri - 1977 (PB 269 655)A10

UCB/EERC-77/05 Unassigned

UCB/EERC-77/06 "Developing Methodologies for Evaluating the Earthquake Safety of Existing Buildings," by No. 1 - B. Bresler; No. 2 - B. Bresler, T. Okada and D. Zisling; No. 3 - T. Okada and B. Bresler; No. 4 - V.V. Bertero and B. Bresler - 1977 (PB 267 354)A08

UCB/EERC-77/07 "A Literature Survey - Transverse Strength of Masonry Walls," by Y. Omote, R.L. Mayes, S.W. Chen and R.W. Clough - 1977 (PB 277 933)A07

UCB/EERC-77/08 "DRAIN-TABS: A Computer Program for Inelastic Earthquake Response of Three Dimensional Buildings," by R. Guendelman-Israel and G.H. Powell - 1977 (PB 270 693)A07

UCB/EERC-77/09 "SUBWALL: A Special Purpose Finite Element Computer Program for Practical Elastic Analysis and Design of Structural Walls with Substructure Option," by D.Q. Le, H. Peterson and E.P. Popov - 1977 (PB 270 567)A05

UCB/EERC-77/10 "Experimental Evaluation of Seismic Design Methods for Broad Cylindrical Tanks," by D.P. Clough (PB 272 280)A13

UCB/EERC-77/11 "Earthquake Engineering Research at Berkeley - 1976," - 1977 (PB 273 507)A09

UCB/EERC-77/12 "Automated Design of Earthquake Resistant Multistory Steel Building Frames," by N.D. Walker, Jr. - 1977 (PB 276 526)A09

UCB/EERC-77/13 "Concrete Confined by Rectangular Hoops Subjected to Axial Loads," by J. Vallenas, V.V. Bertero and E.P. Popov - 1977 (PB 275 165)A06

UCB/EERC-77/14 "Seismic Strain Induced in the Ground During Earthquakes," by Y. Sugimura - 1977 (PB 284 201)A04

UCB/EERC-77/15 Unassigned

UCB/EERC-77/16 "Computer Aided Optimum Design of Ductile Reinforced Concrete Moment Resisting Frames," by S.W. Zagajeski and V.V. Bertero - 1977 (PB 280 137)A07

UCB/EERC-77/17 "Earthquake Simulation Testing of a Stepping Frame with Energy-Absorbing Devices," by J.M. Kelly and D.F. Tsztoo - 1977 (PB 273 506)A04

UCB/EERC-77/18 "Inelastic Behavior of Eccentrically Braced Steel Frames under Cyclic Loadings," by C.W. Roeder and E.P. Popov - 1977 (PB 275 526)A15

UCB/EERC-77/19 "A Simplified Procedure for Estimating Earthquake-Induced Deformations in Dams and Embankments," by F.I. Makdisi and H.B. Seed - 1977 (PB 276 820)A04

UCB/EERC-77/20 "The Performance of Earth Dams during Earthquakes," by H.B. Seed, F.I. Makdisi and P. de Alba - 1977 (PB 276 821)A04

UCB/EERC-77/21 "Dynamic Plastic Analysis Using Stress Resultant Finite Element Formulation," by P. Lukkunapvasit and J.M. Kelly - 1977 (PB 275 453)A04

UCB/EERC-77/22 "Preliminary Experimental Study of Seismic Uplift of a Steel Frame," by R.W. Clough and A.A. Huckelbridge 1977 (PB 278 769)A08

UCB/EERC-77/23 "Earthquake Simulator Tests of a Nine-Story Steel Frame with Columns Allowed to Uplift," by A.A. Huckelbridge - 1977 (PB 277 944)A09

UCB/EERC-77/24 "Nonlinear Soil-Structure Interaction of Skew Highway Bridges," by M.-C. Chen and J. Penzien - 1977 (PB 276 176)A07

UCB/EERC-77/25 "Seismic Analysis of an Offshore Structure Supported on Pile Foundations," by D.D.-N. Liou and J. Penzien 1977 (PB 283 180)A06

UCB/EERC-77/26 "Dynamic Stiffness Matrices for Homogeneous Viscoelastic Half-Planes," by G. Dasgupta and A.K. Chopra - 1977 (PB 279 654)A06

UCB/EERC-77/27 "A Practical Soft Story Earthquake Isolation System," by J.M. Kelly, J.M. Eidinger and C.J. Derham - 1977 (PB 276 814)A07

UCB/EERC-77/28 "Seismic Safety of Existing Buildings and Incentives for Hazard Mitigation in San Francisco: An Exploratory Study," by A.J. Meltsner - 1977 (PB 281 970)A05

UCB/EERC-77/29 "Dynamic Analysis of Electrohydraulic Shaking Tables," by D. Rea, S. Abedi-Hayati and Y. Takahashi 1977 (PB 282 569)A04

UCB/EERC-77/30 "An Approach for Improving Seismic - Resistant Behavior of Reinforced Concrete Interior Joints," by B. Galunic, V.V. Bertero and E.P. Popov - 1977 (PB 290 870)A06

UCB/EERC-78/01 "The Development of Energy-Absorbing Devices for Aseismic Base Isolation Systems," by J.M. Kelly and D.F. Tsztoo - 1978 (PB 284 978)A04

UCB/EERC-78/02 "Effect of Tensile Prestrain on the Cyclic Response of Structural Steel Connections, by J.G. Bouwkamp and A. Mukhopadhyay - 1978

UCB/EERC-78/03 "Experimental Results of an Earthquake Isolation System using Natural Rubber Bearings," by J.M. Eidinger and J.M. Kelly - 1978 (PB 281 686)A04

UCB/EERC-78/04 "Seismic Behavior of Tall Liquid Storage Tanks," by A. Niwa - 1978 (PB 284 017)A14

UCB/EERC-78/05 "Hysteretic Behavior of Reinforced Concrete Columns Subjected to High Axial and Cyclic Shear Forces," by S.W. Zagajeski, V.V. Bertero and J.G. Bouwkamp - 1978 (PB 283 858)A13

UCB/EERC-78/06 "Three Dimensional Inelastic Frame Elements for the ANSR-I Program," by A. Riahi, D.G. Row and G.H. Powell - 1978 (PB 295 755)A04

UCB/EERC-78/07 "Studies of Structural Response to Earthquake Ground Motion," by O.A. Lopez and A.K. Chopra - 1978 (PB 282 790)A05

UCB/EERC-78/08 "A Laboratory Study of the Fluid-Structure Interaction of Submerged Tanks and Caissons in Earthquakes," by R.C. Byrd - 1978 (PB 284 957)A08

UCB/EERC-78/09 "Model for Evaluating Damageability of Structures," by I. Sakamoto and B. Bresler - 1978

UCB/EERC-78/10 "Seismic Performance of Nonstructural and Secondary Structural Elements," by I. Sakamoto - 1978 (PB81 154 593)A05

UCB/EERC-78/11 "Mathematical Modelling of Hysteresis Loops for Reinforced Concrete Columns," by S. Nakata, T. Sproul and J. Penzien - 1978 (PB 298 274)A05

UCB/EERC-78/12 "Damageability in Existing Buildings," by T. Blejwas and B. Bresler - 1978 (PB 80 166 978)A05

UCB/EERC-78/13 "Dynamic Behavior of a Pedestal Base Multistory Building," by R.M. Stephen, E.L. Wilson, J.G. Bouwkamp and M. Button - 1978 (PB 286 650)A08

UCB/EERC-78/14 "Seismic Response of Bridges - Case Studies," by R.A. Imbsen, V. Nutt and J. Penzien - 1978 (PB 286 503)A10

UCB/EERC-78/15 "A Substructure Technique for Nonlinear Static and Dynamic Analysis," by D.G. Row and G.H. Powell - 1978 (PB 288 077)A10

UCB/EERC-78/16 "Seismic Risk Studies for San Francisco and for the Greater San Francisco Bay Area," by C.S. Oliveira - 1978 (PB 81 120 115)A07

UCB/EERC-78/17 "Strength of Timber Roof Connections Subjected to Cyclic Loads," by P. Gülkan, R.L. Mayes and R.W. Clough - 1978 (HUD-000 1491)A07

UCB/EERC-78/18 "Response of K-Braced Steel Frame Models to Lateral Loads," by J.G. Bouwkamp, R.M. Stephen and E.P. Popov - 1978

UCB/EERC-78/19 "Rational Design Methods for Light Equipment in Structures Subjected to Ground Motion," by J.L. Sackman and J.M. Kelly - 1978 (PB 292 357)A04

UCB/EERC-78/20 "Testing of a Wind Restraint for Aseismic Base Isolation," by J.M. Kelly and D.E. Chitty - 1978 (PB 292 833)A03

UCB/EERC-78/21 "APOLLO - A Computer Program for the Analysis of Pore Pressure Generation and Dissipation in Horizontal Sand Layers During Cyclic or Earthquake Loading," by P.P. Martin and H.B. Seed - 1978 (PB 292 835)A04

UCB/EERC-78/22 "Optimal Design of an Earthquake Isolation System," by M.A. Bhatti, K.S. Pister and E. Polak - 1978 (PB 294 735)A06

UCB/EERC-78/23 "MASH - A Computer Program for the Non-Linear Analysis of Vertically Propagating Shear Waves in Horizontally Layered Deposits," by P.P. Martin and H.B. Seed - 1978 (PB 293 101)A05

UCB/EERC-78/24 "Investigation of the Elastic Characteristics of a Three Story Steel Frame Using System Identification," by I. Kaya and H.D. McNiven - 1978 (PB 296 225)A06

UCB/EERC-78/25 "Investigation of the Nonlinear Characteristics of a Three-Story Steel Frame Using System Identification," by I. Kaya and H.D. McNiven - 1978 (PB 301 363)A05

UCB/EERC-78/26 "Studies of Strong Ground Motion in Taiwan," by Y.M. Hsiung, B.A. Bolt and J. Penzien - 1978 (PB 298 436)A06

UCB/EERC-78/27 "Cyclic Loading Tests of Masonry Single Piers: Volume 1 - Height to Width Ratio of 2," by P.A. Hidalgo, R.L. Mayes, H.D. McNiven and R.W. Clough - 1978 (PB 296 211)A07

UCB/EERC-78/28 "Cyclic Loading Tests of Masonry Single Piers: Volume 2 - Height to Width Ratio of 1," by S.-W.J. Chen, P.A. Hidalgo, R.L. Mayes, R.W. Clough and H.D. McNiven - 1978 (PB 296 212)A09

UCB/EERC-78/29 "Analytical Procedures in Soil Dynamics," by J. Lysmer - 1978 (PB 298 445)A06

UCB/EERC-79/01 "Hysteretic Behavior of Lightweight Reinforced Concrete Beam-Column Subassemblages," by B. Forzani, E.P. Popov and V.V. Bertero - April 1979(PB 298 267)A06

UCB/EERC-79/02 "The Development of a Mathematical Model to Predict the Flexural Response of Reinforced Concrete Beams to Cyclic Loads, Using System Identification," by J. Stanton & H. McNiven - Jan. 1979(PB 295 875)A10

UCB/EERC-79/03 "Linear and Nonlinear Earthquake Response of Simple Torsionally Coupled Systems," by C.L. Kan and A.K. Chopra - Feb. 1979(PB 298 262)A06

UCB/EERC-79/04 "A Mathematical Model of Masonry for Predicting its Linear Seismic Response Characteristics," by Y. Mengi and H.D. McNiven - Feb. 1979(PB 298 266)A06

UCB/EERC-79/05 "Mechanical Behavior of Lightweight Concrete Confined by Different Types of Lateral Reinforcement," by M.A. Manrique, V.V. Bertero and E.P. Popov - May 1979(PB 301 114)A06

UCB/EERC-79/06 "Static Tilt Tests of a Tall Cylindrical Liquid Storage Tank," by R.W. Clough and A. Niwa - Feb. 1979 (PB 301 167)A06

UCB/EERC-79/07 "The Design of Steel Energy Absorbing Restrainers and Their Incorporation into Nuclear Power Plants for Enhanced Safety: Volume 1 - Summary Report," by P.N. Spencer, V.F. Zackay, and E.R. Parker - Feb. 1979(UCB/EERC-79/07)A09

UCB/EERC-79/08 "The Design of Steel Energy Absorbing Restrainers and Their Incorporation into Nuclear Power Plants for Enhanced Safety: Volume 2 - The Development of Analyses for Reactor System Piping," "Simple Systems" by M.C. Lee, J. Penzien, A.K. Chopra and K. Suzuki "Complex Systems" by G.H. Powell, E.L. Wilson, R.W. Clough and D.G. Row - Feb. 1979(UCB/EERC-79/08)A10

UCB/EERC-79/09 "The Design of Steel Energy Absorbing Restrainers and Their Incorporation into Nuclear Power Plants for Enhanced Safety: Volume 3 - Evaluation of Commercial Steels," by W.S. Owen, R.M.N. Pelloux, R.O. Ritchie, M. Faral, T. Ohhashi, J. Toplosky, S.J. Hartman, V.F. Zackay and E.R. Parker - Feb. 1979(UCB/EERC-79/09)A04

UCB/EERC-79/10 "The Design of Steel Energy Absorbing Restrainers and Their Incorporation into Nuclear Power Plants for Enhanced Safety: Volume 4 - A Review of Energy-Absorbing Devices," by J.M. Kelly and M.S. Skinner - Feb. 1979(UCB/EERC-79/10)A04

UCB/EERC-79/11 "Conservatism In Summation Rules for Closely Spaced Modes," by J.M. Kelly and J.L. Sackman - May 1979(PB 301 328)A03

UCB/EERC-79/12 "Cyclic Loading Tests of Masonry Single Piers; Volume 3 - Height to Width Ratio of 0.5," by P.A. Hidalgo, R.L. Mayes, H.D. McNiven and R.W. Clough - May 1979(PB 301 321)A08

UCB/EERC-79/13 "Cyclic Behavior of Dense Course-Grained Materials in Relation to the Seismic Stability of Dams," by N.G. Banerjee, H.B. Seed and C.K. Chan - June 1979(PB 301 373)A13

UCB/EERC-79/14 "Seismic Behavior of Reinforced Concrete Interior Beam-Column Subassemblages," by S. Viwathanatepa, E.P. Popov and V.V. Bertero - June 1979(PB 301 326)A10

UCB/EERC-79/15 "Optimal Design of Localized Nonlinear Systems with Dual Performance Criteria Under Earthquake Excitations," by M.A. Bhatti - July 1979(PB 80 167 109)A06

UCB/EERC-79/16 "OPTDYN - A General Purpose Optimization Program for Problems with or without Dynamic Constraints," by M.A. Bhatti, E. Polak and K.S. Pister - July 1979(PB 80 167 091)A05

UCB/EERC-79/17 "ANSR-II, Analysis of Nonlinear Structural Response, Users Manual," by D.P. Mondkar and G.H. Powell - July 1979(PB 80 113 301)A05

UCB/EERC-79/18 "Soil Structure Interaction in Different Seismic Environments," A. Gomez-Masso, J. Lysmer, J.-C. Chen and H.B. Seed - August 1979(PB 80 101 520)A04

UCB/EERC-79/19 "ARMA Models for Earthquake Ground Motions," by M.K. Chang, J.W. Kwiatkowski, R.F. Nau, R.M. Oliver and K.S. Pister - July 1979(PB 301 166)A05

UCB/EERC-79/20 "Hysteretic Behavior of Reinforced Concrete Structural Walls," by J.M. Vallenas, V.V. Bertero and E.P. Popov - August 1979(PB 80 165 905)A12

UCB/EERC-79/21 "Studies on High-Frequency Vibrations of Buildings - 1: The Column Effect," by J. Lubliner - August 1979 (PB 80 158 553)A03

UCB/EERC-79/22 "Effects of Generalized Loadings on Bond Reinforcing Bars Embedded in Confined Concrete Blocks," by S. Viwathanatepa, E.P. Popov and V.V. Bertero - August 1979

UCB/EERC-79/23 "Shaking Table Study of Single-Story Masonry Houses, Volume 1: Test Structures 1 and 2," by P. Gülkan, R.L. Mayes and R.W. Clough - Sept. 1979

UCB/EERC-79/24 "Shaking Table Study of Single-Story Masonry Houses, Volume 2: Test Structures 3 and 4," by P. Gülkan, R.L. Mayes and R.W. Clough - Sept. 1979

UCB/EERC-79/25 "Shaking Table Study of Single-Story Masonry Houses, Volume 3: Summary, Conclusions and Recommendations," by R.W. Clough, R.L. Mayes and P. Gülkan - Sept. 1979

UCB/EERC-79/26 "Recommendations for a U.S.-Japan Cooperative Research Program Utilizing Large-Scale Testing Facilities," by U.S.-Japan Planning Group - Sept. 1979(PB 301 407)A06

UCB/EERC-79/27 "Earthquake-Induced Liquefaction Near Lake Amatitlan, Guatemala," by H.B. Seed, I. Arango, C.K. Chan, A. Gomez-Masso and R. Grant de Ascoli - Sept. 1979(NUREG-CR1341)A03

UCB/EERC-79/28 "Infill Panels: Their Influence on Seismic Response of Buildings," by J.W. Axley and V.V. Bertero - Sept. 1979(PB 80 163 371)A10

UCB/EERC-79/29 "3D Truss Bar Element (Type 1) for the ANSR-II Program," by D.P. Mondkar and G.H. Powell - Nov. 1979 (PB 80 169 709)A02

UCB/EERC-79/30 "2D Beam-Column Element (Type 5 - Parallel Element Theory) for the ANSR-II Program," by D.G. Row, G.H. Powell and D.P. Mondkar - Dec. 1979(PB 80 167 224)A03

UCB/EERC-79/31 "3D Beam-Column Element (Type 2 - Parallel Element Theory) for the ANSR-II Program," by A. Riahi, G.H. Powell and D.P. Mondkar - Dec. 1979(PB 80 167 216)A03

UCB/EERC-79/32 "On Response of Structures to Stationary Excitation," by A. Der Kiureghian - Dec. 1979(PB 80 166 929)A03

UCB/EERC-79/33 "Undisturbed Sampling and Cyclic Load Testing of Sands," by S. Singh, H.B. Seed and C.K. Chan - Dec. 1979(

UCB/EERC-79/34 "Interaction Effects of Simultaneous Torsional and Compressional Cyclic Loading of Sand," by P.M. Griffin and W.N. Houston - Dec. 1979

UCB/EERC-80/01 "Earthquake Response of Concrete Gravity Dams Including Hydrodynamic and Foundation Interaction Effects," by A.K. Chopra, P. Chakrabarti and S. Gupta - Jan. 1980(AD-A087297)A10

UCB/EERC-80/02 "Rocking Response of Rigid Blocks to Earthquakes," by C.S. Yim, A.K. Chopra and J. Penzien - Jan. 1980 (PB80 166 002)A04

UCB/EERC-80/03 "Optimum Inelastic Design of Seismic-Resistant Reinforced Concrete Frame Structures," by S.W. Zagajeski and V.V. Bertero - Jan. 1980(PB80 164 635)A06

UCB/EERC-80/04 "Effects of Amount and Arrangement of Wall-Panel Reinforcement on Hysteretic Behavior of Reinforced Concrete Walls," by R. Iliya and V.V. Bertero - Feb. 1980(PB81 122 525)A09

UCB/EERC-80/05 "Shaking Table Research on Concrete Dam Models," by A. Niwa and R.W. Clough - Sept. 1980(PB81 122 368)A06

UCB/EERC-80/06 "The Design of Steel Energy-Absorbing Restrainers and their Incorporation into Nuclear Power Plants for Enhanced Safety (Vol 1A): Piping with Energy Absorbing Restrainers: Parameter Study on Small Systems," by G.H. Powell, C. Oughourlian and J. Simons - June 1980

UCB/EERC-80/07 "Inelastic Torsional Response of Structures Subjected to Earthquake Ground Motions," by Y. Yamazaki April 1980(PB81 122 327)A08

UCB/EERC-80/08 "Study of X-Braced Steel Frame Structures Under Earthquake Simulation," by Y. Ghanaat - April 1980 (PB81 122 335)A11

UCB/EERC-80/09 "Hybrid Modelling of Soil-Structure Interaction," by S. Gupta, T.W. Lin, J. Penzien and C.S. Yeh May 1980(PB81 122 319)A07

UCB/EERC-80/10 "General Applicability of a Nonlinear Model of a One Story Steel Frame," by B.I. Sveinsson and H.D. McNiven - May 1980(PB81 124 877)A06

UCB/EERC-80/11 "A Green-Function Method for Wave Interaction with a Submerged Body," by W. Kioka - April 1980 (PB81 122 269)A07

UCB/EERC-80/12 "Hydrodynamic Pressure and Added Mass for Axisymmetric Bodies," by F. Nilrat - May 1980(PB81 122 343)A08

UCB/EERC-80/13 "Treatment of Non-Linear Drag Forces Acting on Offshore Platforms," by B.V. Dao and J. Penzien May 1980(PB81 153 413)A07

UCB/EERC-80/14 "2D Plane/Axisymmetric Solid Element (Type 3 - Elastic or Elastic-Perfectly Plastic) for the ANSR-II Program," by D.P. Mondkar and G.H. Powell - July 1980(PB81 122 350)A03

UCB/EERC-80/15 "A Response Spectrum Method for Random Vibrations," by A. Der Kiureghian - June 1980(PB81 122 301)A03

UCB/EERC-80/16 "Cyclic Inelastic Buckling of Tubular Steel Braces," by V.A. Zayas, E.P. Popov and S.A. Mahin June 1980(PB81 124 885)A10

UCB/EERC-80/17 "Dynamic Response of Simple Arch Dams Including Hydrodynamic Interaction," by C.S. Porter and A.K. Chopra - July 1980(PB81 124 000)A13

UCB/EERC-80/18 "Experimental Testing of a Friction Damped Aseismic Base Isolation System with Fail-Safe Characteristics," by J.M. Kelly, K.E. Beucke and M.S. Skinner - July 1980(PB81 148 595)A04

UCB/EERC-80/19 "The Design of Steel Energy-Absorbing Restrainers and their Incorporation into Nuclear Power Plants for Enhanced Safety (Vol 1B): Stochastic Seismic Analyses of Nuclear Power Plant Structures and Piping Systems Subjected to Multiple Support Excitations," by M.C. Lee and J. Penzien - June 1980

UCB/EERC-80/20 "The Design of Steel Energy-Absorbing Restrainers and their Incorporation into Nuclear Power Plants for Enhanced Safety (Vol 1C): Numerical Method for Dynamic Substructure Analysis," by J.M. Dickens and E.L. Wilson - June 1980

UCB/EERC-80/21 "The Design of Steel Energy-Absorbing Restrainers and their Incorporation into Nuclear Power Plants for Enhanced Safety (Vol 2): Development and Testing of Restraints for Nuclear Piping Systems," by J.M. Kelly and M.S. Skinner - June 1980

UCB/EERC-80/22 "3D Solid Element (Type 4-Elastic or Elastic-Perfectly-Plastic) for the ANSR-II Program," by D.P. Mondkar and G.H. Powell - July 1980(PB81 123 242)A03

UCB/EERC-80/23 "Gap-Friction Element (Type 5) for the ANSR-II Program," by D.P. Mondkar and G.H. Powell - July 1980 (PB81 122 285)A03

UCB/EERC-80/24 "U-Bar Restraint Element (Type 11) for the ANSR-II Program," by C. Oughourlian and G.H. Powell July 1980(PB81 122 293)A03

UCB/EERC-80/25 "Testing of a Natural Rubber Base Isolation System by an Explosively Simulated Earthquake," by J.M. Kelly - August 1980

UCB/EERC-80/26 "Input Identification from Structural Vibrational Response," by Y. Hu - August 1980(PB81 152 308)A05

UCB/EERC-80/27 "Cyclic Inelastic Behavior of Steel Offshore Structures," by V.A. Zayas, S.A. Mahin and E.P. Popov August 1980

UCB/EERC-80/28 "Shaking Table Testing of a Reinforced Concrete Frame with Biaxial Response," by M.G. Oliva October 1980(PB81 154 304)A10

UCB/EERC-80/29 "Dynamic Properties of a Twelve-Story Prefabricated Panel Building," by J.G. Bouwkamp, J.P. Kollegger and R.M. Stephen - October 1980

UCB/EERC-80/30 "Dynamic Properties of an Eight-Story Prefabricated Panel Building," by J.G. Bouwkamp, J.P. Kollegger and R.M. Stephen - October 1980

UCB/EERC-80/31 "Predictive Dynamic Response of Panel Type Structures Under Earthquakes," by J.P. Kollegger and J.G. Bouwkamp - October 1980(PB81 152 316)A04

UCB/EERC-80/32 "The Design of Steel Energy-Absorbing Restrainers and their Incorporation into Nuclear Power Plants for Enhanced Safety (Vol 3): Testing of Commercial Steels in Low-Cycle Torsional Fatigue," by P. Spencer, E.R. Parker, E. Jongewaard and M. Drory

UCB/EERC-80/33 "The Design of Steel Energy-Absorbing Restrainers and their Incorporation into Nuclear Power Plants for Enhanced Safety (Vol 4): Shaking Table Tests of Piping Systems with Energy-Absorbing Restrainers," by S.F. Stiemer and W.G. Godden - Sept. 1980

UCB/EERC-80/34 "The Design of Steel Energy-Absorbing Restrainers and their Incorporation into Nuclear Power Plants for Enhanced Safety (Vol 5): Summary Report," by P. Spencer

UCB/EERC-80/35 "Experimental Testing of an Energy-Absorbing Base Isolation System," by J.M. Kelly, M.S. Skinner and K.E. Beucke - October 1980(PB81 154 072)A04

UCB/EERC-80/36 "Simulating and Analyzing Artificial Non-Stationary Earthquake Ground Motions," by R.F. Nau, R.M. Oliver and K.S. Pister - October 1980(PB81 153 397)A04

UCB/EERC-80/37 "Earthquake Engineering at Berkeley - 1980," - Sept. 1980

UCB/EERC-80/38 "Inelastic Seismic Analysis of Large Panel Buildings," by V. Schricker and G.H. Powell - Sept. 1980 (PB81 154 338)A13

UCB/EERC-80/39 "Dynamic Response of Embankment, Concrete-Gravity and Arch Dams Including Hydrodynamic Interaction," by J.F. Hall and A.K. Chopra - October 1980(PB81 152 324)A11

UCB/EERC-80/40 "Inelastic Buckling of Steel Struts Under Cyclic Load Reversal," by R.G. Black, W.A. Wenger and E.P. Popov - October 1980(PB81 154 312)A08

UCB/EERC-80/41 "Influence of Site Characteristics on Building Damage During the October 3, 1974 Lima Earthquake," by P. Repetto, I. Arango and H.B. Seed - Sept. 1980(PB81 161 739)A05

UCB/EERC-80/42 "Evaluation of a Shaking Table Test Program on Response Behavior of a Two Story Reinforced Concrete Frame," by J.M. Blondet, R.W. Clough and S.A. Mahin

UCB/EERC-80/43 "Modelling of Soil-Structure Interaction by Finite and Infinite Elements," by F. Medina

UCB/EERC-81/01 "Control of Seismic Response of Piping Systems and Other Structures by Base Isolation," edited by J.M. Kelly - 1981

UCB/EERC-81/02 "OPTNSR - An Interactive Software System for Optimal Design of Statically and Dynamically Loaded Structures with Nonlinear Response," by M.A. Bhatti, V. Ciampi and K.S. Pister - 1981

UCB/EERC-81/03 "Analysis of Local Variations in Free Field Seismic Ground Motion," by J.-C. Chen, J. Lysmer and H.B. Seed 1981

UCB/EERC-81/04 "Inelastic Offshore Platforms for Seismic Loading," by V.A. Zayas, P. Shum, B. Shing, S.A. Mahin and E.P. Popov 1981

UCB/EERC-81/05 "Dynamic Response of Light Equipment in Structures," by A. Der Kiureghian, J.L. Sackman and B. Nour-Omid - 1981

UCB/EERC-81/06 "Preliminary Experimental Investigation of a Broad Base Liquid Storage Tank," by J.G. Bouwkamp, J.P. Kollegger and R.M. Stephen - 1981